Groundwater dynamics and streamflow generation in a mountainous headwater catchment

Process understanding from field experiments and modeling studies

Thèse présentée à la Faculté Science, Centre d'hydrogéologie et géothermie (CHYN), Université de Neuchâtel

Pour l'obtention du grade de docteur ès Science

Par

Jana von Freyberg

Acceptée sur proposition du jury:

Prof. Mario Schirmer
University of Neuchâtel, Switzerland, directeur de these

Prof. Daniel Hunkeler
University of Neuchâtel, Switzerland, co-directeur de these

Prof. Philip Brunner
University of Neuchâtel, Switzerland, rapporteur

Prof. P. Suresh C. Rao
Purdue University, USA, rapporteur

Dr. Ilja van Meerveld
University of Zurich, Switzerland, rapporteur

Soutenue le 14 Janvier 2015

Université de Neuchâtel 2015

UNIVERSITÉ DE NEUCHÂTEL

Faculté des sciences
Secrétariat-décanat de Faculté
Rue Emile-Argand 11
2000 Neuchâtel - Suisse
Tél: + 41 (0)32 718 2100
E-mail: secretariat.sciences@unine.ch

IMPRIMATUR POUR THESE DE DOCTORAT

La Faculté des sciences de l'Université de Neuchâtel autorise l'impression de la présente thèse soutenue par

Madame Jana von FREYBERG

Titre:

"Groundwater dynamics and streamflow generation in a mountainous headwater catchment – Process understanding from field experiments and modeling studies"

sur le rapport des membres du jury composé comme suit:

- Prof. ass. Mario Schirmer, Université de Neuchâtel, directeur de thèse
- Prof. Daniel Hunkeler, co-directeur de thèse, Université de Neuchâtel
- Prof. Philip Brunner, Université de Neuchâtel
- Prof. Suresh Rao, Purdue University, USA
- Dr Ilja van Meerveld, Université de Zürich

Neuchâtel, le 2 mars 2015

Le Doyen, Prof. B. Colbois

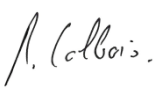

Mots clés: décharge, nappe phréatique, propriétés de la terre, modélisation, versant amont, chute de pluie – ruissellement, recharge, génération de débits, seuils, domaines contribuant variable

Keywords: discharge, groundwater, landscape properties, modeling, mountainous headwater catchment, rainfall-runoff, recharge, streamflow generation, thresholds, variable contributing areas

SUMMARY

Mountainous headwater catchments are often characterized by a high intrinsic variability of climatic and physiographic properties with steep gradients. As temperature, precipitation as well as soil types, vegetation cover and surface topography change with altitude, complex interrelations between the different variables of the water cycle occur and a broad range of hydro(geo)logical regimes and can be found on a rather small scale. In many regions of the world, small headwater catchments in mountainous regions are one of the most important sources of freshwater. However, environmental changes due to human interference, such as agriculture, pollution and water consumption, are likely to negatively affect quality and quantity of ground- and surface water is such catchments. In order to protect and sustainably manage these fragile hydro(geo)logic systems in high elevations, not only does our mechanistic understanding of groundwater flow and streamflow-generation processes in mountainous headwater catchments has to be improved, but also the complex land-atmosphere interactions with groundwater have to be understood.

In order to close that research gap, four particular aspects of the hydro(geo)logic processes in mountainous catchment systems were investigated within this PhD project. These aspects relate the first-order controls on groundwater recharge (i.e., climatic forcing and landscape properties) and the responses driven by groundwater discharge (i.e., streamflow generation and solute transport). In order to adequately describe hydrogeologic processes in mountainous headwater catchments, a holistic approach was pursued, which involved field experiments and analytical modeling. Hydro-climatic data from a dense observation network in the Swiss pre-Alpine upper Rietholzbach Research Catchment (URHB, ~1km^2) were used, where the major variables of the water cycle are continuously monitored at high temporal and spatial resolution.

The processes of groundwater recharge (GR) were investigated through a systematic assessment of of six frequently used GR estimation methods that differ in terms of the underlying concepts and complexity. These methods utilize experimental data (lysimeter, river streamflow, groundwater-table variations) as well as soil-water-balance and physically-based modeling concepts. From the inconsistencies among the applied GR estimation methods first-

order controls of GR were identified that helped to better understand GR mechanisms. It could be shown that the effects of snowmelt-driven GR and water losses through evapotranspiration are very pronounced in the shallow aquifer in the valley bottom (unconsolidated Moraine deposits). Compared to this, GR recharge into the deep, fractured-rock aquifer at higher elevations is less affected by climatic variability. In essence, this project illustrates that a correct interpretation of the GR estimates requires knowledge about the dominant hydro(geo-)logical properties of the catchment because a direct evaluation with detailed GR observations at the plot scale (e.g., lysimeter data) is often not possible.

A more detailed analysis of groundwater dynamics at the event-time scale revealed that groundwater from the shallow aquifer in the valley bottom of the URHB represents the dominant fraction of peak flow during most rainfall periods. When high-intensity rainfall events coincide with wet antecedent moisture conditions, the shallow groundwater table intersects the upper, generally more permeable soil layers at the bottom of the hillslopes, leading to return flow and shallow subsurface stormflow. In addition, surface runoff is generated at the saturated, flat areas in the valley bottom of the catchment (riparian zones). Since the hillslopes are also agricultural areas, nutrient concentrations in river water largely reflect the hydrochemical signal of the groundwater from the shallow aquifer. The riparian zones, however, likely act as sink for solutes (e.g., phosphorous), which are discharged from the agriculturally used hillslopes. During rainfall events, flushing of solutes from the riparian zone can be expected, which may alter the chemograph of the RHB-river.

The conceptual description of the hydro(geo)logic system in the URHB was evaluated with an analytical model that consists of two linear reservoirs for event-flow generation and a baseflow storage with relatively constant discharge rates. Here, rainfall-driven event flow is generated in the riparian zones and the adjacent hillslopes, while baseflow was assumed to originate from the deep fractured-rock aquifer and to be rather constant. The model adequately reproduced the observed streamflow signal, however, the performance improved after implementation of the variable contributing area concept. Although the shrinking/expansion of the riparian zones is small compared to the total catchment area (up to 14 %), this process strongly controls the streamflow hydrograph when wet antecedent moisture conditions coincide with high-intensity rainfall periods.

This PhD project compiles various a practical approaches to analyze and characterize groundwater systems and streamflow-generation mechanisms in mountainous headwater catchments. By focusing on the two dominant drivers, climate and subsurface properties, an important foundation for future research is provided that deals with potential negative effects of climate change and land use on water quality and quantity in mountainous headwater catchments.

ZUSAMMENFASSUNG

Einzugsgebiete in Gebirgen sind häufig durch eine grosse Variabilität klimatischer und physiografischer Einflussgrössen mit steilen Gradienten charakterisiert. Die höhenabhängige Veränderung von Temperatur- und Niederschlagsregimen, Bodentypen und –bedeckung, als auch der Topographie führen zu komplexen Wechselwirkungen mit den verschiedenen Grössen des Wasserkreislaufs und somit einer weiten Bandbreite hydro(geo)logischer Systeme auf kleinem Raum. Weltweit bilden solche Kopfeinzugsgebiete in Gebirgen eine bedeutende Trinkwasserressource für die dicht besiedelten Regionen in den tiefer gelegenen Ebenen. Die hohe Qualität und Quantität dieser Ressourcen ist jedoch häufig bedroht durch zunehmende Umwelteinflüsse, wie zum Beispiel Landwirtschaft ,Verschmutzung oder Wasserentnahme. Es ist daher notwendig, ein umfassendes mechanistisches Verständnis der Grundwasserfliessprozesse und der Abflussbildung unter Einbeziehung der Land-Atmosphären-Wechselwirkungen zu entwickeln, um diese (potentiellen) Probleme richtig zu erfassen und eine nachhaltige Nutzung dieser fragilen hydro(geo)logischen Systeme zu ermöglichen.

Das Ziel dieser Doktorarbeit war es somit, vier verschiedene Aspekte der Hydrogeologie von Kopfeinzugsgebieten im Gebirge zu untersuchen, welche sich auf die wichtigsten Einflussfaktoren auf die Grundwasserneubildung (d.h. Klima und Landschaftseigenschaften) und den Auswirkungen von Grundwasserabfluss (d.h. Prozesse der Abflussbildung und Stofftransport) konzentrieren. Um eine repräsentative und genaue Beschreibung hydrogeologische Prozesse zu ermöglichen, wurde ein holistischer Forschungsansatz verfolgt, der feld-basierte Experimente und numerische Modellierung kombiniert. Im vor-Alpinen Kopfeinzugsgebiet des Rietholzbachs (RHB, ,~3km^2) wurde ein dichtes hydrogeologisches Beobachtungsnetzwerk installiert, welches die bereits existierende meteorologische und hydrologische Messstation erweitert. Dieser Aufbau ermöglicht eine simultane Beobachtung der wesentlichen Variablen des Wasserkreislaufs in sehr hoher zeitlicher und räumlicher Auflösung.

Durch die systematische Auswertung verschiedener Verfahren zur Abschätzung der Grundwasserneubildung unter Einbeziehung von Langzeitmessdaten eines Wägelysimeters

konnten die relevanten Einflussfaktoren auf Infiltrationsprozesse identifiziert und beschrieben werden. Es konnte gezeigt werden, dass die Hydrogeologie im RHB-Einzugsgebiet durch einen tiefen (verfestigte Molassesedimente) und einen flachen (unverfestigte Moränenschotter) Grundwasserleiter geprägt ist, was sich in einer grossen Variabilität der Verweilzeiten im Untergrund niederschlägt. Grundwasserneubildung in den unverfestigten Moränenschottern in der Talebene und den unteren Hängen wird meistens durch vertikale Versickerung durch die Bodenmatrix bestimmt. Dieser Teil der Doktorarbeit demonstrierte zudem, dass eine richtige Interpretation von Grundwasserneubildungsraten nur gewährleistet werden kann, wenn die wesentlichen hydraulischen Eigenschaften des Einzugsgebiets bekannt sind.

Eine detaillierte Untersuchung von Niederschlagsereignissen über einen Zeitraum von zwei Jahren zeigte, dass ein wesentlicher Anteil des Gebietsabflusses der flachen Talsohle sowie den angrenzenden Hängen entstammt. Schneller Grundwasserabfluss in den oberen, besser durchlässigen Bodenschichten tritt jedoch häufig erst dann auf, wenn Starkniederschläge mit einer hohen Vorfeuchte einhergehen. Zusätzlich kommt es zum Oberflächenabfluss auf den gesättigten Flächen in der Talsohle Kopfeinzugsgebietes. Da diese Hänge auch landwirtschaftlich genutzt werden, zum Beispiel als Weideland oder Mähwiesen, spiegeln sich die Nährstoffkonzentrationen im flachen Grundwasserleiter auch im Flusswasser während mittlerer Fliessraten wider. Die angrenzende Talsohle hingegen wirkt vermutlich als Speicher für Nährstoffe (z. Bsp. Phosphor) durch das kontinuierlich anströmende Grundwasser von den Hängen. Während Niederschlagsereignissen kann es daher verstärkt zu einer Auswaschung dieser Substanzen in das Gewässer kommen.

Die konzeptionelle Beschreibung des Grundwasserregimes und der beteiligten Prozesse bei der Abflussbildung im RHB-Einzugsgebiet wurde mithilfe eines numerischen Modells überprüft. Es besteht in Wesentlichen aus zwei linearen Speichern (Hänge und flache Talsohle), die während eines Niederschlagsereignisses nur wenig verzögert zum Abfluss beitragen. Zudem wurde angenommen, dass der Basisabfluss dem tiefen Grundwasserleiter entspringt und daher nur eine geringe zeitliche Variabilität aufweist. Auf der Grundlage von unveränderlichen Flächenanteilen der beiden Speicher relativ zum Gesamteinzugsgebiet gaben die Modellberechnungen das beobachtete Abflussregime relativ gut wieder. Jedoch verbesserte sich die Simulation deutlich, wenn das Konzept der variablen beitragenden Flächen in das Modell implementiert wurde. Mit Hilfe des Modells konnte eine maximale Ausdehnung der gesättigten Flächen in der Talsohle um 14% bestimmt werden, was somit die feldbasierten Beobachtungen bestätigte und quantifizierte.

Die Ergebnisse dieser Doktorarbeit stellen einen möglichen Arbeitsansatz vor, welcher der Erfassung von hydrogeologischen Systemen und relevanter Abflussbildungsprozesse in Kopfeinzugsgebieten mit ähnlichen Landschaftsmerkmalen dient. Die gewonnenen Erkenntnisse leisten zudem einen wesentlichen Beitrag zu einem besseren Verständnis der beteiligten Faktoren (z. Bsp. Klima, Eigenschaften des Untergrundes), welche die hydrogeologischen Prozesse in solchen Gebieten steuern. Dieses Prozessverständnis bildet die notwendige Grundlage für ein nachhaltiges Wasserressourcenmanagement in gebirgigen Einzugsgebieten.

ACKNOWLEDGEMENTS

First of all, I wish to express my sincere thanks to my main supervisor, Prof. Mario Schirmer, who initiated this project, raised the financial support and invited me to work in his group at Eawag. I very much appreciate his trust in my work, his positivity and the scientific freedom that allowed me to develop my own ideas.

I would also like to thank my second supervisor, Prof. Suresh Rao for all the interesting discussions and new ideas, his kindness and contagious curiosity. Further, I wish to thank Prof. Daniel Hunkeler for his help and Prof. James Kirchner for supporting me during the last months of this project. Thank you Dr. Ilja van Meerveld and Prof. Philip Brunner for joining the jury and for taking the time to read this thesis.

I wish to acknowledge the financial support from the Swiss National Science Foundation for the project "Alpine Hydrogeology and Climate Change" and the Doc-Mobility grant that allowed me to visit the Universities of Purdue and PennState.

For sharing the data sets from Rietholzbach and valuable scientific feedback, I would like to thank the groups of Prof. Sonia Seneviratne from ETH Zurich, especially Dr. Irene Lehner and Dr. Martin Hirschi, as well as of Prof. Jan Seibert from the University of Zurich. Very helpful support during fieldwork and in the lab was generously provided by Andy Raffainer, Roger Mégroz, Armand Rochat, Julien Nikiéma, Bahareh Kianfar, Marco Fleischmann, Numa Pfenninger and the AuA-lab team, in particular Denise Freudemann and Madlene Langmeier. I highly appreciate the generosity of the family Sennhauser in Gähwil, who allowed me to conduct the field experiments in the Rietholzbach catchment.

This PhD would not have been possible without the support and the positive spirit I received from so many colleagues and friends at Eawag, ETH Zurich and Purdue University! Thanks a lot to all of you: Ann-Kathrin and Chris McCall, Bas Vriens, Nina Franz, Natallia Zaremba, Lina Tyroller, Elham Rouholahnejad, David Machac, Rebekka Gulde, Vidhya Chittoor Viswanathan, Sabine Hoffmann, Behnam Doulatyari, Stefano Basso, Anna Senn, Anne-Marie Kurth and Mehdi Ghasemizade! Special thanks to Dirk Radny and Christian Möck, whose jokes made my day even in the most stressful situations. For making me feel at home and for being a great flat mate, many thanks to Anja Bretzler. Thanks to Heather Gall, who showed me how to achieve true greatness by inviting me into her life.

I am very grateful to my grandparents, my parents and my brother Henri for always being there for me. I gained most of my confidence from their love and proudness that makes me feel very lucky.

For endless encouragement and companionship and for beeing a unique part of this journey: Tim, let me say thank you with all of my heart!

TABLE OF CONTENTS

FIGURES

TABLES

LIST OF SYMBOLS

Latin symbols

A_e	Event-flow generating area	%
A_h	Areal portion of the hillslopes	%
A_{rz}	Areal portion of the riparian zones	%
A_{tot}	Total catchment area	L^3
C_R	Runoff coefficient	-
D	Drought duration	T
D_h	Estimated hillslope groundwater discharge	$L\ T^{-1}$
D_h'	Simulated hillslope groundwater discharge	$L\ T^{-1}$
EC_O	Electrical conductivity of the river water	$\mu S\ cm^{-1}$
EC_{GW}	Electrical conductivity of the groundwater	$\mu S\ cm^{-1}$
ET, AET	Actual evapotranspiration	$L\ T^{-1}$
GR	Groundwater recharge	$L\ T^{-1}$
GW_{max}	Maximum groundwater table elevation	L
h	Depth to groundwater table	L
k_{gw}	Hillslope groundwater recession constant	T^{-1}
P	Rainfall	$L\ T^{-1}$
P_e	Effective rainfall	L
PET	Potential evapotranspiration	$L\ T^{-1}$
P_{sum}	Cumulative rainfall during one event	L
Q	Total URHB-river streamflow	$L\ T^{-1}$
Q_e	Event flow (streamflow minus baseflow)	$L\ T^{-1}$
Q_e'	Simulated event flow	$L\ T^{-1}$
Q_{ini}	Initial river streamflow	$L\ T^{-1}$
Q_{max}	Maximum river streamflow	$L\ T^{-1}$
R_h	Estimated hillslope groundwater recharge	$L\ T^{-1}$
R_h'	Simulated hillslope groundwater recharge	$L\ T^{-1}$
R^2	Coefficient of determination for simple linear regression	-
S	Storage	L
T_{lag}	Lag time between GW_{max} and Q_{max}	T
T_{res}	Response time	T
V	Drought deficit volume	L
V_{gw}	Estimated hillslope groundwater volume	$L^3\ T^{-1}$
V_{gw}'	Simulated hillslope groundwater volume	$L^3\ T^{-1}$
z_{conf}	Depth to confining layer	L
z_{gw}	Depth of groundwater table	L

z_r	Depth of active soil layer	L
z_{gw}	Depth to groundwater table	L

Greek symbols

α	Direction of flow	°
φ	Aquifer effective porosity	-
σ_y	Specific yield	-
θ	Soil moisture content	-
θ_{def}	Soil moisture deficit	-
θ^*	Soil moisture threshold	-
θ_w	Permanent wilting point	-

INTRODUCTION

Water is involved fundamentally in many physical, chemical and socio-economic processes and thus is essential for the development of all life. One of the most important sources of freshwater are small headwater catchments in mountainous regions whose river discharge significantly sustains water bodies in the lowlands (WOODWELL, 2004; VIVIROLI et al., 2003). In Switzerland, around 80 % of the total river network is comprised by high-elevation catchments (MUNZ et al., 2012) that serve as a major resource for drinking water production from spring discharge and groundwater aquifers (FREIBURGHAUS, 2012). Mountainous headwater catchments also provide essential habitats for unique, highly adapted species (MEYER et al., 2007).

Many mountainous environments are characterized by a high intrinsic variability of climatic and physiographic properties with steep gradients, where temperature, precipitation as well as soil types, vegetation cover and surface topography change with altitude (BURLANDO et al., 2002). Hence, a broad range of hydro(geo)logical regimes and feedback mechanisms can be found on a rather small scale (WEINGARTNER et al., 2003). Mountainous headwater catchments are thus inherently interesting study sites that allow for a holistic investigation of surface and subsurface water flow processes and land-atmosphere interactions. This is of particular importance for the evaluation of possible effects of climate- and land use change on these environments.

Hydro(geo)logical systems in mountainous regions are known to be very sensitive to environmental changes associated with human interference such as agriculture, pollution and water consumption (e.g., HEILLWELL et al., 2008; PLATE, 1998). For instance, small rivers from Swiss pre-Alpine headwater catchments were found to exhibit much higher peak concentrations of pesticides during rainfall events compared to larger catchments (MUNZ et al., 2012). This is attributed to the extensive use of small catchments for agriculture and as pastureland (STRAHM et al., 2013) in combination with generally quick streamflow responses due to short groundwater residence times and overland flow.

Further, climate change is likely to accelerate the hydrologic cycle, which would affect nutrient and bio-geochemical cycles and have negative impacts on water quality and aquatic

ecosystems (e.g., BENISTON and FOX, 1996; JASPER et al., 2004; ZIERL and BUGMANN, 2005). For instance, the Intergovernmental Panel on Climate Change predicted an increase in runoff of 10 - 40 % by mid-century at higher latitudes (IPCC, 2007). Higher air temperatures in spring cause earlier snow- and glacier melt in the mountains that may lead to destructive floods in the lowlands (e.g., BARNETT et al., 2005; ECKHARDT and ULBRICH, 2003; MAXWELL and KOLLET, 2008). On the other hand, mountainous catchments are expected to be very vulnerable to reduced precipitation rates and droughts, which can have cascading effects on local and downstream freshwater bodies (CALANCA, 2007).

A sustainable management of freshwater resources, however, requires an integrated understanding of the dominant physical feedback mechanisms between components of the hydrologic cycle. Over the last decades, numerous studies have focused dominantly on near-surface processes, for instance spatio-temporal variability of soil moisture, streamflow dynamics or water quality in rivers. However, groundwater is known to contribute a large fraction of the streamflow hydrograph (SKLASH and FARVOLDEN, 1979), especially in mountainous catchments where steep hydraulic gradients form effluent river systems. Groundwater discharge also affects the chemical composition of river streamflow. For example, during precipitation events the hydrochemical signal of the stream may not necessarily reflect the hydrological response because 'old' groundwater with a very different composition becomes mobile (BISHOP et al., 2004; KIRCHNER, 2003). Such highly non-linear interactions between ground- and surface water are a major feature of hydro(geo)logic systems in mountainous regions that are often correlated to the exceedance of site-specific thresholds of antecedent moisture conditions or rainfall intensity (e.g., MCGRATH et al., 2007; TROMP-VAN MEERVELD and MCDONNELL, 2006b).

Despite the importance of groundwater to hydrological responses and water quality, investigations of groundwater dynamics in high-altitude catchment systems are comparably rare. Because of steep terrain, missing infrastructure or extreme weather conditions in such areas, the development and implementation of comprehensive hydrogeological investigation and monitoring strategies remains challenging (BURLANDO et al., 2002). Most of the relevant previous work in mountainous catchment hydrogeology is related to fractured rock (e.g., MILLARES et al., 2009; LAUDON and SLAYMAKER, 1997; GABRIELLI et al., 2012), although a number of research groups have also worked on unconsolidated aquifers (ALLEN et al., 2010b; ROY and HAYASHI, 2009).

The description and simulation of hydrologic connectivity between groundwater dynamics and climate drivers in mountainous watersheds require long-term datasets and integrated field experimentation (JENCSO and MCGLYNN, 2011). Due to the fact that hydro(geo)logical functions and patterns cover a wide range of scales (TROCH et al., 2009), measurements at different spatiotemporal scales have to be integrated. For instance, at the catchment scale SIMONI et al. (2011) observed a significant impact of spatial variability of meteorological forcing (precipitation and temperature) on streamflow generation in a field-based study in the Swiss Alps. This observation is further supported by the findings of ZLOTNIK et al. (2011) that indicate that small- and large-scale anisotropy of hydraulic conductivity strongly control the structure of topography driven groundwater flow. Frequently, a threshold dependent connectivity between the valley bottom and the hillslopes can be

observed in mountainous catchments, which also affects small-scale flow dynamics like groundwater-surface water-interaction in the riparian zone (e.g., BENCALA et al., 2011; DETTY and MCGUIRE, 2010; TETZLAFF et al., 2007). The water flow through the very last meters of the valley bottom before entering the stream is seen as a significant first-order control on stream water chemistry and ecosystem functioning (SEIBERT et al., 2009). These examples emphasize the necessity of a general framework for monitoring and describing subsurface flow processes in mountainous headwater catchments. However, many studies mention a lack of detailed long-term data that allow the investigation of the natural wide range of control factors on groundwater dynamics and streamflow responses (JAMES and ROULET, 2009).

RESEARCH OBJECTIVES

This PhD thesis investigates groundwater dynamics and its role for river water quantity and quality in mountainous headwater catchments under consideration of four particular aspects. These aspects refer to the first-order controls of groundwater recharge (i.e., climate forcing and landscape properties) as well as to the responses driven by groundwater discharge (i.e., streamflow generation and solute transport). By applying field and modeling techniques at an experimental site in the Swiss pre-Alps, this PhD thesis addresses some of the many complexities of hydrogeology in mountainous environments at different spatio-temporal scales. Specifically, the research objectives of this research are the following:

- Investigation of groundwater recharge mechanisms through the systematic comparison of groundwater recharge estimation methods at different spatio-temporal scales and for average and extreme climatic conditions;
- Identification of dominant streamflow-generating mechanisms and threshold-responses with focus on groundwater discharge;
- Evaluation of the impact of agricultural land use and related transport of solutes and nutrients towards the river by groundwater discharge.
- Development of a conceptual rainfall-runoff model at the hillslope- and the catchment scale, which is validated with an analytical model;

STRUCTURE OF THE THESIS

According to the research objectives stated above, this PhD thesis consists of three parts, which focus on four different aspects of hydro(geo)logic processes in mountainous headwater catchments.

Part I GROUNDWATER RECHARGE

Various established groundwater estimation methods were compared among each other and against lysimeter seepage measurements at different time scales in order to systematically evaluate the implications of model complexity and initial assumptions on their

predictive strengths. From the model performances, important physical mechanisms regarding catchment functioning and groundwater recharge processes were identified.

Part II STREAMFLOW-GENERATING MECHANISMS AND NUTRIENT TRANSPORT

This chapter presents an extensive analysis of continuous time series of groundwater table depth, rainfall, streamflow and water quality at the hillslope- and the catchment scale at an experimental site in the Swiss pre-Alps. In particular, short-term responses to rainfall events were investigated in order to identify site-specific threshold responses. Based on this assumption, a conceptual model of streamflow generation and nutrient transport from the agricultural areas into the stream were developed.

Part III EVALUATION OF THE CONCEPTUAL MODEL AND SIMULATION OF EVENT-FLOW GENERATION

The conceptual model developed in parts I and II was evaluated by means of a semi-distributed, minimalistic modeling scheme that consists of two parallel linear storage reservoirs. These reservoirs represent the main hydrologic landscape elements at the experimental site that differ in terms of their dominant streamflow-generating properties. The application of the analytical model revealed the importance of variable contributing areas for peak flow rates. Particularly, during long and high-intensity rainfall events the area of saturation-overland-flow generation increases, which has implications on peak flow rates and nutrients export.

In the **CONCLUSIONS AND OUTLOOK** section at the end of this thesis the key findings are summarized and conclusions are drawn. This also includes an outlook on possible challenges for future research that arise from this thesis.

View over the western part of the Rietholzbach research catchment towards east.

PART I

GROUNDWATER RECHARGE

A reliable quantification of groundwater recharge (GR) is essential for sustainable water resources management. This is particularly relevant when considering climate change and predicted increase in the duration and frequency of drought events. Although there exists a large variety of GR estimation methods, their results can differ considerably for a site due to the spatio-temporal scales and complexities they represent. Therefore, it is crucial to evaluate the potential range of GR estimates to allow for consistency and objective inter-comparison of modeling results among different sites. This motivates the present study, which systematically assesses the performance of six frequently used GR estimation methods that differ in terms of the underlying concepts and complexity. These methods utilize experimental data (lysimeter, river streamflow, groundwater-table variations) as well as soil-water-balance and physically-based modeling concepts. 13 years of hydro-climatic data were analyzed from the Swiss Rietholzbach research catchment under consideration of different temporal resolutions and extreme climatic conditions (i.e., dry periods). The major limitations and strengths of the six methods were identified and summarized in a comprehensive overview that may assist future studies to choose an adequate technique for the estimation of GR.

JANA VON FREYBERG, CHRISTIAN MOECK, MARIO SCHIRMER, **Estimation of groundwater recharge and drought severity with varying model complexity**, Journal of Hydrology (*submitted*[1]).

[1] Please note that this is the revised version of an article submitted to *Journal of Hydrology* in February 2015. For the final version consult the homepage of *Journal of Hydrology*.

I - 1 INTRODUCTION

Groundwater recharge (GR) is a driver of many hydrologic processes, which makes it an important variable in the water cycle (BAKKER et al., 2013). Thus, for sustainable water resources management a reliable quantification of GR is essential, particularly considering the effects of climate change on water resources (e.g., GREEN et al., 2011; MIDDELKOOP et al., 2001; VAN ROOSMALEN et al., 2009). A large number of methods exist, which aim at the quantification of GR from available hydro(geo-)logic and climatic measurements (BAKKER et al., 2013). Frequently used physical techniques for GR estimation utilize direct measurements of lysimeters (e.g., HEPPNER et al., 2007; RISSER et al., 2005; XU and CHEN, 2005), temporal variations of river streamflow (e.g., ARNOLD and ALLEN, 1999; COMBALICER et al., 2008; NATHAN and MCMAHON, 1990; RORABAUGH, 1964) or groundwater-table (e.g. CROSBIE et al., 2005; HEALY and COOK, 2002; MARÉCHAL et al., 2006). Furthermore, unsaturated-zone modeling can be applied to estimate GR, such as analytic soil water balance models (e.g., BOND, 1998; FINCH, 1998; RODRIGUEZ-ITURBE et al., 1999) or numerical modeling using Richards' equation (e.g., CROSBIE et al., 2011; JYRKAMA and SYKES, 2007; KEESE et al., 2005; SIMUNEK and VAN GENUCHTEN, 2008; VAN ROOSMALEN et al., 2009). Because GR estimation is very sensitive to the underlying climatic forcing functions and the parameters of the chosen method (RISSER et al., 2005; SAVENIJE, 2004; SCANLON et al., 2002), it is generally recommended to apply several techniques and to compare the GR estimates among each other (NIMMO, 2003; HEALY and COOK, 2002). This, however, is not always practicable because of limited data availability. For example, many climate change impact studies apply solely one GR estimation method (e.g., ALLEN et al., 2010a; GODERNIAUX et al., 2009; ORDENS et al., 2014; VAN ROOSMALEN et al., 2009). Typically, the uncertainty, which is introduced by the chosen GR estimation method, cannot be evaluated objectively and may lead to controversy results. This might be of importance also for drought risk assessment studies in hydrological systems where GR is closely linked to catchment storage and the streamflow regime (e.g., BENISTON and FOX, 1996; CALANCA, 2007; JASPER et al., 2004; VANHAM et al., 2009). Therefore, GR estimation methods should also be analyzed with respect to both, mean and extreme climatic conditions to allow for an accurate assessment. This could be achieved, for instance, by comparing different GR time series during very dry climatic conditions by means of drought characteristics (e.g., duration and severity, MISHRA and SINGH, 2010). Although there are several comparison studies focusing on GR (e.g., ALLISON et al., 1994 FLINT et al., 2002; GEE and HILLEL, 1988; LERNER et al., 1990; SCANLON et al., 2002; SIMMERS, 1998; SOPHOCLEOUS, 1991; SORENSEN et al., 2014; XU and CHEN, 2005), still little research work systematically evaluated the accuracy and the validity of the applied GR estimation techniques under this important aspect.

In addition, a comprehensive comparison of GR estimation methods can serve as a valuable learning tool that helps to identify first-order controls on GR recharge and to improve our mechanistic understanding of the involved hydro(geo)logic processes (e.g., BEVEN, 2007; DUNN et al., 2008; FENICIA et al., 2014). As a reference for estimated GR, experimental data from large lysimeters (>2 m depth, >1-2 m^2 area) can be used. Despite certain limitations of lysimeters (SCANLON et al., 2002), they provide a unique technology for direct measurements of the soil water balance that is also representative for larger scales (SENEVIRATNE et al., 2012;

YOUNG et al., 1996). These systems that extend below the rooting depth of plants, are assumed to provide reliable estimates of GR that will reach the groundwater table without further loss mechanisms (HEPPNER et al., 2007). To our knowledge, there only exists one study in which data from a large lysimeter were compared against GR estimates based on evapotranspiration models used in water balance equations (XU and CHEN, 2005). Since appropriate systems are difficult to construct and require high maintenance, there are only a few comparison studies employing long-term lysimeter data, however, from smaller systems (e.g., HEPPNER et al., 2007; RISSER et al., 2005).

In order to provide a comprehensive evaluation of six widely established GR estimation methods, the main objectives of this study are: (i) to identify the major strengths and limitations of the methods at different time scales and climatic conditions by using measurements from a large lysimeter system and to employ drought characteristics; (ii) to learn from the inconsistencies among the applied GR estimation methods to identify first-order controls and to better understand GR mechanisms.

The GR estimation methods tested in this study span a large variety of approaches and complexities (i.e., number of model parameters and type of input variables) as well as different spatial scales (i.e., plot to catchment scale). These methods are: (a) large lysimeter measurements; (b) streamflow-based automated recession-curve displacement method (RORA, RUTLEDGE and DANIEL, 1994); (c) groundwater-table fluctuation method (WTF, HEALY and COOK, 2002); soil water balance models with (d) one (SWB, RODRIGUEZ-ITURBE et al., 1999) and (e) four soil layers (FINCH, FINCH, 1998) and (f) a physically-based, one-dimensional model (HYDRUS, SIMUNEK and VAN GENUCHTEN, 2008). Daily hydro-climatic data from the Swiss Rietholzbach research catchment were used, spanning a 13-year period (2000-2013) that coves a sufficiently large variability of climatic conditions.

First, all methods were compared on an annual and monthly basis against each other by using field and literature data as initial model parameters. The same analysis was carried out after calibrating methods (b) to (f) against lysimeter data (calibrated models are marked with a "*"-sign). This allows for a more robust assessment of the performance and meaningful comparison of the methods, despite the differences in the underlying modeling concepts. In the second part of this chapter, drought characteristics were calculated from monthly GR time series to systematically evaluate the performance of the different methods during very dry climatic conditions. These results are then discussed to identify the main strengths and limitations of the six methods. From this, conclusions about flow processes and streamflow generation in the studied catchment are derived and recommendations for the effective estimation of GR at different spatio-temporal scales are provided.

I - 2 MATERIALS AND METHODS

I - 2.1 Study site and observed data

The Rietholzbach research catchment is located in the pre-Alpine headwaters of the Thur river in north-east Switzerland (Figure 1c). Its western sub-catchment (upper

Rietholzbach, URHB, red line in Figure 1a) covers an area of 0.94 km^2, from which around 72 % is pastureland, 19 % is forested, 4 % is settlement and pavement and 5 % is a wetland located in the central valley bottom. Elevations in the URHB range from 744 to 910 masl with a more gentle topography in the valley bottom, which is underlain by Pleistocene glacial moraine deposits (Figure 1a).

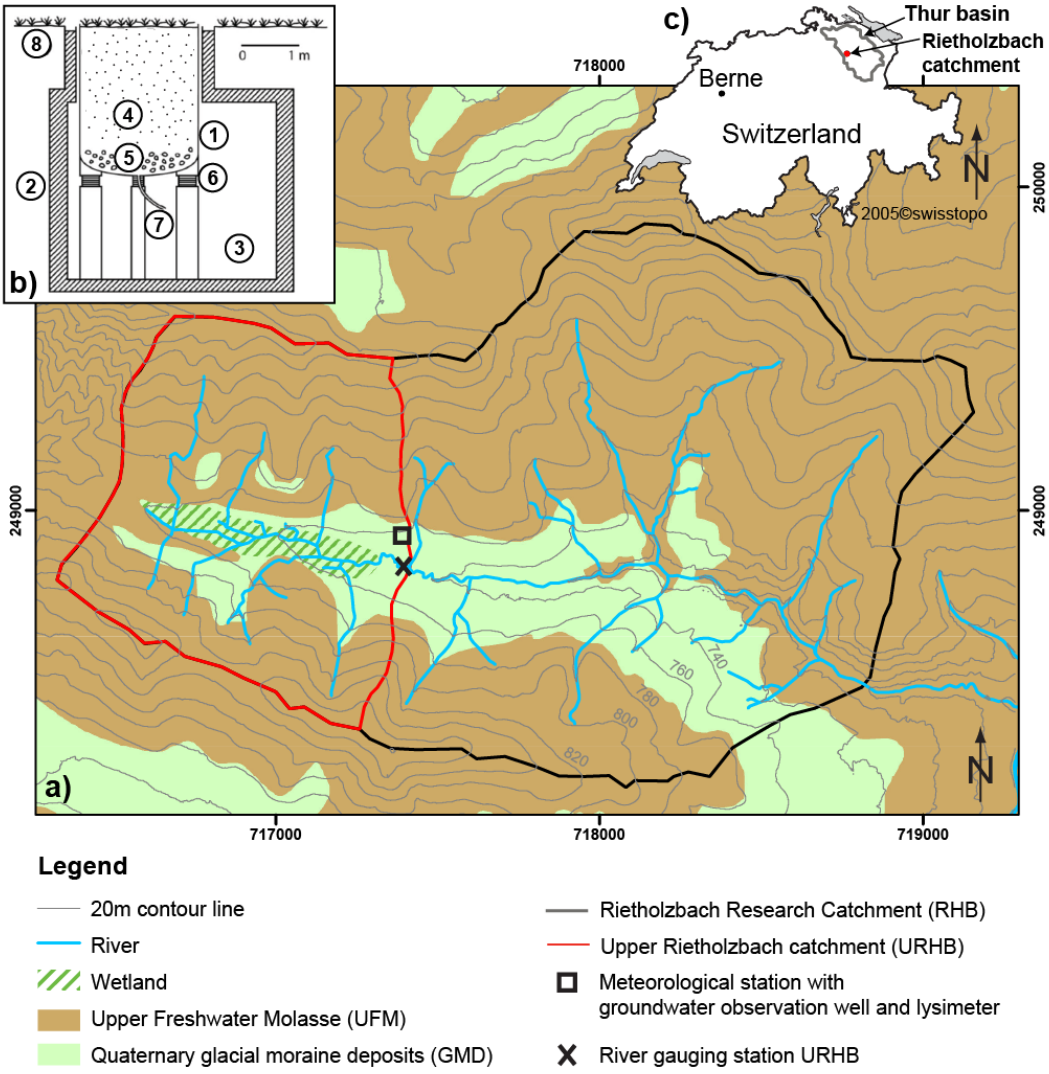

Figure 1 The upper Rietholzbach catchment (URHB) in the western part of the Rietholzbach research catchment (RHB) and location of the meteorological station (black box) and the river gauge (black cross) near the outlet of the URHB; (a) Schematic description of the lysimeter system (modified after SENEVIRATNE *et al. (2012)): (1) Container, (2) concrete wall, (3) cellar, (4) soil, (5) filter (sand and gravel), (6) electronic scales, (7) drainage outlet, (8) grass; (b) Location of the URHB in the Thur basin in north-east Switzerland.*

The moraine deposits are a heterogeneous composition of unconsolidated conglomerates and Quaternary gravel pockets that form a shallow, unconfined groundwater aquifer with an average hydraulic conductivity of $2x10^{-3}$ m s^{-1} (BALDERER, 1980). The bedrock is formed by the Upper Freshwater Molasse, that is layers of consolidated conglomerates, sandstone, marl and freshwater limestone, with hydraulic conductivities between $1.5x10^{-6}$ m s^{-1} and $1.1x10^{-4}$ m s^{-1} (BALDERER, 1983). Vertical groundwater flow between the two aquifers is assumed to be minor due to a confining low-permeability layer of clay and silt beneath the

moraine deposits (VON FREYBERG et al., 2014). The soils in the valley bottom areas are mainly peaty soils and Gleysols, whereas on the hills and slopes Cambisols and Regosols are dominant (GERMANN, 1981).

All hydro-climatic variables (such as river streamflow, precipitation, groundwater-table depth) are measured at the experimental field site 'Büel' that is located near the URHB-catchment outlet (Figure 1a). Further details about the instrumentation of the Büel site and data post-processing are provided in the supplementary information of part I (Table SI- 1) and in Seneviratne et al. (2012). Data used in this study span from 1 January 2000 to 31 December 2012 and cover variable climatic conditions from very wet to very dry periods (Figure SI- 1). For instance, in the year 2003, an extreme summer heat wave occurred that affected large parts of central Europe (CASTY et al., 2005). Other years with less severe dry periods in the Swiss north-eastern pre-Alps were 2009 and 2011 (METEOSWISS, 2009; METEOSWISS, 2011). Wet periods with several high-intensity precipitation events or a significant accumulation of snow occurred in 2001, 2002 and 2007 (Figure SI- 1a). During the 13-year period, average annual values of precipitation, actual evapotranspiration, river streamflow and lysimeter seepage were 1465 mm, 649 mm, 1188 mm and 1003 mm, respectively. The hydroclimatology of the catchment is representative for the eastern Swiss Plateau (SENEVIRATNE et al., 2012).

I - 2.2 Recharge estimation methods

Large lysimeter

The large weighting lysimeter (2.5m deep, 2m diameter) is located at the experimental field site 'Büel' near the URHB-catchment outlet (Figure 1a,b). The lysimeter cylinder was filled with an undisturbed soil column from the same location in 1976. The system imitates the surrounding surface and subsurface properties, which allows a direct measurement of actual evapotranspiration and drainage through the unsaturated zone at the plot scale (e.g., SENEVIRATNE et al., 2012; STUMPP and MALOSZEWSKI, 2010). Since groundwater table depths at the site are generally shallow (< 5 m beneath ground surface, Figure SI- 1d) and the average rooting depth is around 0.3 m (GERMANN, 1981) it is assumed that measured lysimeter drainage is a good indicator for GR at daily temporal resolution. Uncertainties might be introduced by a distorted soil-moisture and pressure-head profile due to the open drainage collection system (SCANLON et al., 2002) and preferential flow along the inner lysimeter wall. However, considering the size and age of the lysimeter, these effects are likely to be minor. Although, only local processes at the plot scale are captured within the lysimeter, the observed recharge correlates well with the RHB river-streamflow signal (SENEVIRATNE et al., 2012).

RORA model

The computer program RORA (RUTLEDGE and DANIEL, 1994; RUTLEDGE, 2007) estimates GR from daily streamflow records by using the recession-curve displacement method after Rorabaugh (1964**)**. The method is based on a one-dimensional analytical model that assumes streamflow recessions to represent instantaneous groundwater discharge in a

homogeneous aquifer with uniform recharge. The hydraulic soil properties are indirectly represented through the recession index (K), which is defined as the average time required for groundwater discharge to recede by one log cycle (RUTLEDGE and DANIEL, 1994). An initial K-value of 25.6 days was obtained for the nearly linear parts of the streamflow hydrographs of the URHB river. For this, the automated master recession curve separation tool of Posavec et al. (2010) was applied. For the calibrated RORA* model, a value of K of 13 days was calculated from the lysimeter data instead. As recommended by Rutledge and Daniel (1994) daily data from September to April in 2000-2002 were used for the calculation of K, when the effect of evapotranspiration on streamflow recession rates is likely to be small. Because of the simplifying assumptions inherent in the RORA model it is generally recommended to apply the program at time scales not shorter than one month (RUTLEDGE, 2002).

Water table fluctuation method (WTF)

The groundwater-table fluctuation method (WTF) is a widely established procedure for the estimation of GR in unconfined aquifers (HEALY and COOK, 2002). It presumes a linear correlation between groundwater-table rise (Δh) and GR with the coefficient σ_y (specific yield):

$$GR = \Delta h \cdot \sigma_y \quad (1)$$

The absolute value of Δh was approximated by fitting an exponential function to the receding limbs of the site-specific groundwater table time series (HEPPNER et al., 2007). With an automated fitting procedure in the "MRCR" computer program of Heppner and Nimmo (2005) GR was then estimated from daily groundwater table depths accordingly. An initial value of 0.075 was used for σ_y, which is the average of pumping-test results in a neighboring catchment with a similar geology (BALDERER, 1984). A calibration of σ_y for the first two years of the observation period was carried out. However, model performance did not improve considerably and therefore, σ_y was calibrated through fitting cumulative GR to lysimeter seepage over the entire observation period (WTF*). This resulted in a value of 0.0601 that still lies well within the range of the field-based observations. It also has to be noted that the location of the groundwater observation well at a gentle hillslope might bias the GR estimation due to lateral drainage. Nevertheless, this effect is assumed to be small because of a significantly larger vertical hydraulic gradient compared to the lateral hydraulic gradient at the site.

Simplistic soil water balance model (SWB)

Estimation of daily GR with a frequently applied simplistic soil-water balance model (SWB, e.g. BASU et al., 2010; RODRIGUEZ-ITURBE et al., 1999; VON FREYBERG et al., 2015) is based on the following equation for the unsaturated zone:

$$\Delta S = P - AET - GR \quad (2)$$

It is assumed that the water budget of an isotropic and homogeneous soil column is solely governed by the change in soil water storage (ΔS) in an uppermost "active" soil layer, which generally corresponds to the average depth of the plant roots. GR occurs when infiltrating rainfall (P) overcomes the soil moisture deficit in this zone, i.e., when the soil

water content exceeds field capacity. A deficit in soil moisture is caused by actual evapotranspiration (AET), which is calculated from potential evapotranspiration (PET, ALLEN et al., 1997; ALLEN et al., 1998). AET is assumed to be maximal when moisture conditions are at field capacity and to decrease in a linear fashion at smaller water contents up to the wilting point, where AET is zero (RODRIGUEZ-ITURBE et al., 1999; Eq. (3) - (4) in HARMAN et al., 2011). Surface runoff and lateral flow are neglected in the SWB model. During days with frozen ground and snow cover, AET was reduced by 60 % (ALLEN et al., 1998). To account for delayed infiltration of snowmelt water within this and the following GR estimation methods, the snow water equivalent (SWE) was calculated with the 'SnowMelt' function in the R-project Software 'EcoHydRology' package (WALTER et al., 2005). The uncalibrated SWB model is based on only 3 physically-based parameters that were adapted from site-specific measurements and literature values (field capacity, wilting point, rooting depth, Table SI-2). For this and the following GR estimation methods, calibration of the parameters against daily lysimeter seepage was carried out with the parameter estimation software PEST (DOHERTY, 2011) for the first two years of the observation period. A warm-up phase of 180 days before the start of the observation period was found sufficient for this and the following GR estimation methods to minimize effects due to state-value initialization. More details can be found in Table SI- 2 in the supporting information.

FINCH model

This soil-water balance model includes canopy interception, surface runoff, bypass flow and plant water uptake in the root zone of the soil column into the daily water balance equation (FINCH, 1998). The model assumes a 4-layered root zone where a GR-signal is simulated when water inflow into the fourth layer at the bottom exceeds field capacity. In each layer, AET is governed by current available water content and root density. Since most of the URHB catchment is covered with grass, the canopy reference parameters for annual short vegetation as given in Finch (1998) and Allen et al. (1994) were used for the uncalibrated FINCH model. Parameters describing the hydraulic soil properties were obtained from literature data and field-based observations (Table SI- 2, Table SI- 3). The calibration procedure follows the approach outlined above.

HYDRUS model

The physically-based one-dimensional HYDRUS model (SIMUNEK and VAN GENUCHTEN, 2008) was used to simulate water flow in a variably saturated porous medium by numerically solving the Richards' equation. On the top of the soil column a flux boundary with daily precipitation and PET was applied (without uptake compensation), while the bottom was represented by a seepage boundary with atmospheric pressure conditions in order to represent lysimeter seepage. For the purpose of simplicity and easy transferability, a homogeneous soil structure was assumed with hydraulic model parameters as in the formulation of van Genuchten (1980). Root water uptake was simulated for grass cover following the model in Feddes et al. (1974). For the un-calibrated HYDRUS model, the hydraulic soil-property parameters were adapted from site-specific measurements and literature values (Table SI- 2,

Table SI- 3). Calibration was carried out solely for these parameters, while the parameters of the Feddes et al. (1974) model remained unchanged.

I - 2.3 Drought characteristics

For the calculation of drought characteristics, the 20th percentile of the time series was applied as a fixed threshold (x_0, Figure 2), following the methods used in Tallaksen and van Lanen (2004), Talleksen et al. (2009) and Andreadis et al. (2005). Based on this, we calculated the duration (D_x) and the deficit volume (V_x) of the time series ($x(t)$, e.g. precipitation, lysimeter seepage, Figure 2). D_x is defined as the number of consecutive periods (e.g. months) in which the moving average of x falls below x_0. V_x was calculated as the sum of the deficit volumes ($V_x(t)$) over a continuous period of time, e.g. one month or the duration of an event (TALLAKSEN et al., 2009).

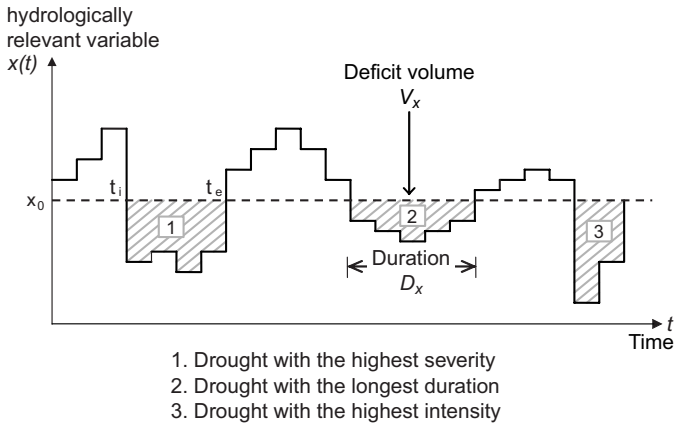

Figure 2 Drought characteristics (modified after MISHRA and SINGH (2010)).

Another frequently used metric for the characterization and classification of regional meteorological droughts is the Palmer drought severity index (PDSI, PALMER, 1965). Since the PDSI is calculated solely from mean-monthly precipitation, air temperature and the local available water content of the soil, it is used as an indicator for hydrological droughts in this study. Similarly to the soil-water balance models for GR estimation, precipitation was corrected for the snow water equivalent based on the procedure described in Walter et al. (2005) and a field capacity value of 0.34 was used. Calculations were carried out with the Matlab® code provided by Jacobi et al. (2013). PDSI-values between -0.5 and 0.5 represent moisture conditions near normal, whereas values below -4 and above 4 indicate severe drought or very wet conditions, respectively (ALLEY, 1984).

For the ongoing analysis, daily GR estimates were aggregated to monthly and annual sums to reduce the strong temporal variability, that is often inherent in daily time series, and to allow for the precise discretization of dry periods (TALLAKSEN et al., 1997).

I - 3 RESULTS

I - 3.1 Comparison of annual GR estimates

In order to capture the inter-annual variability of the GR signal, the comparison of methods is first carried out on an annual basis. This is also in line with previous long-term water budget studies and large-scale applications (e.g., ALLEN et al., 2010a; KEESE et al., 2005; SCANLON et al., 2006). Except for the lysimeter, all GR estimation methods were applied with uncalibrated (literature and field-based data) and calibrated (against lysimeter data, marked with "*") parameter sets to provide a more robust analysis of the performance and to minimize the uncertainty originating from the field-based parameter values. The methods are compared against lysimeter data by means of model error (*ME*), Pearson's correlation coefficients (*PCC*, PEARSON, 1895) and Nash-Sutcliffe efficiency (*NSE*, NASH and SUTCLIFFE, 1970). Using lysimeter data as reference GR allows for an objective evaluation of the concepts inherent in the GR estimation methods.

Estimated yearly GR and model performance criteria are shown in Figure 3 and Table 1, respectively. For the lysimeter, estimated median GR (1037mm) accounts for around 71 % of median precipitation (1470mm). The uncalibrated models simulate a considerably large variability of yearly GR rates with median values between 663 mm a^{-1} (FINCH) and 1178 mm a^{-1} (WTF). In contrast, the yearly GR rates obtained with the calibrated methods vary less. Here, median yearly GR varied from 816 mm a^{-1} (FINCH*) to 1013 mm a^{-1} (HYDRUS*, Figure 3). The median values and lower ranges of the SWB/SWB* and HYDRUS/HYDRUS* boxplots compare very closely to the lysimeter data with and without adapted parameter values.

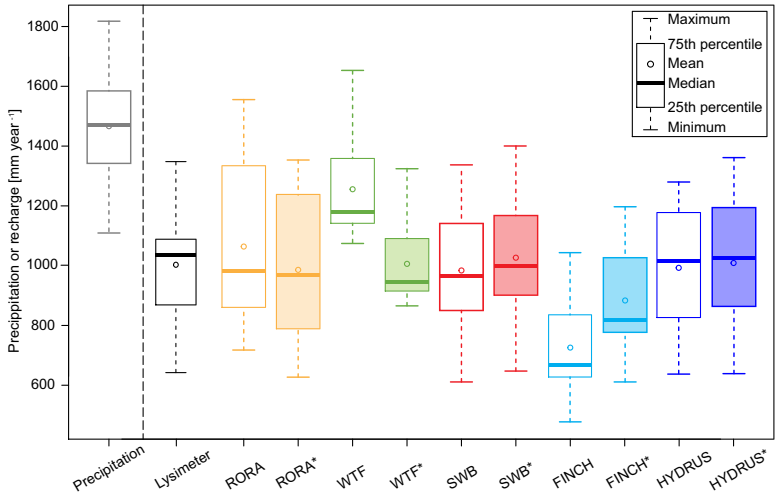

Figure 3 (a) Boxplots of annual sums of snow water equivalent (SWE), observed and simulated groundwater recharge for the observation period 2000-2012; (b) Mean annual sums of lysimeter seepage (grey bars) and groundwater recharge estimates (colored lines) based on daily data for the observation period 2000-2012, plotted on the left-hand axis. The right-hand axis shows values of annual mean sums of SWE (solid grey line) and the long-term average of SWE (dashed grey line).

Table 1 Yearly sums of lysimeter seepage and model performance criteria (model error, Pearson's correlation coefficient (PCC), Nash-Sutcliffe efficiency (NSE)) of yearly GR estimates relative to observed lysimeter data. Calibrated GR estimation methods are marked with a ""-sign.*

Year	Model error [%]									
	RORA	RORA*	WTF	WTF*	SWB	SWB*	FINCH	FINCH*	HYDRUS	HYDRUS*
2000	-31.2	-37.1	1.7	-18.5	-11.5	-8.3	-39.2	-25.4	-6.9	-5.9
2001	-27.4	-28.3	9.2	-12.5	-0.9	3.8	-23	-11.3	-5.2	0.9
2002	-20	-16.3	-8.1	-26.4	-16.6	-14.1	-32.7	-21.5	-14.3	-15.5
2003	14.1	4.3	67.8	34.4	-5.8	0.3	-26.1	-5.4	-1.3	-1.1
2004	15.2	14.7	43.9	15.3	-4.3	1.3	-25.5	-8.3	-2.5	2.1
2005	18	8.4	43.3	14.8	-7	-0.9	-33.4	-15	2.3	-1.2
2006	-4.5	-16.6	13.9	-8.7	6.6	12.2	-19.1	-0.5	3.8	2
2007	23.8	14.2	51.7	21.6	12.5	16.9	-14.3	0.6	13	14.1
2008	46.3	26.8	8.5	-13	-11.5	-6.3	-40.3	-23.5	-13	-13.1
2009	53.4	36.2	35.6	8.7	-2.2	3.2	-28.2	-10.9	-5.2	-0.9
2010	32.6	21.8	32.3	6	8.4	10.9	-22.6	-8.1	11.9	13.4
2011	8.2	-5.4	62.8	30.5	15.5	21.1	-28.3	-4	10.6	17.6
2012	-17.3	-24.5	16.9	-6.3	-1.9	-0.7	-30.6	-15.3	1	3.8
Mean	8.5	-0.1	29.2	3.5	-1.4	3	-27.9	-11.5	-0.4	1.2
PCC	0.37	0.5	0.6	0.6	0.9	0.9	0.9	0.9	0.91	0.9
NSE	-0.55	-0.08	-0.82	0.36	0.8	0.79	-0.68	0.53	0.83	0.8

The inter-annual comparison of the methods in Figure 4 reveals a large climatic variability during the observation period that caused a wide range of yearly GR rates. A graphical evaluation of Figure 4 shows that the different GR estimation methods were capable of reproducing the alternations of wet and dry seasons. All methods estimated the highest GR in 2001/2002, 2007 and 2010, which relates well to the time series of precipitation in Figure 4.

Overall, deviations from the lysimeter data were smallest for the uncalibrated and calibrated SWB/SWB*, FINCH* and HYDRUS/HYDRUS* models. The WTF method consistently overestimated GR in all years after 2002, but the performance of improved considerably when the WTF*-method was applied with a smaller σ_y-value (e.g., mean ME reduced from 29.2% to 3.5%). Although the uncalibrated RORA model simulates a similar median annual GR as the lysimeter, it exhibits a strong tendency towards higher GR. For the calibrated RORA* model, Table 1 indicates an improvement mainly for the years 2007-2010, however, GR is still overestimated for the remaining years. The poorer performance of WTF method and the RORA model compared to the remaining methods can largely be related to the underlying assumptions as will be discussed further below.

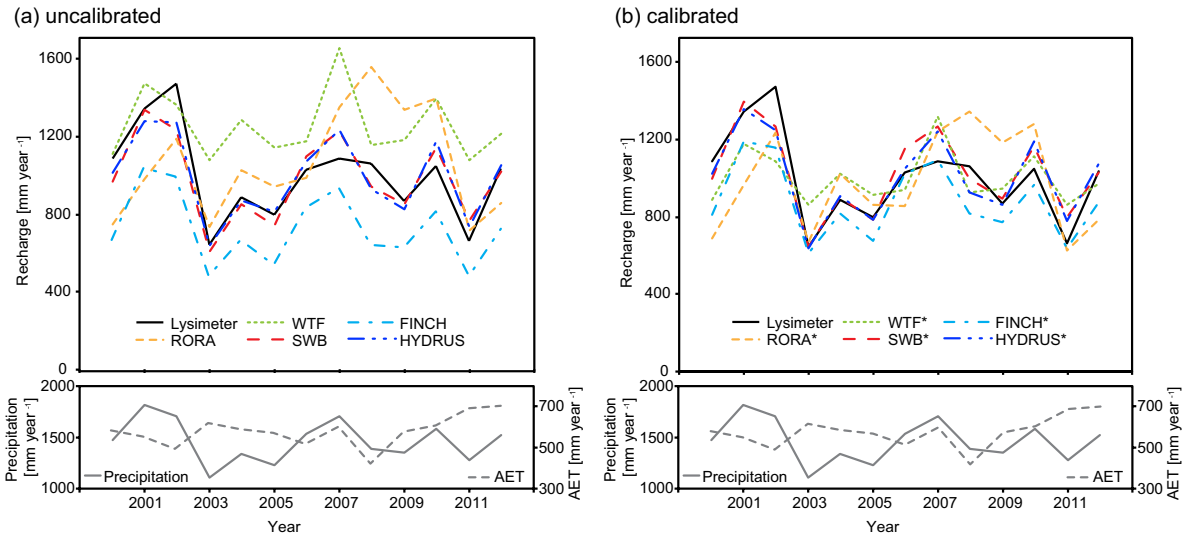

Figure 4 Yearly GR estimates (lysimeter: black, RORA: orange, WTF: green, SWB: red, FINCH: light blue, HYDRUS: dark blue) for the observation period 2000-2012 with GR-values on the left-hand axis. The right-hand axis shows values of yearly precipitation (solid grey line) and the long-term average of precipitation (dashed grey line). (a) GR estimation methods with uncalibrated model parameters, (b) GR estimation methods with calibrated parameters ("").*

I - 3.2 Comparison of monthly recharge estimates

To systematically evaluate the ability of the GR estimation methods to capture monthly and seasonal variability, the six GR estimation methods were compared on a monthly basis. Figure 5 depicts mean-monthly GR estimates from the lysimeter, as well as from the uncalibrated and calibrated (*) methods. The lysimeter data indicate a distinct seasonality in the GR signal with highest recharge rates in spring and autumn, which can be related to the occurrence of snowmelt around March as well as decreasing temperatures and AET around September, respectively (grey lines in Figure 5). GR is generally reduced in summer due to higher temperatures and AET-rates between May-August.

It can be seen that the observed seasonal pattern was captured by most methods. However, Figure 5a shows that the uncalibrated models cover a much wider range of mean-monthly GR, with values up to 67 % larger (WTF) and 48 % smaller (FINCH) than the lysimeter data (Table 2). From the uncalibrated GR estimation methods, the SWB model performed best relative to the lysimeter ($NSE = 0.48$, mean $ME = 0\%$). After calibration, GR was more overestimated between May-July, however, no overall improvement of the SWB* model suggests that the initial parameter set already reflects natural conditions adequately. The RORA/RORA* model and the WTF/WTF* method estimated a more damped mean-monthly GR signal between July and November compared to the other methods, which results in an overestimation of GR in the dry season (May-August, Figure 5). In addition, both methods simulated an increase of GR between January and February, while the remaining methods indicate a drop in GR. The calibrated RORA* model performed slightly better when the calibrated recession index K is used (Table 2). The performance of the calibrated WTF* method improved from January to August. However, the linear relationship between σ_y and

GR also worsened the performance from September to November, when GR was underestimated by up to 35 %.

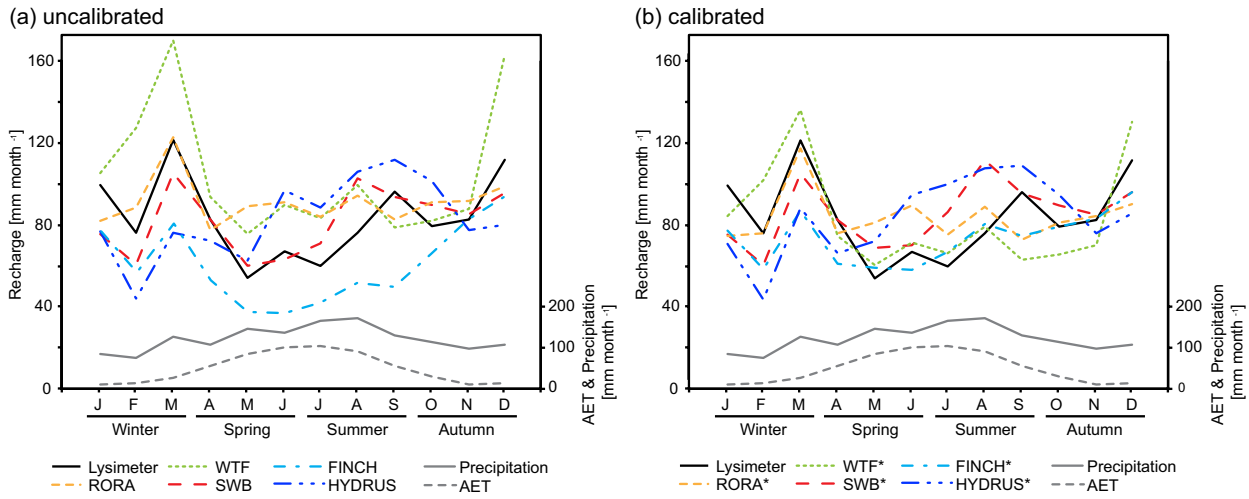

Figure 5 Mean-monthly GR estimates (lysimeter: black, RORA: orange, WTF: green, SWB: red, FINCH: light blue, HYDRUS: dark blue) for the observation period 2000-2012 with GR-values on the left-hand axis. The right-hand axis shows values of mean-monthly actual evapotranspiration (AET, dashed grey line) and mean-monthly precipitation (solid grey line). (a) GR estimation methods with uncalibrated model parameters, (b) GR estimation methods with calibrated parameters ("").*

The precipitation-driven models SWB-, FINCH- and HYDRUS underestimated GR in winter by more than 13 %, even after calibration (Table 2). The largest differences to lysimeter data were found for the HYDRUS* model (up to 43 % in February). In addition, HYDRUS/HYDRUS* estimated the highest GR rates between June and September, which was not indicated by any other GR estimation method.

Table 2 Mean-monthly sums of lysimeter seepage and model performance criteria (model error, Pearson's correlation coefficient (PCC), Nash-Sutcliffe efficiency (NSE)) of mean-monthly GR estimates relative to observed lysimeter data for the observation period 2000-2012. Calibrated GR estimation methods are marked with a ""-sign.*

Month	*ME* for mean-monthly GR estimates [%]									
	RORA	RORA*	GTF	GTF*	SWB	SWB*	FINCH	FINCH*	HYDRUS	HYDRUS*
January	-17.3	-24.5	6.1	-15	-23.9	-23.9	-22.8	-22	-22.7	-28.7
February	16.3	-0.5	67.3	34.1	-20.9	-20.9	-25.7	-23.5	-42.4	-42.8
March	0.9	-3.4	40	12.2	-13.4	-13.4	-33.6	-28.2	-37.3	-27.5
April	-6	-7.7	13.5	-9	0.1	0.1	-35.9	-25.7	-12.3	-19.5
May	65.6	51.1	40.6	12.7	11.6	28.1	-31.4	9.6	15.9	33.8
June	35.7	34	33.6	7.1	-5.6	4.8	-45.5	-13.2	44.4	41.7
July	40.5	26.9	39.4	11.7	19	45.1	-29.7	12.2	48.1	67.5
August	23.8	17	30	4.1	34.8	46.3	-33	5.3	38.4	41
September	-14.3	-24.2	-18.5	-34.7	-2.8	-0.8	-48.4	-21.9	16.4	13.7
October	15	2.5	3.2	-17.3	12.8	13.4	-17	0.4	28.1	20.1
November	11.3	2.8	6.3	-14.8	3.2	3.2	0	1.2	-6.4	-8
December	-11.9	-19.4	45.8	16.8	-14.6	-14.2	-16.4	-13.8	-28.2	-23.5

	RORA	RORA*	GTF	GTF*	SWB	SWB*	FINCH	FINCH*	HYDRUS	HYDRUS*
Mean *ME* [%]	13.3	4.5	25.6	0.7	0	5.6	-28.3	-10	3.5	5.7
PCC	0.55	0.51	0.76	0.76	0.7	0.51	0.8	0.75	0.06	0.05
NSE	0.16	0.25	-1.26	0.31	0.48	0.19	-0.84	0.27	-0.8	-0.8
For monthly GR estimates [%]										
Mean *ME* [%]	66.3	45.3	39.7	11.9	10.3	32	-28.7	7.1	37.7	33
PCC	0.69	0.75	0.81	0.81	0.89	0.87	0.9	0.9	0.76	0.81
NSE	0.45	0.55	0.37	0.63	0.78	0.74	0.65	0.78	0.56	0.63

I - 3.3 Comparison of drought characteristics

In shallow groundwater systems, such as in the URHB, a reduction of GR rates during dry climatic conditions can have a strong impact on water resources and the streamflow regime. Therefore, GR estimation methods should be analyzed with respect to both, mean and extreme climatic conditions to allow for an accurate assessment of their performance. Here, we focus on severe dry periods and apply drought characteristics and the Palmer drought severity index (PDSI). Because most studies of drought characteristics employ data at monthly temporal resolution, the same time scale was used here. This is also consistent with the optimal time scales of the RORA model (RUTLEDGE, 2002) and the PDSI (HEIM, 2002).

I - 3.3.1 Drought deficit and duration

Figure 6 presents cumulative probability plots (*cpp*) of the drought deficit volumes (V_x) for the respective time series *x(t)* (precipitation and GR estimates from uncalibrated and calibrated methods). Here, deficit volumes for each month (mm month^{-1}, Figure 6a, b) and the whole event (mm event^{-1}, Figure 6c, d) are shown. Table 3 lists the largest deficit volumes as well as the durations of dry periods for all GR estimation methods.

The *cpp* of $V_{precipitation}$ indicates many short dry periods with large deficit volumes of up to 63 mm month^{-1} and 76 mm event^{-1} (February-March 2012) that are caused by the distinct short-term variability of precipitation- or snowmelt events. Compared to this, the GR estimates indicate a more dampened response resulting in more steep *cpp*'s and generally smaller deficit volumes than for precipitation. However, for the lysimeter similarly high values were reached during the most severe dry periods (e.g., $V_{lysimeter}$ = 86 mm event^{-1} in June - September 2003), while the maximum monthly deficit volume was considerably smaller (Table 3). The deficit volumes of the GR estimation methods WTF, RORA and HYDRUS with uncalibrated model parameters exhibit a large scatter and relate more to the *cpp* of $V_{precipitation}$ (Figure 6a, c). The uncalibrated WTF-method resulted in the highest number of dry periods (24 events) with a tendency towards more severe events similar to precipitation. This behavior could only partly be improved with a calibrated σ_y.-value, mainly for the larger deficit volumes (Figure 6d). The uncalibrated RORA- and HYDRUS models exhibit very similar *cpp*'s and mostly overestimated the deficit volumes relative to the lysimeter. After calibration, the performance of both methods improves considerably, although the HYDRUS* model is the only method

that captured the most severe dry event as measured by the lysimeter (83 mm event^{-1}, Table 3). The steep slope of the *cpp* of V_{FINCH} indicates a distinct underestimation of the deficit volumes, which is caused by the overall small GR estimates obtained with the uncalibrated model parameters (Figure 6). Even after calibration, the more severe events (> 20 mm event^{-1}) were not captured by the FINCH* model. The SWB model best reproduced the *cpp* of the lysimeter, particularly for smaller dry periods (< 20 mm event^{-1}). However, like the FINCH model the uncalibrated SWB model slightly underestimated the most severe dry periods.

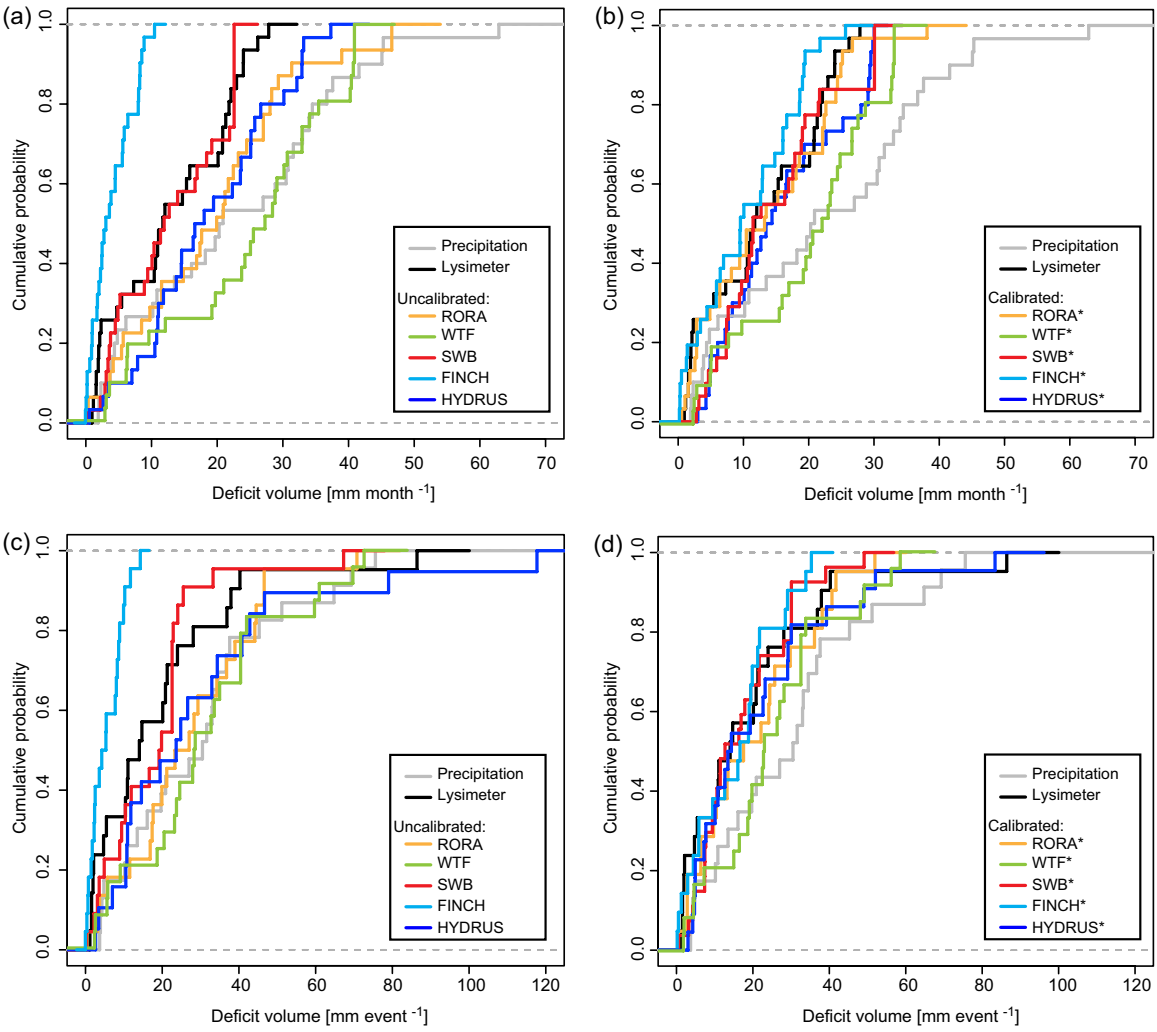

Figure 6 Cumulative distribution plots of deficit volumes of dry period for the six GR estimation methods and precipitation. The line colors and GR estimation methods are: lysimeter: black, RORA: orange, WTF: green, SWB: red, FINCH: light blue, HYDRUS: dark blue. (a) and (b) Deficit volume per month for GR estimates with uncalibrated and calibrated ("") model parameters, respectively; (c) and (d) deficit volume per event for GR estimates with uncalibrated and calibrated ("*") model parameters, respectively. The respective threshold values and the number of events are provided in Table 3.*

Table 3 Drought characteristics for the hydrological time series precipitation and GR estimates based on monthly data.

Parameter	Precipitation	Lysimeter	RORA	RORA*	WTF	WTF*	SWB	SWB*	FINCH	FINCH*	HYDRUS	HYDRUS*
Drought threshold value [mm month^{-1}]	63.9	29.3	46.5	38.1	40.8	32.7	22.6	30.1	10.6	25.6	39.8	30
Number of dry months	30	31	31	31	31	31	31	31	31	31	30	30
Number of dry events	26	22	22	21	25	25	23	28	22	21	20	22
Largest deficit volume per year [mm year^{-1}]	134.1	88	99.1	79.9	111	89	67.3	61.8	21.3	57.5	144.3	113.4
Largest deficit volume per month [mm month^{-1}]	62.9	27.8	46.6	38.1	40.8	32.7	22.6	30.1	10.6	25.6	37.3	30
Largest deficit volume per event [mm event^{-1}]	75.6	86.4	70.8	51.9	73.1	58.6	67.3	49.1	14.6	35.3	117.7	83.4

I - 3.3.2 Historical most severe dry periods

Finally, the GR estimation methods were compared in terms of their ability to capture the most severe dry periods between 2000 and 2012. For this, the Palmer drought severity index (PDSI) was used as additional reference for historical drought durations and severity. Around 47 % of the time the PDSI simulated incipient to mild drought conditions (-2 < PDSI < -0.5, Figure 7). For 8 % of all months, the PDSI indicated moderate to severe drought conditions (PDSI < -2), for instance in winter when a closed snow cover and frozen soil reduces GR (e.g., December 2004, March 2005, December 2005 - January 2006). Other severe dry periods were generated through the combined effect of low precipitation- and high evapotranspiration rates in summer, having a prolonged effect on catchment storage up to late autumn (e.g., July - December 2003, September - October 2009, April 2011, Figure 7).

Figure 8 depicts the drought characteristics (V_x in mm a^{-1}, D_x in months) of dry periods for precipitation and all GR estimates based on monthly data. Because V_x differed considerably among the hydrological variables, normalized values of V_x relative to the maximum value were used in the following analysis to allow for an objective comparison of the GR estimation methods. The individual maximum values are provided in Table 3.

The lysimeter data agree well with the PDSI and rank 2003 the year with the most severe dry period (Figure 8b). For precipitation, however, the deficit volume of 2003 is ranked only 5th indicating that high air temperature and AET were the dominant drivers for this event. In fact, the heat wave in 2003, which also affected large parts of Europe, was driven by extremely hot and dry meteorological conditions in summer (BADER, 2004; SCHÄR and JENDRITZKY, 2004). Except for the WTF method, all other models ranked 2003 the 1st or 2nd

most severe dry year and estimated durations between 4 - 5 months, which are in the same range as the lysimeter data (5 months). With the WTF/WTF* method, the dry period in 2003 was only 3 months long, and therefore the drought deficit was relatively small.

The year 2009 was ranked 2nd relative to the deficit volume based on lysimeter data. Similarly, all GR estimation methods except for the RORA/RORA* model estimated periods with large GR deficits during 3 - 5 months. The GR estimates from the RORA/RORA* model seemed unaffected by the dry climatic conditions in 2009. Instead, the model indicated the 3rd most severe dry period in 2001 (Figure 8c, d). Also the WTF/WTF* method shows an elevated deficit volume in 2001, although here this year was ranked only 5th (Figure 8e, f).

The dry period in 2011 was characterized by very low rainfall rates, particularly during spring and autumn (Figure 8a, Figure SI- 1, METEOSWISS, 2011). This resulted in the 3rd most severe dry period based on lysimeter data. Most GR estimation methods ranked this year 1st or 2nd (e.g. RORA*, WTF/WTF*, FINCH and HYDRUS/HYDRUS*), however, with similar durations as the lysimeter (5 months). For 2011, the calibrated SWB* model related most closely to the lysimeter with respect to the normalized deficit volume, but underestimated the duration by one month.

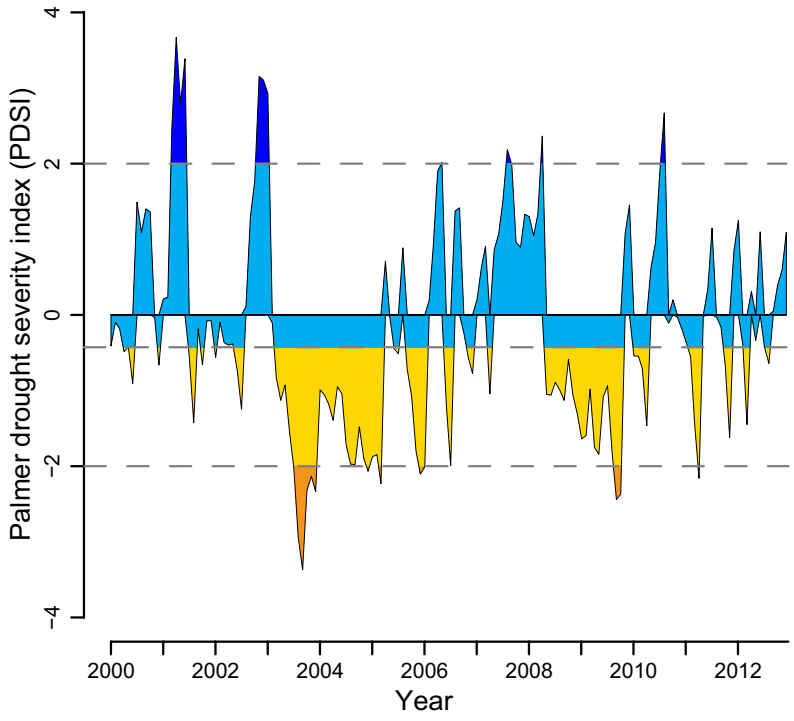

Figure 7 Palmer drought severity index (PDSI) for the URHB, 2000-2012.

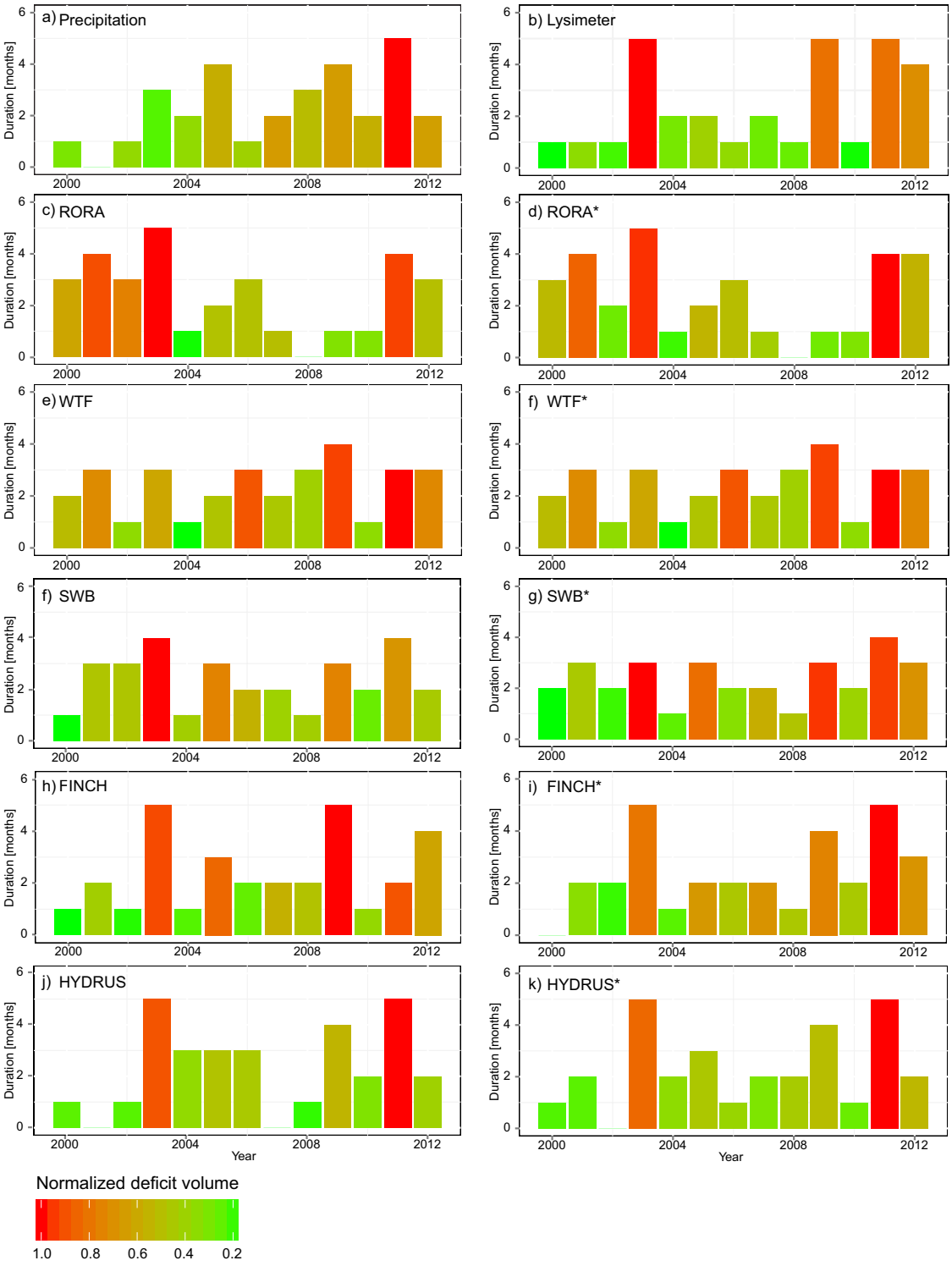

Figure 8 Drought duration and normalized deficit volumes for all GR estimation methods for each year of the observation period based on monthly data. The length of the bar indicates the number of dry periods (months) per year. The color scale represents the severity of the droughts per year, i.e. high or low deficit volumes are indicated by a reddish or greenish color, respectively.

I - 4 STRENGTHS AND LIMITATIONS OF THE GR ESTIMATION METHODS

In the following section the limitations and strengths of the six GR estimation methods are discussed to develop some broad guidelines that may assist in identifying appropriate techniques for future GR studies. The systematic comparison of lysimeter data with the GR estimation methods based on field- and literature data and after calibration reveals important information about physical processes, their representation in the models and potential sources of uncertainty. The main conclusions drawn from this analysis are summarized in Table 4. It incorporates the findings of the present study into the existing reviews of GR estimation methods by Healy and Scanlon (2010) and Scanlon et al. (2002).

Overall, the GR estimation methods showed a stronger consistency at annual time scales because short-term variations (e.g., precipitation events) were mainly averaged out. This results in reasonable estimates of yearly GR for most methods even without calibration, particularly as for the SWB- and the HYDRUS models. Nevertheless, the large lysimeter remains the only method allowing for direct GR measurements (SENEVIRATNE et al., 2012; YOUNG et al., 1996). For instance, mean-monthly time series of the lysimeter data indicate a distinct seasonality of the GR signal that is driven by climatic forcing and vegetation. Although this general behavior was captured by all of the remaining five GR estimation methods, there was a large variability of GR particularly between November and May (Figure 5). This is likely to be related to the alternating effects of frozen soil and snow cover (November-February) compared to periods with snowmelt events and low AET (March-May). Thus, a realistic representation of snow accumulation and snowmelt is essential for GR-estimation methods utilizing climatic forcing functions. Despite the implementation of a process-based snowmelt model (WALTER et al., 2005), the methods SWB, FINCH and HYDRUS often underestimated snowmelt-driven GR in late winter and spring relative to the lysimeter. This can be explained with measurement uncertainties for solid precipitation of up to 60 % with the standard rain gauge at the Büel site (GURTZ et al., 2003a). This explanation is supported further by the good performance of the RORA model and the WTF method during these seasons. Their application does not require climatic forcing functions and so these methods already indirectly account for snow accumulation and snowmelt-driven GR. Consequently, these methods are likely to provide more reliable GR estimates at snowmelt-dominated catchments.

Furthermore, to be consistent with most GR studies where no AET measurements are available for model calibration, we did not consider the observed AET data from the lysimeter in the model calibration process. This procedure, however, might introduce an additional source of uncertainty and model bias. For instance, a comparison of monthly sums of AET from the lysimeter versus the model reveals a strong linear correlation for the SWB model (slope = 0.86, R^2 = 0.84, *NSE* = 0.82, respectively). In contrast to this, the performance in terms of AET is less good for the HYDRUS* model (slope = 0.49, R^2 = 0.39, *NSE* = 0.23), because it underestimated AET particularly in summer. This indicates that the calibrated model parameters in HYDRUS* try to compensate the misfit of snowmelt-fed GR during winter and spring, which is caused by uncertain precipitation measurements and snow-melt

calculations. As a result, satisfactory GR rates can still be obtained for annual time scales, although the differences between lysimeter and HYDRUS* model data are much larger for seasonal time scales (Table 1, Table 2).

The very similar behavior of the mean-monthly GR estimates from the RORA and WTF methods between January-February and July-November was not reflected by the lysimeter data (Figure 5). This suggests that a reduction of GR-rates due to evapotranspiration is more pronounced in the upper soil profile at the Büel site (i.e., lysimeter soil column) than at the catchment scale. The analysis of drought characteristics of both RORA and WTF methods indicates that they represent a more integrative measure of GR since they are based solely on river streamflow and groundwater table data, where the involved hydro(geo)logical processes capture larger spatio-temporal scales than the lysimeter. Because of the hilly topography and the geological properties of the experimental catchment it seems likely that river streamflow and the near-stream aquifer are fed by groundwater storages further uphill. This is in line with the conceptual model presented in von Freyberg et al. (2014), where catchment hydrology is controlled by two separate groundwater aquifers that are formed by the fractured bedrock (Upper Freshwater Molasse, UFM) and the unconsolidated moraine deposits in the valley bottom. An earlier study also indicated that groundwater discharge from the deep fractured-rock aquifer of the UFM contributes around 50 % of river streamflow in the URHB catchment (VON FREYBERG et al., 2015). Consequently, GR estimates based on RORA and WTF are likely to incorporate the delayed and strongly dampened recharge signal from the deep, fractured aquifer at higher elevations of the URHB. Because these models capture a larger scale than the lysimeter, an objective evaluation of the modeling results with direct lysimeter measurements is difficult. Therefore, absolute values of GR estimates with the RORA and WTF should be considered with caution, particularly when the hydro(geo)logical properties of the site are unknown.

With the WTF method, for instance, significant miscalculations of GR can result from the linear relationship between σ_y and GR in Eq. (1). The results in Table 2 and Table 3 indicate that a constant σ_y-value might not be sufficient for shorter time scales (months to seasons) or in regions with large climatic variability, because antecedent moisture conditions are not considered. In addition, lateral groundwater inflow from further uphill might cause artificial variations of the water table, which cannot be linked directly to vertical GR as represented by the lysimeter. For instance, in dry periods with deep groundwater tables (around 5 m bgs in summer 2003) small fluctuations of the water table indicated the occurrence of GR (Figure 8e, f, Figure SI- 1d). This behavior could not be observed in the lysimeter, which consequently results in large differences between the calculated drought characteristics. In order to account for small groundwater table fluctuations during dry periods that are not caused by vertical GR, a transient σ_y-value would have to be used that better represents the actual storage conditions in the vadose zone (HEALY and COOK, 2002; SHAH and ROSS, 2009). There exist some analytical expressions for transient σ_y (e.g., NACHABE, 2002, DOS SANTOS JÚNIOR and YOUNGS, 1969), however, implementation of these models would obviously increase the complexity of the WTF method. Alternatively, the WTF method can be applied in combination with a soil-water balance model, as proposed by Sophocleous (1991). Over longer time scales (years) and during average climatic conditions, reasonable

results still can be obtained with the WTF method and a constant σ_y-value as demonstrated in this study.

For the RORA model, small differences between the GR estimates based on uncalibrated and calibrated *K* suggest a low sensibility to this parameter, which was also pointed out in earlier studies (e.g., RISSER et al., 2005; RUTLEDGE, 2002). Despite the considerable uncertainty of *K*, the RORA model captured the whole range of GR rates measured with the lysimeter (Figure 3). Consequently, this method may provide a useful tool for estimating the possible range of GR at a site where only streamflow data are available. A realistic interpretation of the results, however, requires detailed knowledge of the dominant flow processes.

From the soil-water balance-based approaches, the SWB/SWB* model showed the better results at annual time scales but was outperformed by the calibrated, more complex FINCH* model at monthly temporal resolution. The strong underestimation of GR with the uncalibrated FINCH model is mainly related to a higher bypass-flow threshold compared to the calibrated value (Table SI- 2). When the threshold value is small, water percolates faster through the soil column and less water is lost because of evapotranspiration (FINCH, 1998). Thus, application of the FINCH model with literature- and field-based parameters can results in significant bias of the GR estimates that are difficult to identify when no reference measurements are available.

Table 4 Evaluation of six established GR estimation methods

GR estimation method	Com-plexity	Governing equations	Model parameters	Required data sets	Time scales	Spatial scales (order of magnitude)	Strengths	Limitations	Sources of uncertainty
Large lysimeter	+++	Experimental approach			Minutes -years	10^{-1} m^2	• Direct measurement of vertical GR at high temporal resolution	• Only representative at the plot scale • Only vertical flux • Expensive and high maintenance requirements	• Preferential flow along the inner lysimeter wall or soil cracks • No estimates of lateral flow
RORA	+	Recession-curve displacement method	1	River streamflow	Months -years	≥ 10^4 m^2	• Simple and easy of use • No assumptions made regarding flow pathways • Indirectly incorporates effects of snow cover and -melt	• Not applicable in un-gauged catchments or catchment with flood-control features or reservoirs • No predictions possible	• Conceptual model has to be known for correct interpretation of results
WTF	+	Linear change in hydraulic head	1 (σ_y)	Groundwater table	Days -years	1 – 10^3 m^2	• Simple and easy of use • No assumptions made regarding flow pathways • Indirectly incorporates effects of snow cover and -melt	• Not applicable for confined aquifers and deep groundwater tables • Measurements from singe well might not be representative • Cannot account for steady GR • No predictions possible	• Proper estimation of specific yield can be difficult • Water table rise due to other factors (ET, barometric pressure, pumping etc.)

GR estimation method	Com-plexity	Governing equations	Model para-meters	Required data sets	Time scales	Spatial scales (order of magnitude)	Strengths	Limitations	Sources of uncertainty
SWB	++	Soil water balance equations	3	Precipitation PET	Days - years	$1 – 10^3$ m^2	• Simple and easy of use • Only few effective parameters describe subsurface properties • Allows prediction of GR	• Does not account for surface runoff • Only vertical flow • Some parameters have no physical meaning • Requires measurements or literature values for parameter calibration	• Representation of snow cover and – melt
FINCH	+++	Soil water balance equations	9	Precipitation PET	Days - years	$1 – 10^3$ m^2	• Only few effective parameters describe subsurface properties • Incorporation of plant-water uptake and bypass flow	• Some parameters have no physical meaning • Requires measurements or literature values for parameter calibration	• Representation of snow cover and – melt
HYDRUS	+++	Non-linear physically-based	5	Precipitation PET	Days - years	$1 – 10^4$ m^2	• Allows prediction of GR • Physically-based parameters describe subsurface properties • Allows prediction of GR	• Only vertical flow • Requires measurements or literature values for parameter calibration	• Representation of snow cover and – melt

I - 5 SUMMARY AND CONCLUSIONS

The objective of this part of the thesis was to identify and discuss strengths and limitations of six frequently used GR estimation techniques (large lysimeter, RORA model, WTF method, soil-water balance models, physical based model) that vary in terms of the underlying concepts, complexity and input variables. For this, a 13-year time series of hydroclimatic data from the upper Rietholzbach research catchment was used. The (relative) performance of the GR estimation methods was systematically assessed with different evaluation metrics for various time scales and climatic conditions. From the major inconsistencies between the methods we gained new insights on the hydro(geo)logical functioning of the catchment and the processes driving GR. The major conclusions from the comparison of methods applied in this study are listed below.

- Different model complexities lead to inconsistencies in estimated GR. Because actual GR is unknown, data from a large lysimeter were used as a reference. By comparing GR from lysimeter data and modeling results, we found that the physically-based HYDRUS model and the soil-water balance model FINCH performed best during monthly time scales. Improved model performance can be observed for the more simplistic approaches (SWB, RORA, WTF) at mean-monthly and annual time scales.

- The uncertainty introduced by using field and literature data as initial model parameters can be significant for both simplistic (e.g., WTF) and complex (e.g., FINCH) GR estimation methods. Nevertheless, all uncalibrated models sufficiently captured the inter-annual and seasonal range of GR variability. A comparison of GR estimates from at least two methods, which employ different input variables, is thus strongly recommended.

- The high uncertainties of snow measurements and the representation of snowmelt in physically based and soil-water balance models (e.g., SWB, FINCH, HYDRUS) might introduce significant model bias. In this case, the additional use of another GR estimation method, which is independent of climatic forcing functions (e.g., RORA, WTF), should be considered to quantify the potential variability of GR.

- GR estimation methods based on river streamflow (RORA) and groundwater table data (WTF) employ integrated signals of hydrological processes and thus allow for an evaluation of GR at larger spatial scales. A correct interpretation of the results requires knowledge about the dominant hydro(geo-)logical properties of the catchment because a direct evaluation with detailed GR observations at the plot scale (e.g., lysimeter data) is often not possible.

The findings of this study provide some broad guidelines on where and at what spatio-temporal scales the discussed GR estimation methods are best applicable. Therefore, it offers valuable information for other studies where no lysimeter facilitates the objective assessment of modeling results. In addition, the systematic comparison of methods gave insight into the hydro(geo)logic processes taking place at the studied catchment.

SUPPLEMENTARY INFORMATION OF PART I

Table SI- 1 Instrumentation and measured variables at the Büel site in the Upper Rietholzbach catchment (URHB)

Variable	Symbol (unit)	Instrument	Data gaps	Interpolation method
Actual evapotranspiration	AET (mm d^{-1})	Weighting lysimeter, depth = 2.5 m, diameter = 2.0 m	-	Negative ET-values were proportionally corrected with positive ET-values to fit average daily ET; all ET-values were set to zero when daily $\|\Sigma neg\| > \Sigma pos$; only negative ET-values were set to zero when $5x\|\Sigma neg\| < \Sigma pos$;
Air temperature	T (°C)	Meteolabor 'Thygan VTP6', 2m above ground	-	-
Groundwater table depth	GW (m bsf.)	OTT 'PS1', steel pressure cell	11 - 21 Dec 2006, 30 Dec 2006 - 9 Feb 2007, 25-26 Feb 2007, 4 - 10 Mar 2007, 3 Sep -9 Oct 2008, 2 Nov-14 Dec 2008	Trends were removed from data between Jan 2000 - Dec 2006, interpolation of data gaps ≤ 7 days with linear regression
Long-wave incoming radiation	LDA1 (W m^{-2})	Kipp & Zonen 'Pyrgeometer CG4', ventilated, heated	-	-
Long-wave outgoing radiation	LUA1 (W m^{-2})	Kipp & Zonen 'Pyrgeometer CG4', ventilated, heated	-	-
Lysimeter seepage	L (mm)	Weighting lysimeter, depth = 2.5 m, diameter = 2.0 m	-	-
Precipitation	P (mm)	Lambrecht '1518-H3', heated tipping bucket 1.5 m above the ground	-	Unrealistic high P values between 2 Dec 2011 and 10 Jan 2012 due to snow accumulation in the rain gauge were replaced by linearly interpolated P values from the nearby weather station 'Hörnli' No. 2705 (Federal Office of Meteorology and Climatology, MeteoSwiss)
River streamflow Upper Rietholzbach	Q (mm d^{-1})	OTT 'ODS4', ceramic pressure cell	01 Jan - 3 Apr 2000, 24 Sep 2002, 3 - 6 Aug 2003, 9 - 12 Aug 2007, 4 Sep - 10 Oct 2007, 7 - 13 Jul 2008, 2 Sep - 9 Oct 2008, 27 Nov - 18 Dec 2008	Data gaps were interpolated with discharge data from gauging station 'Rietholzbach' No. 2414 (Federal Office of the Environment, FOEN), which show a high correlation

Variable	Symbol (unit)	Instrument	Data gaps	Interpolation method
Short-wave incoming radiation	SDA1 (W m^{-2})	Kipp & Zonen 'Pyranometer CM21', ventilated, heated	-	-
Short-wave outgoing radiation	SUA1 (W m^{-2})	Kipp & Zonen 'Pyranometer CM21', ventilated, heated	-	-
Sunshine duration	SD (d)	Meteoservis 'SD4'	Measurements started 19 Dec 2011	Data before 19 Dec 2001 were used from the meteorological station 'Hörnli' No. 2705 (Federal Office of Meteorology and Climatology, MeteoSwiss)
Relative humidity	RH (%)	2000-2005: Meteolabor 'Thygan VTP6', 2m above ground	-	-
		2006-2012: ROTRONIC 'HC2-S3', 2m above ground	-	-
Wind speed	W (m s^{-1})	Young '05103'	-	-

Table SI- 2 Field- and literature-based as well as calibrated model parameters for the GR estimation methods

Method	Parameter name	Initial parameter	Calibrated parameter	References for initial parameters
RORA program (RORA) (RUTLEDGE and DANIEL, 1994; RUTLEDGE, 2007)	Recession index (K)	25.6 d	13 d	Based on site-specific observations (lysimeter seepage)
Groundwater- table fluctuation method (GTF) (HEPPNER and NIMMO, 2005)	Specific yield (σ_y)	0.075	0.0601[c]	BALDERER, 1984
Soil water balance model[a] (SWB) (RODRIGUEZ-ITURBE et al., 1999)	Soil moisture threshold	0.34	0.30	Based on Dingmann (2002) and site-specific observations (clay loam) (MITTELBACH, 2011)
	Permanent wilting point	0.16	0.23	Based on Dingmann (2002) and site-specific observations (clay loam) (MITTELBACH, 2011)
	Depth of active soil layer	300 mm	300 mm	Site-specific observations (GERMANN, 1981 and SENEVIRATNE et al., 2012)

Method	Parameter name	Initial parameter	Calibrated parameter	References for initial parameters
FINCH model[a,b] (FINCH, 1998)	Field capacity layer 1	0.34	0.31	Based on Dingmann (2002) and site-specific observation (clay loam) (MITTELBACH, 2011)
	First day (0 to 1)	1	1	
	Wilting point layer 1	0.16	0.24	Based on Dingmann (2002) and site-specific observations (clay loam) (MITTELBACH, 2011)
	Water saturation layer 1 (0.05 to 0.4)	0.5196	0.55	From ROSETTA model (SCHAAP et al., 2001) based on site-specific observations (MITTELBACH, 2011)
	Bypass-flow threshold (0 to 20 mm)	5.0 mm	0.2 mm	Reference value in Finch (1998)
	Proportion bypass flow (0 to 0.5)	0.1	0.2	Reference value in Finch (1998)
	Root proportions in layers (1 [=equal] to 5 [=most in layer 1])	5	5	Reference value in Finch (1998)
	Rooting depth (0.2 to 3 m)	1.2 m	1.2 m	Reference value for annual short vegetation in Finch (1998)
	Number of layers (1 to 10)	4	4	Based on site-specific observation (MITTELBACH, 2011)
HYDRUS-1D[a,b] (SIMUNEK and VAN GENUCHTEN, 2008)	Residual water content	0.075	0.075	All parameters from ROSETTA model (SCHAAP et al., 2001) based on site-specific observations (MITTELBACH, 2011)
	Saturated water content	0.432	0.428	
	van-Genuchten parameter (α)	0.0122 cm^{-1}	0.0027 cm^{-1}	
	van-Genuchten parameter (β)	1.442	1.54	
	Saturated hydraulic conductivity	17.91 cm d^{-1}	3.34 cm d^{-1}	

Table SI- 3 Soil properties used for initial parameters of the FINCH and HYDRUS models (data from Mittelbach (2011), hydraulic soil properties obtained with the ROSETTA model (SCHAAP et al., 2001)).

Depth (cm)			Bulk density (g cm^{-3})	Particle size distribution (%)			Texture	Organic fraction (%)	van-Genuchten parameters				
From	To	Middle		Clay	Silt	Sand			α (cm^{-1})	β (-)	Saturated hydraulic conductivity k_s (cm d^{-1})	Residual water content (-)	Saturated water content (-)
0	15	7.5	1.08	30.6	35.9	33.5	clay loam	4.7	0.0109	1.4778	56.35	0.088	0.5196
15	23	19	1.37	30.8	31	38.2	clay loam	2.5	0.0127	1.4379	12.11	0.08	0.4425
23	70	46.5	1.5	25.6	32.7	41.7	loam	1.3	0.013	1.4276	7.69	0.068	0.3981
70	120	95	1.5	26.9	34.4	38.7	loam	1.7	0.0122	1.4335	6.71	0.0703	0.4002
120	200	160	1.5	26.9	34.4	38.7	loam	2.7	0.0122	1.4335	6.71	0.0703	0.4002

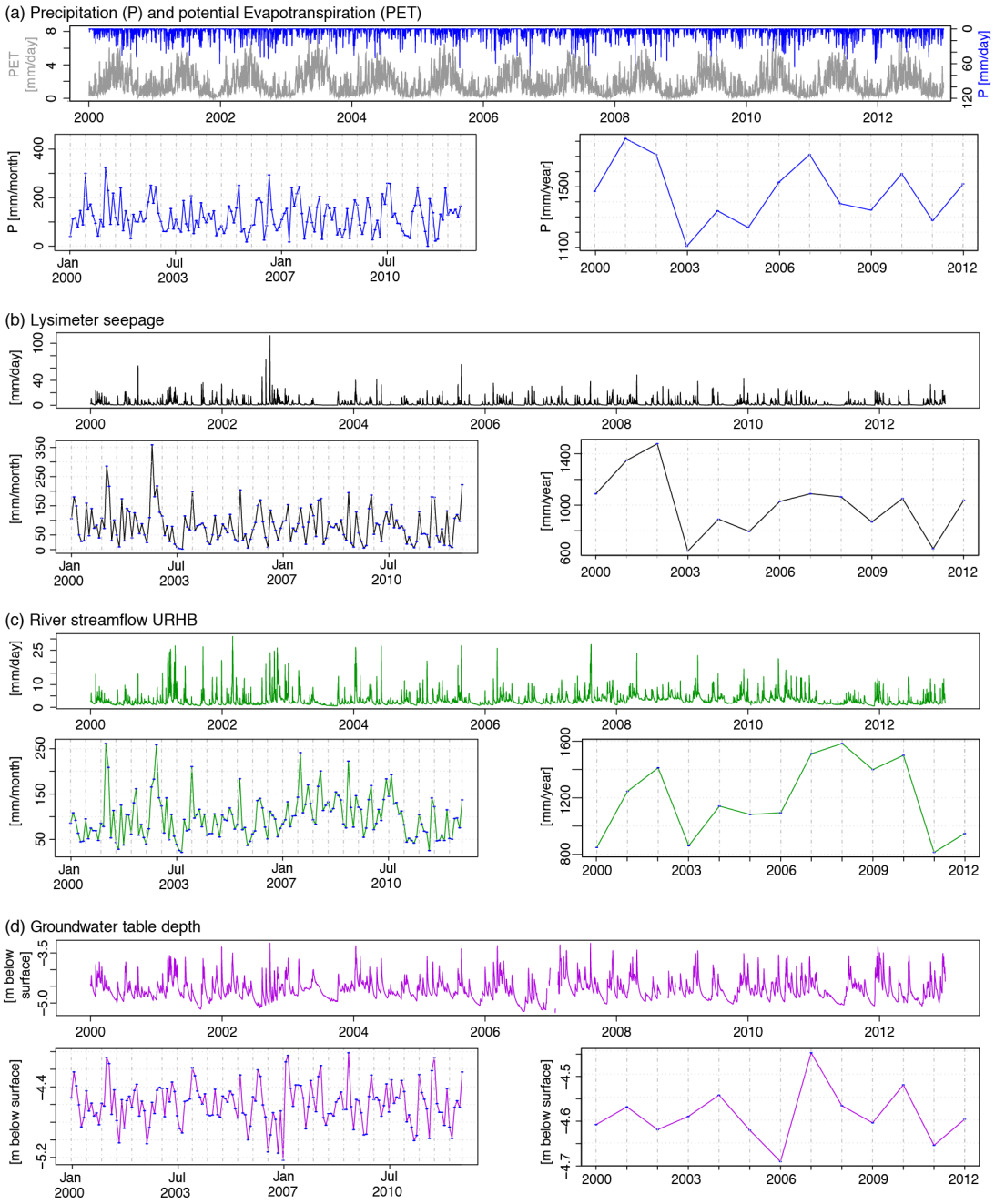

Figure SI- 1 Daily, monthly and annual data of observed values in the Upper Rietholzbach catchment (URHB) between 1 January 2000 and 31 December 2012; (a) Precipitation and potential evapotranspiration (only daily data); (b) Lysimeter seepage; (c) River streamflow measured at the outlet of the URHB; (d) Groundwater table depth at the observation well in the URHB (monthly and annual data are mean values obtained from daily data).

PART II

STREAMFLOW-GENERATING MECHANISMS AND SOLUTE TRANSPORT

Hydrological responses in mountainous headwater catchments are often highly non-linear with a distinct threshold-related behavior, which is associated to steep hillslopes, shallow soils and strong climatic variability. A holistic understanding of the dominant physical processes that control streamflow generation and non-linearity is required in order to assess potential negative effects of agricultural land use and water management in those areas. Therefore, streamflow generation in a small pre-Alpine headwater catchment (Upper Rietholzbach (URHB), ~1 km^2) was analyzed over a 2-year period by means of rainfall-response analysis and water quality data under explicit consideration of the joint behaviours of climate forcing and shallow groundwater dynamics. The runoff coefficients indicate that only a small fraction of the total catchment area (1 – 26 %) generates streamflow during rainfall events. Hereby, the valley bottom areas (riparian zones) were the most important event-water source, whereas only the lower parts of the hillslopes became hydrologically connected to the river network during higher antecedent moisture conditions. However, a distinct threshold-like behavior could not be observed, suggesting a more continuous shift from a riparian-zone to a more hillslope-dominated streamflow hydrograph. Regular manure application on the hillslopes in combination with lateral hillslope groundwater flow and long groundwater residence times in the riparian zones resulted in a higher mineralization (e.g., total phosphorous) and significant denitrification in the valley bottom area. Despite the important role of the riparian zones for event-flow generation in the URHB, their nutrient buffer capacity is expected to be small due to the low permeability of the local subsurface material. The findings of this integrated analysis are summarized in a conceptual framework describing the hydrological functioning of hillslopes and riparian zones in the URHB.

JANA VON FREYBERG, DIRK RADNY, HEATHER E. GALL, MARIO SCHIRMER (2014)
Implications of hydrologic connectivity between hillslopes and riparian zones on streamflow composition, Journal of Contaminant Hydrology, 169:62-76, doi: http://dx.doi.org/10.1016/j.jconhyd.2014.07.005.

II – 1 INTRODUCTION

Understanding the hydrologic connectivity between hillslopes and the river system as well as the dominant groundwater-flow pathways can help to assess the implications of land use on river water quality (e.g., BURT and PINAY, 2005; PRINGLE, 2003; TETZLAFF et al., 2007). Thus, long-term, seasonal or event-based monitoring of river water quality (i.e., solutes used as environmental tracers) provides valuable information about the source zones of catchment streamflow (e.g., quickflow, baseflow) and groundwater-surface water interaction processes (e.g., COOK and HERCZEG, 2000; LEIBUNDGUT and SEIBERT, 2011). Various studies found a rapid and significant increase of nutrient export rates when potential source areas become hydrologically connected to the river system during rainfall events (e.g., DOPPLER et al., 2012; OCAMPO et al., 2006; STIEGLITZ et al., 2003).

In mountainous catchments the hillslopes are often agriculturally used (e.g., pastureland, cattle grazing), which is generally accompanied with the application of fertilizers. Thus their hydraulic and hydrological connectivity with the rivers and riverine areas is inextricably linked to the mobilization and transport of solutes, such as nutrients and pollutants, to the surface waters fed by mountainous catchments (e.g., JENCSO et al., 2010; THOMPSON et al., 2012; VAN VERSEVELD et al., 2009). The flushing out and drainage of such substances from agriculturally used hillslope areas can have a negative effect on the riverine ecosystem and may harm aquatic organisms in these particularly vulnerable high-elevation environments.

Landscape properties (e.g., topography, vegetation patterns, soil type distributions) have been identified as important drivers for catchment hydrology, which makes them an appropriate tool for investigating runoff generation mechanisms at various spatial scales (MCGLYNN et al., 2004). In mountainous regions large portions of the landscape are hillslopes, which makes them the dominant landscape unit that essentially act as filter for climatic and biogeochemical responses (BACHMAIR and WEILER, 2011). Numerous hillslope and catchment-scale studies focused on the investigation of subsurface flow mechanisms and characteristic threshold responses that drive non-linear hydrological processes. Hereby, valuable information can be obtained by investigating the response dynamics of river flow, hydrochemistry and shallow groundwater tables to rainfall events. For instance, HAGA et al. (2005) found a clear shift in lag time (time between peak rainfall and peak discharge) a suitable proxy for the activation of hillslope groundwater flux towards the river system. Many of these studies proved a strong dependency of the rainfall-responses on antecedent moisture conditions (e.g., JAMES and ROULET, 2009; PENNA et al., 2011; SIDLE et al., 1995; TROMP-VAN MEERVELD and MCDONNELL, 2006c), which is a proxy for the overall degree of hydrologic connectivity among the active landscape units (e.g., hillslopes) with the river system. Generally, during "wet" conditions a larger portion of the catchment contributes to streamflow (i.e., high degree of connectivity) compared to "dry" conditions in which the hydrologically active zones are small (i.e., low degree of connectivity) (JAMES and ROULET, 2009).

Further, total rainfall and rainfall intensity (e.g., ANDERSON et al., 2009; TROMP-VAN MEERVELD and MCDONNELL, 2006c), shallow groundwater flow pathways (e.g., DETTY and

MCGUIRE, 2010; RODHE and SEIBERT, 2011; HAUGHT and MEERVELD, 2011; WIENHÖFER et al., 2009), and subsurface properties (e.g., GRAHAM et al., 2010) were found as important first-order controls on streamflow response and solute export (BURT and PINAY, 2005). In complex landscapes such as mountainous catchments, a mechanistic understanding of the hillslope groundwater re- and discharge dynamics and the interrelations between the other landscape units builds the foundation for the conceptualization of the catchment's hydrological behavior, which is relevant in the context of water quality management or flood prediction.

Thus, the rationale for the present work is to improve the mechanistic understanding of stream-landscape connectivity and to highlight possible implications on nutrient transport from agriculturally used hillslopes. For this, a small pre-Alpine headwater catchment (~ 1 km^2) in Switzerland was chosen as a case study since its hydro-climatology was shown to be representative for the wider region of the eastern Swiss Plateau (SENEVIRATNE et al., 2012). The present study investigates the hydrological functioning of this catchment with a focus on shallow groundwater variations at the hillslope-scale and its implications on nutrient export from agricultural areas. The integrated analysis is carried out by means of spatially dense and high-frequency hydrometric observations and a detailed investigation of rainfall-response dynamics.

This chapter is organized as follows: Section II - 2 provides information about the small pre-Alpine headwater catchment and experimental set-up. In section II - 3.1 a conceptual model of the dominant groundwater flow processes at the hillslope scale is derived based on hydrometric observations and rainfall-response analysis. In section II - 3.2, the analysis of streamflow-rainfall response facilitates the transfer of the conceptual model from the hillslope- to the catchment scale. Section II - 3.3 compares seasonal effects of hydro-climatic variables on river- and groundwater quality under consideration of the conceptual model. In section II - 3.4, the respective portions of streamflow-generating areas are estimated and possible implications for solute export from those landscape units are derived. The present work is critically evaluated and put into the broader context of hydrological behavior of mountainous catchments in the conclusions-section.

II - 2 MATERIALS AND METHODS

II - 2.1 Site description and Instrumentation

The Rietholzbach Research Catchment (RHB, ~ 3 km2) is a first-order watershed of the Thur river that is located in the pre-Alps in north-east Switzerland (Figure 9a). The present study focuses on the Upper Rietholzbach sub-catchment (URHB, ~ 0.94 km2) that comprises the western part of the RHB. The local climate is characterized by temperate humid conditions with a higher thunderstorm frequency in summer (METEOSWISS, 2013). The landscape is predominantly used for cattle grazing and hay production, which is associated with regular manure application. Around 19 % is forested and settlements and streets cover approximately 4 % of the catchment area.

The geology of the URHB is characterized primarily by the Tertiary Upper Freshwater Molasse (UFM, consolidated clastic sediments and layers of marls, sandstones and freshwater limestone) and quaternary moraine deposits from the Würm glacial period (QMD, unconsolidated gravel pockets). The latter is accumulated primary in the valley bottoms and the lower hillslopes, whereas the UFM-unit generates steep slopes and hilltops in the URHB (Figure 17a). Generally, shallow Regosols developed on the UFM-unit. On the hillslopes of the QMD locally several meter thick Cambisols can be found, which become Gleysols and peaty soils in the more shallow areas and in the valley bottoms (Figure 9a). Here, hydraulic conductivities are very low resulting in a limited infiltration capacity of the Gleysols and peaty soils (GERMANN, 1981).

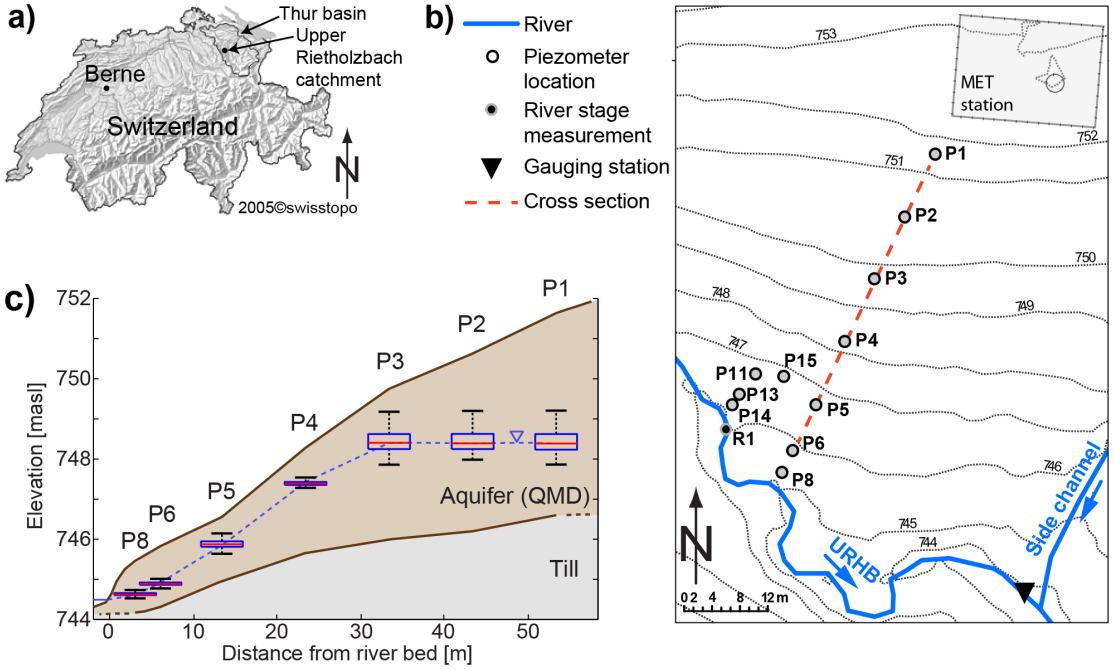

Figure 9 (a) Location of the Upper Rietholzbach sub-catchment (URHB) as part of the Thur catchment in NE Switzerland; (b) Field site Büel with meteorological (MET) station and piezometers; (c) Cross section along the piezometer transect P1 – P8 of the field site Büel in the URHB sub-catchment. Depth of the lithological units are based on electrical resistivity tomography surveys and soil core sampling. Box-plots of groundwater table variations during 1 June 2011 and 31 August 2013 along the transect P1-P8 (red line: median, box: 10th and 90th percentile, whiskers: 25th and 75th percentile).

An extensive groundwater-monitoring network (Büel site) is located on the south-facing slope in close vicinity to the outlet of the URHB (Figure 9b). Here, a dense cluster of standard 2''-groundwater observation pipes (i.e., piezometers with pipe diameter of 5.08 cm) was installed in the shallow QMD-aquifer along the hillslope and the bottom area using Direct Push Technology (*Geoprobe*®, USA). Along with piezometer installation soil cores were sampled with the Direct Push Technology in order to determine the thickness of the QMD-aquifer and to study the local soil properties. It was found that the QMD-aquifer is underlain by an impermeable till layer, which is more than 10 m thick in the valley bottom area of the Büel site. In combination with electrical resistivity tomography surveys and the soil core samplings at piezometer locations P1, P2, P3, P4 and P8 the slope of the confining till layer was linearly interpolated as shown in Figure 9c.

The piezometers at the Büel site were arranged in one long transect and three short transects and screened over the entire thickness of the aquifer (Figure 9b, Table 5). All piezometers were equipped with pressure, temperature and electrical conductivity (P-T-EC) transducers (DL/N 70, measuring interval 15 minutes, SensorTechnik Sirnach Switzerland). A P-T-EC transducer in the river (R1, Figure 9b) continuously monitored river water stage, stream temperature and EC (DL/N 70, measuring interval 15 minutes, SensorTechnik Sirnach Switzerland).

Table 5 Properties of piezometers at the Büel site in the URHB. Local slopes were computed with the "Local Morphometry" module in the open source software SAGA GIS based on a 2 m x 2 m digital elevation model (DEM) with vertical resolution of 0.5 m (SwissALTI3D, swisstopo)

Piezometer	Distance to river bank (m)	Land surface elevation above river bed (m)	Local slope (°)	Thickness of aquifer (m)	Depth of piezometer screen below surface (m)
P1	53.3	7.0	10.5	5.0	1.2-4.2
P2	43.3	5.9	2.5	4.4	1.2-4.2
P3	33.3	5.1	9.5	3.8	1.2-3.2
P4	23.3	3.6	9.5	2.4	1.1-2.1
P5	13.3	2.0	8.5	1.9[a]	1.1-2.1
P6	5.7	1.2	5.5	1.6[a]	1.0-2.0
P8	2.9	0.8	9.0	1.5	0.7-1.7
P12	8.2	1.4	7.5	-	1.1-2.1
P13	4.7	1.0	5.0	-	1.0-2.0
P14	2.8	0.9	6.4	-	1.0-2.0

[a] Interpolated from nearby measurements

A meteorological station with a weighting lysimeter is located at the upper part of the Büel site (Figure 9b). Here, rainfall was measured hourly at a standard rain gauge at 1.5 m above ground. Actual evapotranspiration was determined directly by a weighting lysimeter (2.5 m deep, 2 m diameter) that imitates the surrounding subsurface and land use (GURTZ et al., 2003a; SENEVIRATNE et al., 2012). River discharge was monitored at a gauging station at the outlet of the URHB (Figure 9b).

River- and groundwater was sampled weekly or biweekly near the URHB-gauging station and at the piezometer locations P2 and P13 (Figure 9b). The water samples were filtered through washed 0.45 µm CN Membrane filters and analyzed for calcium (Ca^{2+}, as indicator for geogenic mineralization), chloride (Cl^-, assumed conservative and as indicator of groundwater sources), silicate (H_4SiO_4, as indicator for groundwater residence time in the shallow subsurface), nitrogen (NO^{3-}) and total phosphorous (TP). Details about the analysis method and detection limits are provided in Table SI-5.

II - 2.2 Rainfall characteristics and antecedent moisture conditions (AMC)

Figure 10 gives an overview of the calculated event features used in this study. The response time (T_{res}) is defined as the time between the first peak of the maximum 1h-rainfall intensity (PI_{max}) and the peak river discharge (Q_{max}) (HAGA et al., 2005). The time delay of groundwater level peak (GW_{max}) to peak river discharge (Q_{max}) is referred to as lag time (T_{lag}) in this study. In order to provide consistency to the analysis, the observed discharge and groundwater table data were related to the initial values Q_{ini} (discharge) and GW_{ini} (groundwater table), respectively. Hereby, the initial values were computed as the 1 h-average before the onset of rain following HAGA et al. (2005). The constant-k method described in BLUME et al. (2007) was used to determine the end of the event-flow hydrograph, for calculating the duration as well as the portion of event flow (Q_e) in the streamflow signal. This method was selected since it is fully automated and objectively identifies the point in time when the streamflow hydrograph is comprised entirely of baseflow. The mean rainfall intensity (PI) is the total event rainfall (P_{sum}) divided by the time rainfall was detected. Runoff coefficients (C_R) are defined as total event discharge (Q_e) divided by P_{sum}.

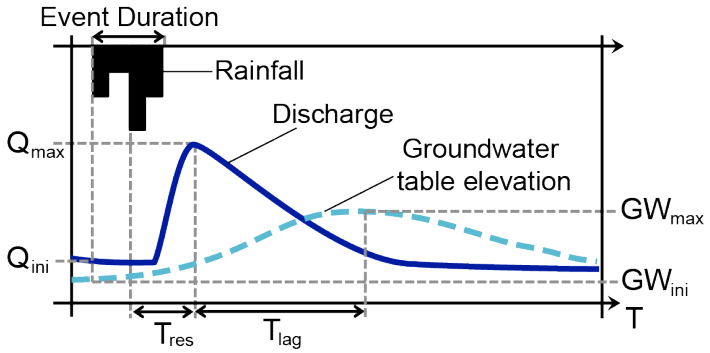

Figure 10 Schematic description of calculated event features.

Many studies name antecedent catchment moisture a controlling factor for streamflow-generation mechanisms, since it regulates the timing and amplitude of groundwater table fluctuations (e.g., HAGA et al., 2005; INAMDAR and MITCHELL, 2007; JAMES and ROULET, 2009; TROMP-VAN MEERVELD and MCDONNELL, 2006a). However, the quantitative metrics of catchment wetness state and their determination are not consistent (e.g. shallow soil moisture in DETTY and MCGUIRE (2010); PENNA et al (2011); antecedent precipitation indices in INAMDAR and MITCHELL (2007); JAMES and ROULET (2007); initial groundwater table depth in JAMES and ROULET (2009)), which hampers an objective comparison between different sites. In mountainous catchments the spatial distribution of shallow soil moisture is generally very heterogeneous with ranges of continuity of several tens of meters (JAMES and ROULET, 2009). In the URHB it can be assumed that volumetric soil moisture content, measured at the meteorological station near the Büel site is not representative of the wetness state of the entire basin. Hence, we introduced two parameters as surrogates for antecedent moisture conditions (AMC) of the entire URHB sub-catchment. Initial discharge (Q_{ini}) can be applied as AMC-proxy under the assumption that catchment outflow is an integrated signal of all hydrological and climatic processes within the basin, thus it is equivalent to changes in storage. In this context, TEULING et al. (2010) explicitly showed that storage and discharge can

be directly correlated with each other for the RHB (of which the URHB comprises the western part). The second proxy for AMC, the antecedent precipitation index (AP_7), is defined as cumulative rainfall within 7 days prior to the first detection of rainfall according to INAMDAR and MITCHELL (2007). Here, AP_7 was corrected additionally for cumulative ET in order to account for the loss of soil water during this period.

II – 2.3 Topographic analysis and groundwater flow directions

Topographic analysis on the URHB is based on a 2 m x 2 m digital elevation model (DEM) with a vertical resolution of 0.5 m (SwissALTI3D, swisstopo), which was smoothed to 5 m x 5 m in order to reduce noise and artifacts from buildings and streets. The slopes of the landscape (TARBOTON, 1997) were computed with the "Local Morphometry" module in the open source software SAGA GIS (CONRAD, 2006; BÖHNER et al., 2008). Likewise, the topographic wetness index (TWI) (BEVEN and KIRKBY, 1979), which is an established measure as a proxy for spatial shallow groundwater table distribution, was obtained by running the "Terrain Analysis – Hydrology" module of this software.

In order to investigate the spatial variability of groundwater directions at the field site, the direction of groundwater flow was calculated following the approach described by RODHE and SEIBERT (2011). Hereby, the groundwater surface is assumed a plane spanning between three piezometers. From the normal vector describing the position of this plane in the xyz-space, the direction of groundwater flow (α) of the plane can be obtained. For the following four piezometer triplets (with the triangle name in brackets) the flow direction was calculated: P3-P5-P15 (A), P6-P12-P15 (B), P8-P12-P14 (C), P6-P8-P14 (D), R1-P8-P14 (E).

II - 3 RESULTS AND DISCUSSION

II - 3.1 Groundwater flow processes at the hillslope-scale

Long-term variations of groundwater tables along the transect P1-P8 are depicted as boxplots in Figure 9c. The absolute variability of groundwater tables is largest at uphill piezometers (maximum range at P1: ~ 1.8 m) and decreases further downhill (maximum range at P8: ~ 0.5 m). In the uphill part (P1-P3), the groundwater surface forms a plateau whereas further downhill groundwater tables are more or less parallel to the land surface. This causes a thicker unsaturated zone in the uphill transect and very shallow groundwater tables on the lower slope, indicating the occurrence of near saturation at these downhill areas (i.e., at P5 and P8). It further suggests that the average groundwater tables are controlled by the surface topography of the confining till layer and the permeability of the aquifer material. Soil core sampling revealed that the slope of the confining till layer at P1, P2 and P3 is smaller than for the further downhill piezometer locations (P4-P8, Table 5, Figure 9c). Additionally, soil cores at P4 contained a clay-rich heterogeneous composition of gravel and sand between 1.6 m and 2.4 m depth. This might cause a local low-transmissivity zone above the till layer, which is indicated also by the small variability of groundwater tables at P4 (Figure 9c). Based on the

hydrometric observations and following the framework presented by SEIBERT and MCGLYNN (2005), the Büel site was divided into a hillslope section (piezometers P1-P4) and a riparian zone (piezometers P5-P8).

II – 3.1.1 The role of antecedent moisture conditions (AMC) and rainfall characteristics

In order to identify the dominant groundwater flow mechanisms at the hillslope-scale that account for streamflow generation and solute transport in the URHB, response times and groundwater table variations after rainfall events were investigated under explicit consideration of antecedent moisture conditions and rainfall properties. The following analysis is based on 31 rainfall events during the snow-free periods in 2011 and 2012 as representative examples, with their calculated characteristics summarized in Table SI-4 in the supplementary information of part II.

The rainfall responses of hillslope and riparian groundwater tables at the Büel site can be correlated to the local landscape and subsurface properties. As evident from Table SI-4 and Figure 11a, riparian zone groundwater tables increased more often than at the upper hillslope and average lag times (T_{lag}) decreased with decreasing distance from the river. For example, groundwater tables at P5 and P8 peaked on average 9.5 h before P1.

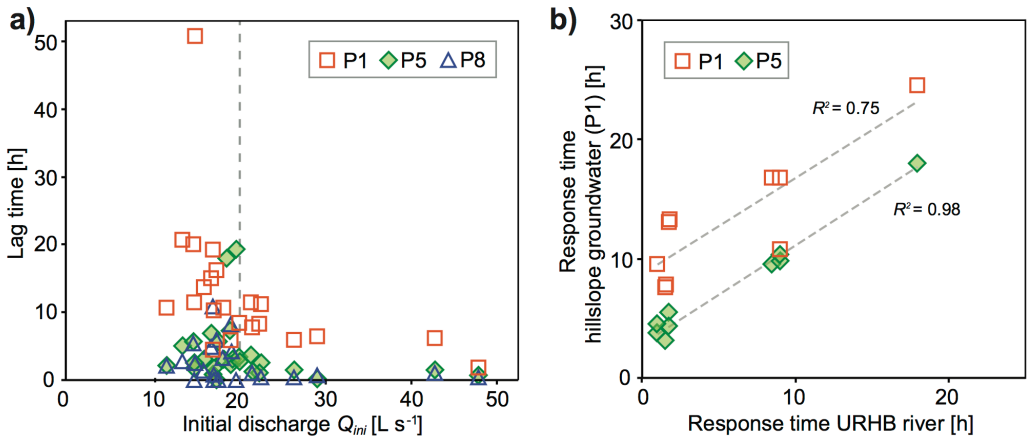

Figure 11 (a) Initial discharge versus lag times of groundwater tables at the hillslope (P1) and riparian zone (P5, P8); (b) Response times of discharge versus response times of groundwater levels at P1 and P5 for rainfall events with $Q_{ini} \geq 20$ L s^{-1}

Further, a similar pattern could be observed for the relation between groundwater table dynamics and AMC. A shift in T_{lag} was found with increasing wetness conditions, especially for initial discharge (Q_{ini}). In Figure 11a, Q_{ini} was compared with T_{lag} at the hillslope (P1) and riparian zone (P5), respectively. The threshold values of Q_{ini} = 21.5 L s^{-1} at the hillslope (P1) and 19.8 L s^{-1} at the riparian zone (P5) marked the storage conditions after which T_{lag} became significantly shorter (Figure 11a). Similar values were found for the other piezometer locations, such as 21.5 L s^{-1} at P3 and 19.2 L s^{-1} at P8. Thus, the threshold value of Q_{ini} at each location decreased the closer the piezometer was located to the stream, i.e. the shallower the groundwater table was. By only considering rainfall events with wet AMC (Q_{ini} > 20 L s^{-1}, i.e., average threshold value along the transect) the temporal variability of hillslope groundwater

tables (P1) and river discharge showed a more synchronous response, as indicated by a significant linear correlation of T_{res} and T_{lag} with a slope of around 0.8 ($R^2 = 0.74$, Figure 11b). It further shows, that groundwater at the hillslope responded on average 9 hours after river discharge. Average T_{lag} for the other piezometer locations during wet AMC ($Q_{ini} > 20$ L s^{-1}) was 3.2 h (P3, $R^2 = 0.73$), 2.6 h (P5, $R^2 = 0.98$) and 0.5 h (P8, $R^2 = 0.99$).

In contrast to Q_{ini}, rainfall in the previous 7 days (AP_7) did not significantly control the timing of groundwater table response at both hydrological landscape units for the considered events. A distinct AMC threshold triggering a shift of response times was not found since long T_{lag} were detected after high pre-event rainfall, and vice versa. For example, at the hillslope (P1) and at the riparian zone (P5) rainfall events with $AP_7 > 0$ mm (wet AMC) and $AP_7 < -10$ mm (very dry AMC) caused similar T_{lag} (Table SI-4).

With respect to rainfall characteristics, the event analysis showed that groundwater tables at the hillslope (P1) and the riparian zone (P5, P8) increased significantly after a rainfall threshold of $P_{sum} > \sim 11$ mm was exceeded (Figure 12a). This rainfall threshold represents losses due to infiltration, interception and depression storage. The dependency on AMC was analyzed by separating the events into wet ($AP_7 > 0$) and dry ($AP_7 < 0$) conditions. For the riparian zone groundwater table, this threshold was unaffected by AP_7. At the hillslope (P1), the required amount of rainfall triggering a comparable rise when $AP_7 > 0$ was much smaller than during drier conditions ($AP_7 < 0$) (Figure 12a). For example, the relative rise of the groundwater table was 0.2 m following a 21.8 mm rainfall event during wet AMC (7 August 2011, $AP_7 = 2.6$ mm) and a 32.2 mm rainfall event during very dry AMC (24 August 2011, $AP_7 = -21.6$ mm, Table SI-1, Figure 12a).

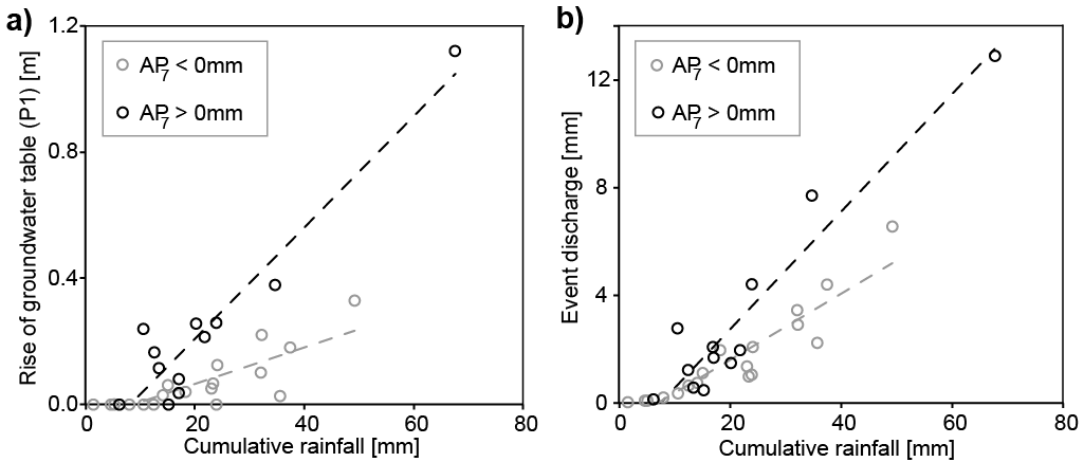

Figure 12 (a) Cumulative rainfall versus absolute rise of groundwater level at piezometer location P1; (b) Cumulative rainfall versus event discharge.

Further, a strong linear relationship existed between P_{sum} and the rise of groundwater table, both for wet and dry conditions. With respect to AP_7, Figure 12a illustrates the rainfall response of hillslope groundwater at P1 ($R^2 = 0.66$ for $AP_7 < 0$, $R^2 = 0.90$ for $AP_7 > 0$). For the hillslope, high pre-event rainfall likely increased the moisture content and the hydraulic permeability of the unsaturated zone and reduced the depth to the groundwater tables. As indicated by the absolute rise of groundwater tables, hillslope groundwater discharge was generally higher during such conditions. This is consistent with observations by GURTZ et al.

(2003b) who suggested increased groundwater recharge rates in the RHB when infiltration and percolation water led to saturation of the soil layers above the groundwater table. At the riparian zone (P5 and P8) a strong linear correlation existed between P_{sum} and the rise of groundwater tables ($R^2 = 0.47$ for P5, $R^2 = 0.70$ for P8), regardless of AP_7. This indicates a very small soil moisture deficit most of the time and supports the previous assumption that the riparian zone is fed continuously by groundwater flux from areas further uphill.

Rainfall event characteristiscs also affected the groundwater flow directions (α) during the snow-free periods in 2011 and 2012 at the transition zone between hillslope and riparian zone at the Büel site (Figure 13a). A rise of near-stream groundwater levels was associated with a change of groundwater flow towards a more west-east oriented direction. In order to assess the effect of P_{sum} on groundwater flow dynamics, the maximum range of α at the four piezometer triangles (A, B, C, D) for the corresponding P_{sum}-values was calculated. A significant positive correlation between the range of α and P_{sum} was found for all triangles (Figure 13b). The smallest change of α occurred at the most uphill location (A) and the highest variability was detected at triangle B. For triangles A, C and D, α increased with rising groundwater tables, indicating that water flowed dominantly towards the stream during rising groundwater tables rather than parallel to it. For triangle B, groundwater flow shifted to the opposite direction during rainfall events. Here, a rise of groundwater tables was associated with fluxes mainly parallel to the river, as indicated by a negative correlation between α and mean triangle-groundwater table. From this, it can be suggested that triangle B marks a mixing zone of hillslope groundwater (direction parallel to the surface topography) and riparian groundwater (direction affected by groundwater-surface water-interaction). Additionally, the cut bank of the river meander at the lower part of the Büel site is likely to affect α and the degree of groundwater-surface water-interaction in the riparian zone. At locations with more straight river stretches a similar shift of α can be expected; however, the mixing zone of hillslope and riparian groundwater flow dynamics might be located closer to the river due to a more lateral flow of the river water (RODHE and SEIBERT, 2011).

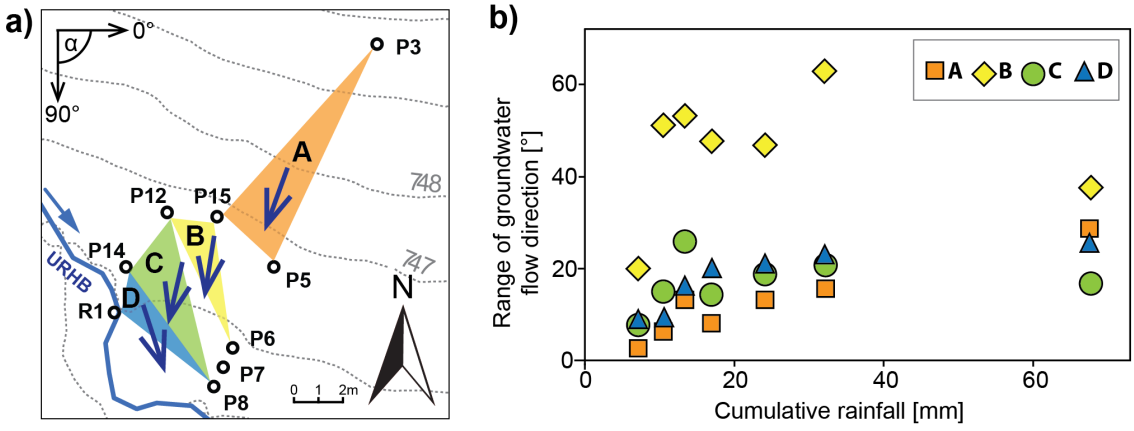

Figure 13 Groundwater flow directions at the field site Büel, (a) locations of the piezometer triangles with average initial groundwater flow directions before the 7 events: 110° (A), 99° (B), 103° (C), 72° (D); (b) Maximum ranges of groundwater flow directions for triangles A, C, D and E during 7 rainfall events in 2012 (12 April, 7 June, 9 June, 18 June, 21 June, 25 June, 29 July).

II - 3.1.2 Towards a conceptual model at the hillslope-scale

Flow processes in the riparian zones are determined dominantly by saturation and infiltration excess (ZEHE and SIVAPALAN, 2009). In the URHB, the aquifer in the riparian zone of the Büel site is very shallow due to the underlying till layer (Figure 9c). The permanent high water level indicates an influx of hillslope groundwater, which suggests stormflow generation from shallow subsurface stormflow and saturation overland flow. The strong correlation between rainfall characteristics and variations of riparian groundwater tables further supports this hypothesis. Variations of AMC are minor in the riparian zone and, therefore, play only a secondary role for stormflow generation and solute export.

Consistent long lag times of hillslope groundwater table responses (Figure 11a) indicate that saturated matrix flow is the dominant transport mechanism in the hillslopes. The shift towards shorter lag times during wet AMC suggests that quick hillslope groundwater flux at the Büel site towards the valley bottom is initiated when the groundwater table reaches more permeable zones in the upper soil column. This is consistent with other experimental hillslope and catchment-scale studies that have found a non-linear relationship between hillslope outflow and cumulative rainfall, which was mostly associated to the activation of preferential flow and transmissivity feedback mechanisms in more permeable soil layers (e.g., ANDERSON et al., 2009; GRAHAM et al., 2010; LEHMANN et al., 2007; PENNA et al., 2011). At the Büel site, hydraulic conductivity decreases with depth due to the increasing clay content (till layer as aquitard, Figure 9c). Hence, lateral flow on the confining till layer, as detected by DETTY and MCGUIRE (2010) in the Hubbard Brook Experimental Forest (NH, USA), is not likely to be the dominant flow pathway in the URHB hillslopes. It rather can be suggested that groundwater flow processes in the deeper hillslope aquifer are slow (matrix flow) so that primarily "young" groundwater is discharged from the hillslopes during rainfall events and wet AMC as shallow subsurface stormflow.

II - 3.2 Streamflow response to rainfall events

Runoff coefficients (C_R) of the URHB streamflow records for all 31 rainfall events ranged from 0.01 to 0.26 with an average value of 0.08 (Table SI-4). The largest runoff coefficients were associated with a higher wetness of the catchment (Figure 14), which is in line with findings of other studies, such as JAMES and ROULET (2009), PENNA et al. (2011) and DETTY and MCGUIRE (2010). For example, the largest values of C_R (> 0.18) are correlated with $AP_7 > 0$ mm and $Q_{ini} > 16$ L s^{-1}, respectively. For the rainfall event on 9 June 2012 only a small runoff coefficient ($C_R = 0.122$) was detected, despite the very wet AMC ($AP_7 = 110$ mm, $Q_{ini} = 48$ L s^{-1}). Due to the previous rainfall period on 7 June with a much higher discharge peak, on 9 June the streamflow hydrograph was likely to be still affected by the receding event-flow signal, which resulted in an underestimation of the total event flow volume and a small C_R. Because of the wider distribution of C_R relative to AMC a moisture threshold, after which the event-flow contributing area expands rapidly, is not as distinct for the URHB sub-catchment compared to the studies mentioned above. Further, the small number of events with very dry AMC hampers the identification of a distinct threshold. Since the URHB is a rather moist watershed (SENEVIRATNE et al., 2012), we can assume the found AMC to be

representative for the overall conditions in the URHB. Based on this, the results rather suggest a more continuous transition to larger event-flow generating areas during long and high-intensity rainfall periods.

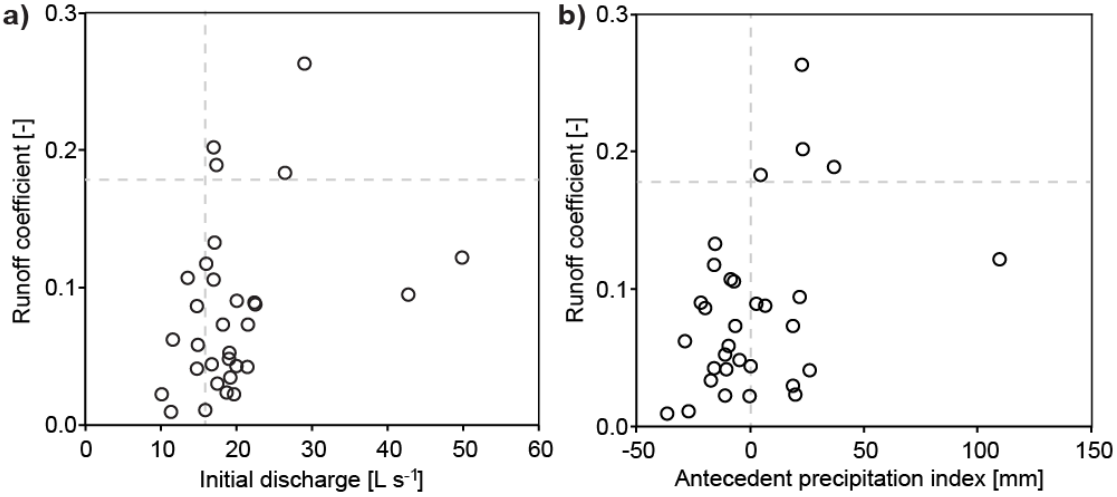

Figure 14 Correlation of AMC and runoff coefficients for all rainfall events. (a) Initial discharge (Q_{ini}); (b) antecedent precipitation index (AP_7).

Runoff coefficients in relation to rainfall intensity reveal a two-fold correlation when separated into very wet and very dry AMC. For example, during very wet conditions ($AP_7 > 10$ mm), low intensity rainfall events (< 2.5 mm h^{-1}) caused the highest runoff coefficients during the study period, whereas C_R did not exceeded 0.13 over a wide range of rainfall intensities when $AP_7 < -10$ mm (Figure 15). For Q_{ini} as proxy for AMC, this correlation was less pronounced as for AP_7. This can be explained with the small range of Q_{ini} that limits the number of observations with very wet and very dry AMC, respectively (Figure 15b). Although, values of $Q_{ini} < 16$ L s^{-1} represent the lower third of all measured AMC values, a similar behavior as for AP_7 for drier conditions can be expected for smaller Q_{ini}, i.e. small C_R during high-intensity rainfall events.

Similar to hillslope groundwater, a strong linear relationship existed between P_{sum} and Q_{event} independent of the AMC ($R^2 = 0.85$ for $AP_7 < 0$, $R^2 = 0.91$ for $AP_7 > 0$) (Figure 12b). However, during drier conditions Q_{event} was generally smaller for similar values of P_{sum}. The majority of the largest flood events ($Q_{event} > 4$ mm) occurred when antecedent precipitation was high and in three cases (21 September, 2012 and 21 June, 2012; 26 September, 2012 and 29 July, 2012; 18 September, 2012 and 11 September, 2012) a similar amount of rainfall led to approximately 3 mm more catchment outflow compared to events with dry AMC. The same rainfall threshold of $P_{sum} >\sim 11$ mm that was found for the hillslope groundwater table (P1, Figure 12a) was also found for the streamflow signal (Figure 12b).

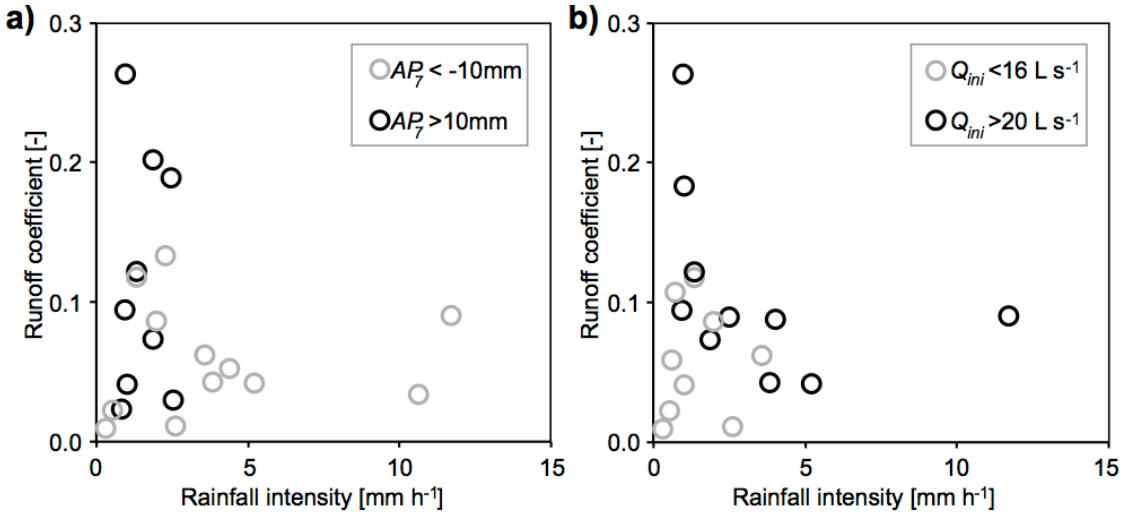

Figure 15 Runoff coefficient versus mean rainfall intensity for events with very wet and dry antecedent moisture conditions (AMC). (a) AMC represented by antecedent precipitation index (AP_7); (b) AMC represented by initial discharge (Q_{ini}).

For the URHB, the previous analysis elucidated that the role of rainfall characteristics for river (and hillslope groundwater) response is highly dependent on AMC. During wet conditions, feedback mechanisms between rainfall and hillslope groundwater re- and discharge are quicker and lead to a more direct response suggesting an increase of hydrologic connectivity between the river and the hillslope. The found rainfall threshold of 11 mm leading to detectable river response is much smaller than values reported from other experimental sites, such as 17 - 23 mm at Maimai, New Zealand (~60 cm thick stony silt loam podzolized yellow brown earths with high density of preferential flow paths, GRAHAM et al., 2010), 23 mm at a small Alpine catchment, Italy (60 – 100 cm thick clay to silty clay Cambisols, PENNA et al., 2011) or 55 mm at the Panola hillslope, Georgia, USA (0 – 186 cm thick unstructured sandy loam, TROMP-VAN MEERVELD and MCDONNELL, 2006c). This suggests that in the URHB the contribution from the riparian zones was likely the major source of event flow during small events and dry AMC. The hillslopes became hydrologically active mainly during more wet AMC. However, frequent rainfall during the snow-free periods in the URHB causes relatively wet AMC throughout the year and thus in most cases the hillslopes contributed to event flow soon after the rainfall threshold of 11 mm was exceeded (Figure 12a).

II - 3.3 Seasonal variability of hydrometric parameters and solute concentrations in riparian zone, hillslope and URHB-river

Figure 16a-f presents the monthly averaged time series data from June 2011 until August 2013 in order to visualize seasonal trends of the hydro-climatic conditions in the URHB. The large variability of monthly rainfall in 2011 – 2013 reflects the temperate humid conditions of the wider region (Figure 16a). On average, the highest rates of rainfall occurred during the summer months when evapotranspiration and air temperatures were at their maximum as well (Figure 16b and c). Monthly streamflow from the URHB showed no marked

seasonal trend. The good linear correlation with the temporal variability of groundwater table depths at P1 and P8 (both $R^2 = 0.69$) implies a direct link with the local aquifer system (Figure 16d-f).

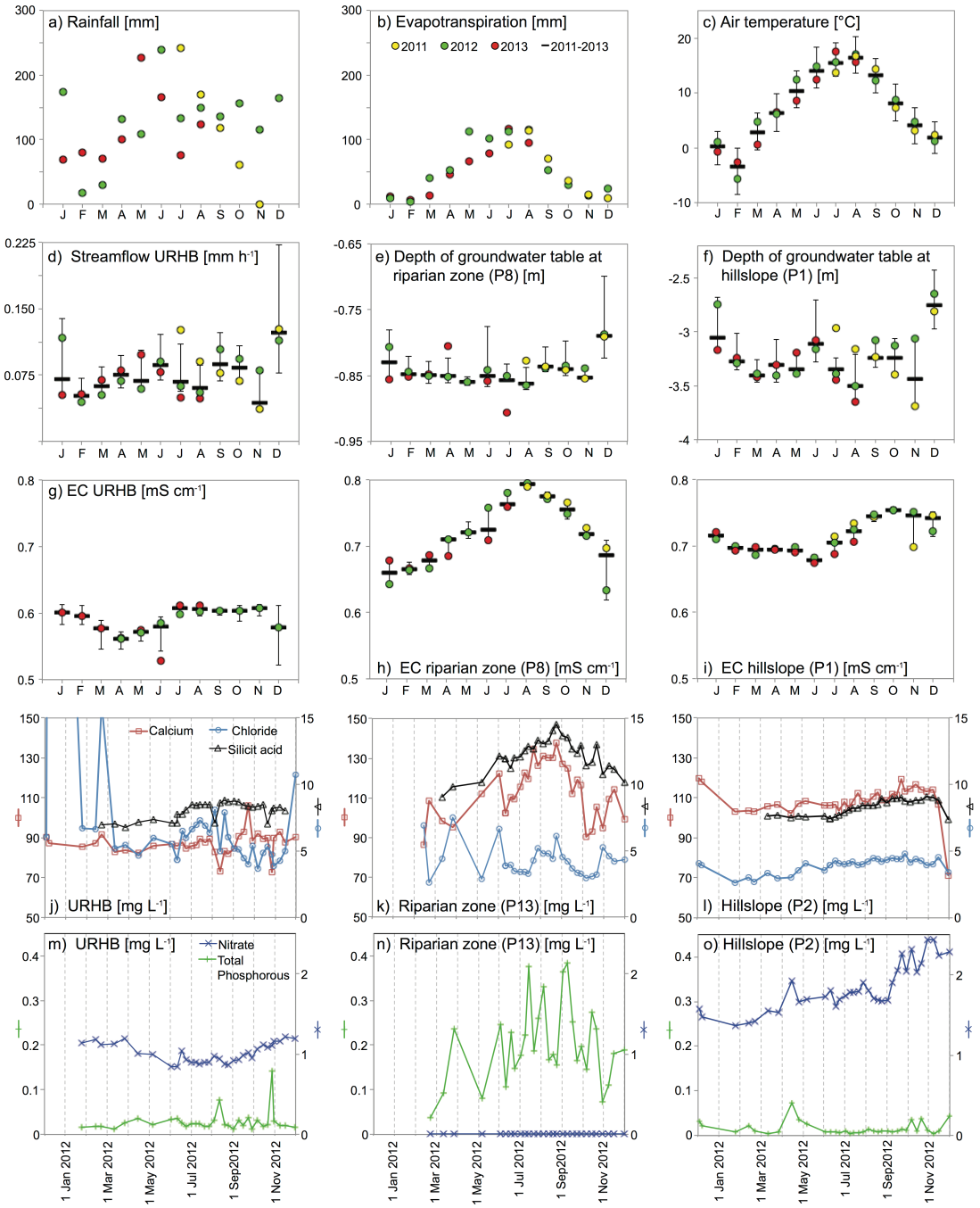

Figure 16 Seasonal variability of hydro-climatic variables and solutes in ground- and river water in the Upper Rietholzbach sub-catchment (URHB); (a-i) (Box) plots of monthly average values or sums from 1 July 2011 till 31 August 2013, with values for 2011 (yellow), 2012 (green) and 2013 (red): a) Rainfall (standard rain gauge at 1.5 m, Dec 2011: 667 mm is not shown); (b) Actual evapotranspiration (lysimeter); (c) Air temperature (2m); (d) Total streamflow; e-f) Groundwater table depth at the riparian zone and hillslope, respectively (due to logger failure there were no data recorded at P8 between 1 May to 30 May 2013 and 16 June to 13 September 2013); (g-i) Electrical conductivity; (j-l) Calcium, chloride and silicit acid concentrations during 2012 (chloride concentrations in

river water on 6 December 2011: 64.7 mg L^{-1} and 22 February 2011: 18.1 mg L^{-1} are not shown); m-o) Nitrate and total phosphorous concentrations during 2012.

In the URHB, monthly mean electrical conductivity in river water (EC_Q) is strongly controlled by geogenic sources as indicated by the high proportions of HCO_3^- (74 %), Ca^{2+} (17 %) and Mg^{2+} (4 %) in river water. In spring, EC_Q declined likely due to dilution with low mineralized snowmelt water (Figure 16g). During late summer and fall EC_Q remained relatively constant at 0.60 mS cm^{-1}, which is in contrast to the EC_{GW}-variations in the riparian groundwater (P8, Figure 16h). Here, EC_{GW} was generally above 0.65 mS cm^{-1} and rose continuously up to 0.80 mS cm^{-1} from January to August and then decreased again until December. Oxygen concentrations, measured occasionally in 2012 (HQ40D and LDO, Hach Lange, Switzerland) at P7 and P5 were mostly below 1 mg L^{-1}, indicating reducing conditions of the shallow near-stream aquifer. At the hillslope (P1) the highest EC_{GW} (0.75 mS cm^{-1}) was detected in October 2011 with a less pronounced seasonal trend and a maximum shift of EC_{GW} from 0.68 to 0.75 mS cm^{-1} between June and October (Figure 16i). Oxygen concentrations were significantly higher at the upper part of the transect (around 6 mg L^{-1} at P2 and P3.

Overall, the seasonality of the H_4SiO_4- and Ca^{2+}-concentrations measured in ground- and surface water in 2012 correlated well with the respective long-term *EC*-variations (Figure 16h and k). From summer to late fall H_4SiO_4- and Ca^{2+}-concentrations rose at all three sampling locations whereas the trend was most pronounced at the riparian zone (P13) with a peak in early September (P13, Figure 16i). This behavior reveals the important role of *ET* for groundwater chemistry in the riparian zones, which is further supported by a good linear correlation of monthly EC_{GW} in the riparian zone (P8) with air temperature ($R^2 = 0.81$) and *ET* ($R^2 = 0.56$). Under the assumption that solute concentrations in the infiltrating rainwater were small and the higher mineralized hillslope groundwater supplied the near-stream areas continuously, an enrichment of solutes occurred when *ET* depleted the local riparian groundwater storage in summer.

Cl^--concentrations in the URHB-river showed strong variations - especially in early spring (Figure 16i, Table SI-5), which can be explained by salt application on the nearby street on the south-facing slope. For the time after 22 February 2012 the average Cl^--concentration in the river water was approximately 6 mg L^{-1} with no distinct seasonal trend, which corresponds to similar concentrations measured in the riparian zone, (between 3 mg L^{-1} and 8 mg L^{-1}) and in the hillslope (between 3 and 5 mg L^{-1}, Figure 16k and l, Table SI-5).

Concentrations NO_3^- and TP in river water were generally low with no marked seasonality (Figure 16m, Table SI-5). In the hillslope groundwater NO_3^--concentrations continuously increased from around 1.3 mg L^{-1} to up to 2.4 mg L^{-1}, which can be correlated to eluviation of NO_3^- from the upper soil layers, especially in fall 2012 when precipitation rates and hillslope groundwater table were high (Figure 16o). TP-concentrations only peaked in the second half of April, but generally remained below 0.04 mg L^{-1}. NO_3^--concentrations of all samples from the riparian zone were below the detection limit, whereas TP-concentrations were more than one magnitude higher than at the other two sampling locations (Figure 16n). With the highest values (TP $\geq$ 0.35 mg L^{-1}) measured between mid of July and mid of September, the riparian TP-concentrations also showed a distinct seasonality. Since a large portion of the URHB area is agriculturally used (i.e., regular manure application at the

hillslopes) NO_3^- input due to atmospheric deposition is negligible. This assumption is further supported by very low sulfate concentrations (SO_4) in ground- and river water that were below detection limit (5 mg L^{-1}) for 97 % of all samples.

These analyses reveal that the overall hydrology of the URHB river is primarily associated with the hillslope groundwater dynamics. Further, at the riparian zone the increasing EC_{GW} in spring in addition to high Ca^{2+}-concentrations in late summer can be seen as indicators of groundwater influx from the hillslopes. However, the strong variability of solutes (e.g., Ca^{2+} and Cl^-) in river water is likely to be correlated to quick flow processes, facilitated by rainfall or snowmelt events and preferential flow pathways.

II - 3.4 Synthesis of hillslope- and catchment-scale hydrological responses: implications for nutrient export

The delineation of hydrological relevant landscape units of a catchment is closely linked to the dominant streamflow-generating mechanisms taking place on those areas (SEIBERT and MCGLYNN, 2005). Several studies applied this concept in combination with tracer experiments and hydrometric data in order to identify the relevant source areas of streamflow and the active flow pathways (e.g., DETTY and MCGUIRE, 2010; JENCSO and MCGLYNN, 2011; MCGLYNN et al., 2004). For many catchments worldwide a separation of the landscape into the two basic units of hillslopes and riparian zones was found to provide an adequate framework for the conceptualization of the overall hydrological behavior.

At the Büel site, the rainfall-response analysis illustrated that event flow is primarily generated from saturated catchment areas that react uniformly to rainfall (i.e., independent from AMC, even for low intensity rainfall events). In order to scale up the findings from the hillslope- to the catchment scale and to locate those areas in the URHB topographic indices can be applied. For example, the topographic wetness index (TWI, BEVEN and KIRKBY, 1979) is widely used in order to identify potential source areas for streamflow contribution and as a proxy for shallow groundwater table distribution (e.g., DETTY and MCGUIRE, 2010; JAMES and ROULET, 2007; SEIBERT and MCGLYNN, 2005).

Figure 17b depicts the distribution of slopes and TWI of the URHB, respectively. A flat area (slope < 5 %) with shallow soils characterizes the central valley bottom (yellow-framed area in Figure 17b). The transition between QMD and UFM is clearly marked by a change in slope of the land surface. Accordingly, the TWI is highest in the flat valley bottom areas (Figure 17c). Overall, the TWI correlates with the distribution of Gleysols and peaty soils that indicate the existence of shallow groundwater tables (Figure 17b and c). Further, most areas underlain by fractured UFM (Figure 17a) are characterized by deep groundwater tables as shown by small TWI-values on the upper hillslopes and plateaus.

From the catchment-wide landscape analysis and the hydrometric observations at the Büel site, it can be suggested that geomorphology is a first-order control of groundwater dynamics and streamflow-generation mechanisms in the URHB. For example, the development of a wetland in the western part of the basin that covers ~5.3 % of the total area indicates that these valley bottom areas are fully saturated most of the year. These results support the discretization of the URHB-landscape into riparian zones and hillslopes following

the framework proposed by SEIBERT and MCGLYNN (2005). In the URHB, riparian zones contain areas with high TWI, which are located predominantly in the valley bottoms with Gleysols and peaty soils. The hillslopes are characterized by deeper groundwater tables, steep terrain and larger distances to the river. With respect to event-flow generation, only the lower parts of the hillslopes adjacent to the riparian zones (i.e., TWI-values between ~7 and ~8) are likely to contribute shallow subsurface stormflow as it was observed at the Büel site.

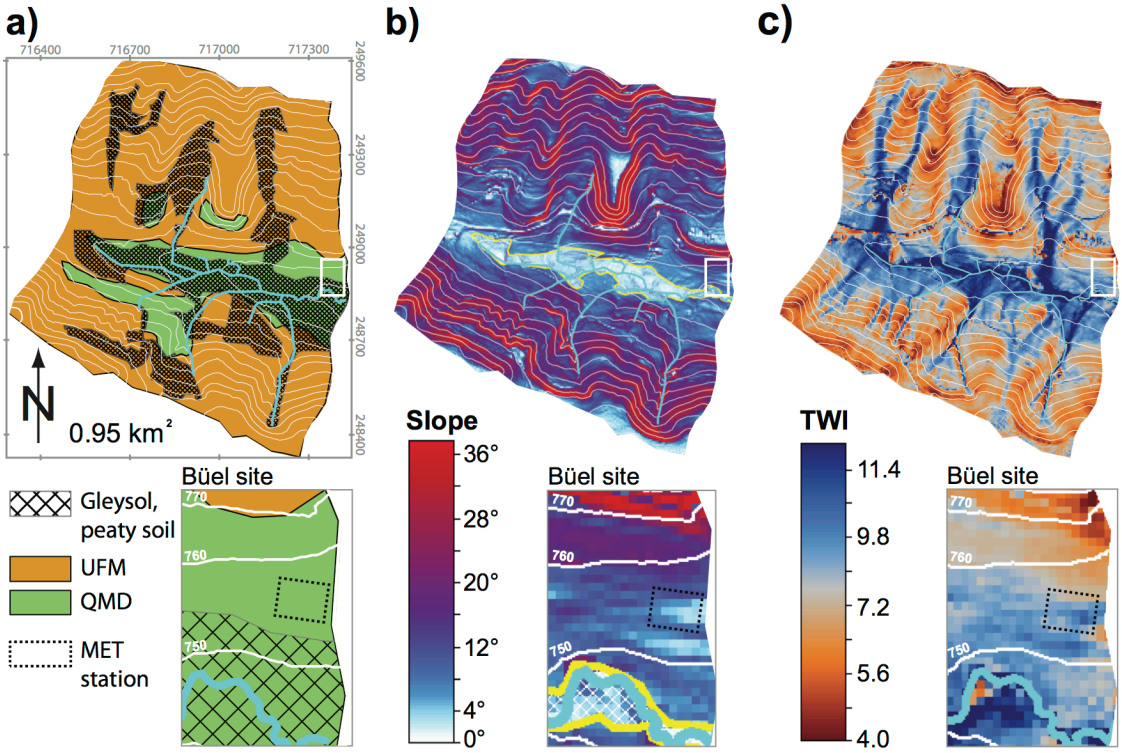

Figure 17 Surface and landscape properties in the Upper Rietholzbach sub-catchment (URHB) and at the Büel site; (a) Geological units (Upper Freshwater Molasse: UFM, quaternary moraine deposits: QMD)) and Gleysol distribution; (b) Slope and riparian zone (yellow-framed area); (c) Topographic wetness Index (TWI); a paved street crosses the catchment on the south-facing slope, which causes locally artificially high TWI-values.

Assuming that C_R is an indicator for the active event flow-contributing area during a rainfall period (BOUGHTON, 1987), the average value of 0.08 suggests that event flow in the URHB is dominantly generated from the permanently saturated areas in the valley bottom (~ 5.3 % of the catchment area, Figure 10b) and impervious, surface runoff-generating surfaces (e.g., settlements and streets cover ~ 4 % of the catchment area). The small values of C_R during dry conditions may reflect spatial limitations and low temporal variability of those quick flow-generating areas in the URHB, for example due to the steep hillslopes. Higher C_R-values during wet conditions together with small rainfall intensities indicate an expansion of the stormflow generating area and an increase of hydrologic connectivity, for example due to the activation of hillslope groundwater flux, which might be associated with solute export from these areas. A detailed analysis carried out for two representative rainfall events (supplementary information of part II, Figure SI-2) corroborates this assumption.

Since in the URHB more than 70 % of the catchment area is used as pastureland with regular manure and fertilizer application, the hillslopes adjacent to the riparian zones (transition zones) can be considered critical source areas (PIONKE et al., 1996) for nutrient input into the river. However, many studies found the riparian zone to significantly buffer the nutrient input from the hillslopes before the groundwater discharges into the stream (e.g., MCGLYNN and SEIBERT, 2003; VIDON and SMITH, 2007). The buffering capacity of the riparian zones is linked to the dominant flow and transport processes as well as to the subsurface properties and biogeochemical conditions that determine the residence time of the groundwater and hence, sorption and degradation rates. The data from the Büel site indicate that the conditions in the riparian zone alter the nutrient concentrations of the hillslope groundwater as it passes through the shallow aquifer valley bottom. Here, a reduction of NO_3^- (denitrification) can be attributed to reduced oxygen-concentrations due to consistently shallow groundwater tables and organic-rich soils that act as electron donors. An enrichment of TP in the riparian zone aquifer indicates the immobilization of mobile phosphorous species (e.g., PO_4^{3-}) that arrive from the upper (agriculturally used) hillslopes. Since the near-stream sediments are characterized by high clay contents (due to the underlying till layer) binding or adsorption on clay particles is likely to be the primary mechanism for PO_4^{3-}-immobilization (DOMAGALSKI and JOHNSON, 2012). Nevertheless, the seasonal URHB chemograph only showed marginal effects of these processes, which indicates that actual groundwater discharge from the riparian zone was minor compared to surface runoff and shallow subsurface stormflow in the more permeable upper soil layers in the hillslopes. Although, the riparian zone may act as an effective buffer zone for NO_3^-, in relation to total catchment outflow the actual NO_3^- removal rate is expected to be small. This is in line with other experimental studies that showed the permeability of the riparian zone aquifer material to be a critical factor for its NO3- buffer capacity (e.g., BURT et al., 1999; INAMDAR et al., 2009; MCGLYNN and MCDONNELL, 2003). With respect to phosphorous, it can be expected that TP-enriched groundwater from the flat valley bottoms is flushed out when riparian groundwater tables reach the land surface during wet periods with high-intensity rainfall events, which then causes TP-peaks in the river water. This hypothesis is supported by findings from other catchments with agriculturally used hillslopes or experimental studies, as for instance PIONKE et al. (1996), SURRIDGE et al. (2007) or VIDON et al. (2010).

II - 4 CONCLUSIONS

The present study focused specifically on the origin of quick streamflow during rainfall events that drives the dynamic hydrology and solute transport in mountainous headwater catchments. In order to gain a mechanistic understanding of stream-landscape connectivity and to highlight possible implications on nutrient export from agriculturally used hillslopes, first-order controls regulating shallow groundwater dynamics and stormflow generation were identified in the western small pre-Alpine URHB catchment.

The results from the integrated analysis at the URHB are consistent with findings in other catchments and environments (e.g., DETTY and MCGUIRE, 2010; INAMDAR and MITCHELL, 2007; MCGUIRE and MCDONNELL, 2010; SEIBERT and MCGLYNN, 2005; SIDLE et al., 1995). With respect to solute transport in the hillslope, similar behaviors could be observed as those described in the conceptual model of BURT and PINAY (2005).

- The event-flow generating area in the URHB comprises a portion of less than 30%. Those areas were localized dominantly in the flat valley bottom (wetland and riparian zones) and the adjacent lower hillslopes where groundwater tables are shallow and local soil moisture deficit is low throughout the year.

- The water level in the riparian zones are a near-steady-state phenomenon with a very limited hydraulic buffering potential of high-intensity rainfall events due to a small storage capacity. Thus, surface runoff and shallow subsurface stormflow dominate in these areas, indicated by short lag times and small groundwater level changes.

- At the adjacent hillslopes, timing and amplitude of groundwater table response to rainfall events are determined by a higher water storage capacity. Thus, AMC is a first-order control of the response times, whereas rainfall characteristics influence groundwater dynamics only during wet conditions. These processes can be highly non-linear, for example when shallow groundwater flow in the upper, generally more permeable soil layers, is initiated.

- The riparian zones likely act as sink for solutes (e.g., phosphorous), which are discharged from the agriculturally used hillslopes. Low permeability and local reducing conditions lead to limited degradation rates. It can be expected, that solutes are flushed from the riparian zones during rainfall events, dominantly by shallow subsurface stormflow and by saturation excess, that may alter the chemograph of the URHB river.

- Low oxygen concentrations in the riparian zone result in a significant immobilization of NO_3^-, likely due to denitrification. Although it might be a buffer zone for NO_3^-, actual groundwater discharge from the riparian zones is likely minor compared to surface runoff and shallow subsurface stormflow that bypasses the denitrification zones during rainfall events.

Hence, the applied integrated approach revealed that river water quality in this mountainous catchment is likely dominated by hillslopes groundwater signature whereas the riparian zones in the valley bottom areas govern its dynamic hydrologic regime.

Future research in mountainous catchments will benefit from the better understanding of the dominant controls on streamflow generation mechanisms by describing the hydrological functioning of the landscape units during rainfall events. Since land use management as well as hydro-climatic and geomorphic properties of the studied mountainous catchment can be considered representative for large parts of the north-eastern Swiss pre-Alps, the presented findings of the dominant hydro-climatic processes in the URHB are expected to be relevant and transferable to other mountainous catchments. This is of particular importance with respect to climate change that is likely to alter mountainous hydrology considerably (BENISTON and FOX, 1996). For the Swiss pre-Alps, extreme events (droughts and floods) are predicted to occur more frequently (METEOSWISS, 2013), which will be accompanied with land-use change, water scarcity, mudslides or avalanches. Thus, the improved understanding of hydrogeological and hydrological processes in the mountainous source areas of major rivers

is of great importance to the water resource management of Switzerland and many other parts of the world. The integrated system understanding from this study also facilitates the development of effective mitigation measures, targeting protection and preservation of the ecological and hydrological functioning of mountainous catchments.

SUPPLEMENTARY INFORMATION OF PART II

Table SI-4 Rainfall characteristics and calculated event features during the snow-free period in 2011

Start of rainfall event	Duration	Total rainfall	Rainfall intensity	Peak rainfall intensity	Antec. Precipitation index	Initial discharge	Runoff coefficient	Peak discharge	Respose time	Lag time T_{lag}			
		P_{sum}	PI	PI_{max}	AP_7	Q_{ini}	C_R	Q_{max}	T_{res}	P1	P3	P5	P8
(dd.mm.yy hh:mm)	(h)	(mm)	(mm h^{-1}) [a]	(mm h^{-1}) [b]	(mm)	(L s^{-1})	(-)	(mm h^{-1}) [c]	(h)	(h)	(h)	(h)	(h)
08.07.11 1:15 AM	4.50	23.4	5.2	13.2	-10.6	21.5	0.042	0.367	1.75	11.50	10.50	3.75	**
05.08.11 7:30 PM	3.25	14.2	4.4	11.7	-10.9	19.1	0.053	0.464	1.25	6.00	0.25	2.25	**
07.08.11 1:15 AM	8.75	21.8	2.5	7.4	2.6	22.4	0.089	0.498	8.50	8.25	0.50	1.00	**
14.08.11 9:45 PM	6.25	24.0	3.8	12.2	-16.0	20.1	0.043	0.441	1.00	*	2.75	3.50	**
24.08.11 8:15 PM	2.75	32.2	11.7	26.0	-21.6	20.2	0.090	0.976	1.00	8.50	1.50	2.75	**
27.08.11 3:30 AM	4.25	17.0	4.0	7.7	6.6	22.6	0.088	0.339	1.75	11.25	1.75	2.50	0.50
04.09.11 1:30 PM	21.50	49.2	2.3	13.0	-15.5	17.2	0.133	1.610	1.00	10.25	5.25	1.75	0.00
11.09.11 5:45 PM	7.50	6.2	0.8	2.4	19.6	18.7	0.023	0.022	6.75	*	*	18.00	*
14.09.11 5:45 AM	6.00	15.2	2.5	6.2	18.5	17.5	0.030	0.093	1.25	*	5.25	6.00	5.75
16.09.11 9:45 PM	6.50	16.3	2.5	8.2	0.3	16.8	0.044	0.137	1.75	15.00	7.75	6.75	4.75
18.09.11 3:15 AM	10.75	20.2	1.9	6.0	18.5	21.6	0.073	0.150	9.00	7.75	2.25	1.25	1.00
09.10.11 9:45 PM	13.50	12.6	0.9	2.9	21.8	42.8	0.095	0.224	1.50	6.25	0.75	1.50	1.25
19.10.11 11:45 AM	8.25	12.5	1.5	3.2	-4.8	19.1	0.048	0.050	2.50	*	6.25	7.25	8.25

[a] Mean rainfall intensity

[b] Maximum 1 h rainfall intensity

[c] Maximum discharge relative to Q_{ini}

* No response was detected, ** No data available

Table SI-5 Summary of biweekly solute concentrations of ground- and surface water samples collected between January through December 2012, including maximum observed concentration, total number of samples, portion of samples with concentrations below detection limit (DL) and coefficient of variation (CV, ratio of standard deviation and mean).

	URHB-river	**P13**	**P2**
	Maximum (mg/L)	Maximum (mg/L)	Maximum (mg/L)
Compound	number of samples	number of samples	number of samples
DL (mg/L)	% < DL	% < DL	% < DL
Measurement	CV	CV	CV
Silicit acid ($H_4SiO_4^-$)	**8.8**	**14.6**	**9.1**
5.0	n = 30	n = 28	n = 30
Auto-Analyzer 3	0 %	0 %	0 %
(Bran+Luebbe - now Seal Analytical, UK)	0.079	0.109	0.070
Calcium (Ca_2^+)	**106.0**	**137.9**	**119.8**
0.5	n = 35	n = 30	n = 35
761 Compact IC	0 %	0 %	0 %
(Metrohm Switzerland)	0.065	0.124	0.074
Chloride (Cl^-)	**64.7**	**7.5**	**4.8**
0.5	n = 35	n = 30	n = 35
761 Compact IC	0 %	0 %	0 %
(Metrohm Switzerland)	1.310	0.286	0.138
Nitrate (NO^{3-})	**1.2**	**< 0.5**	**2.4**
0.5	n = 35	n = 30	n = 35
761 Compact IC	0 %	100 %	0 %
(Metrohm Switzerland)	0.115	-	0.921
Total phosphorous (TP)	**0.141**	**0.384**	**0.074**
0.001	n = 35	n = 30	n = 35
Varian Cary 50 Bio UV/ Visible	0 %	0 %	0 %
Spectrophotometer (Agilent Techn., USA)	0.793	0.485	0.92

Analysis of two exemplary rainfall events to evaluate the conceptual model

In order to evaluate the conceptual description of groundwater dynamics at the hillslope and riparian zone with respect to hydrological behavior of the URHB, two exemplary rainfall events with different runoff coefficients (C_R) were analyzed in detail. Hereby, *EC* of ground- and river water will be utilized as proxy of groundwater contribution to streamflow.

Figure SI-2a shows the large rainfall event from September 4, 2011, where four discharge peaks occurred in response to four high-intensity rainfall periods. Antecedent moisture conditions (AMC) were very dry (AP_7 = -15.5 mm, Q_{ini} = 17.2 L s^{-1}). During the first two rainfall periods of the event 24.8 mm of rain fell, causing a total event discharge of 0.8 mm (C_R = 0.03). During the third and fourth rainfall period, 23.7 mm of rain fell and event discharge became 5.8 mm causing a much higher runoff coefficient of C_R = 0.24. The groundwater tables in the riparian zone (P5) rose synchronously with river stage whereas the hillslope groundwater table (P1) responded only at the onset of the third rainfall event. In order to estimate qualitatively the contribution of rainwater to event flow, the dilution of river water (D_Q) was expressed as the area of the EC_Q-curve per event relative to the initial EC_Q before the onset of rain. Interestingly, the dilution of river water during the third and fourth rainfall period of the event (D_Q = 5.7 mS cm^{-1}) was slightly smaller than during the first and second period (D_Q = 6.3 mS cm^{-1}), although event flow was more than 7-times higher. The delayed activation of higher mineralized hillslope groundwater flux towards the valley bottom that buffered the dilution signal of the rainwater might explain this behavior. This hypothesis is corroborated further by rising EC_{GW}-values in the hillslope and riparian zone groundwater during the third and fourth rainfall event period (Figure SI-2a). Another explanation might be the activation of catchment areas that contribute higher mineralized or nutrient-rich water to the river network (e.g., from pastureland after manure application). However, at the URHB the observed change of dilution patterns mostly occurred independently of the manuring season (spring and fall) but rather indicates a more persistent property of the catchment hydrological behavior such as shallow groundwater flux from the hillslopes.

Figure SI-2b illustrates a rainfall event with a double-peaked hydrograph on 10 October, 2011 that occurred during wet antecedent conditions (AP_7 = 21.8 mm, Q_{ini} = 0.16 mm h^{-1}). Hence, river discharge responded quickly to the two rainfall pulses and reached Q_{max} after only 1 h and 1.25 h after each PI_{max}, respectively. In both cases, discharge decreased quickly and reached pre-event conditions already 2.5 h after rainfall was over. Accordingly, the overall runoff coefficient was relatively small (C_R = 0.095). However, two delayed discharge pulses occurred 7.25 h and 18.25 h after the end of the rainfall event, respectively. During these pulses the EC_Q-values rather remained constant or increased slightly, which is in contrast to the behavior during most rainfall events where the EC_Q-signal indicates dilution. It can be suggested that these discharge pulses are caused by delayed groundwater influx from further upslope areas, which is also supported by the corresponding response of the hillslope groundwater table (P1, T_{lag} = 6.25 h and ΔGW = 0.16 m) and rising EC_{GW}-values. In addition, delayed outflow of (deep) groundwater from the fractured UFM-aquifer might account for the observed increase of discharge after the end of the rainfall event.

Although, overall permeability is small in the UFM, fractures and the lithostratigraphy (i.e., different hydraulic conductivities of consolidated conglomerates, sandstone, fresh water limestone and marl) are likely to facilitate a delayed expulsion of groundwater flux towards the springs that originate from the upper hillslopes of the URHB.

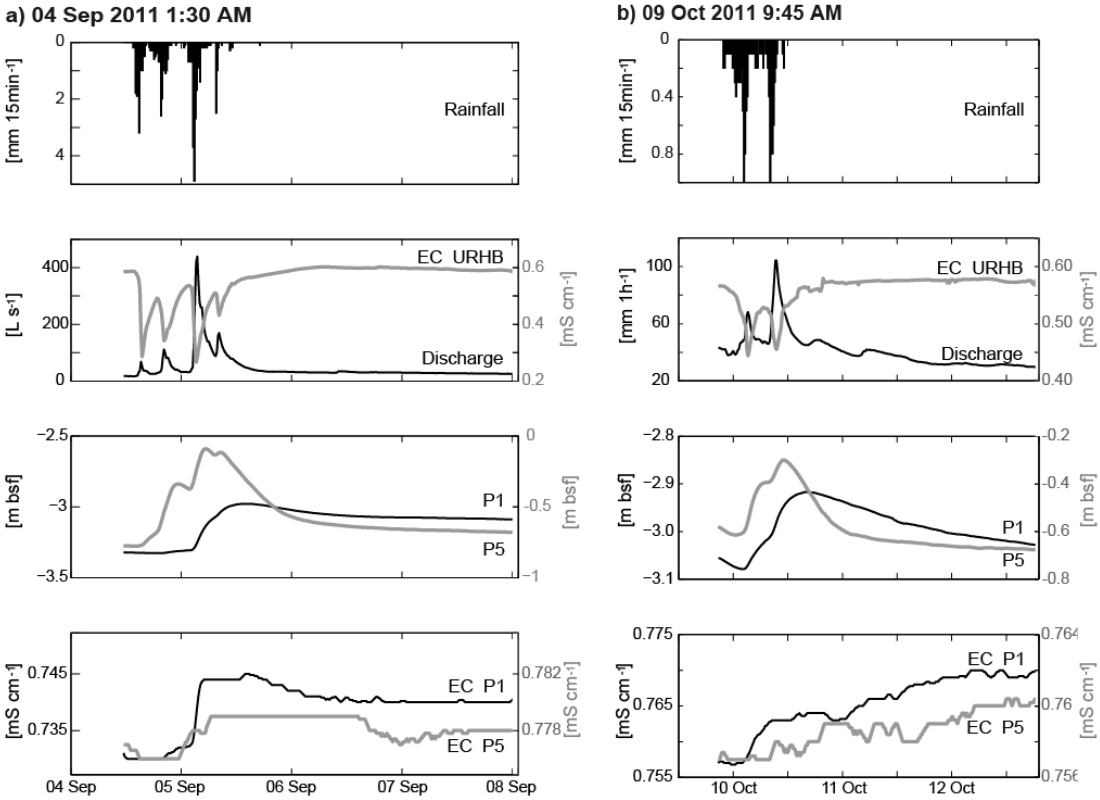

Figure SI-2 Time series of rainfall, discharge, electrical conductivity (EC) and groundwater table depths at piezometer location P1 and P5 during the rainfall events on (a) 4 September, 2011; (b) 9 October, 2011.

PART III

EVALUATION OF THE CONCEPTUAL MODEL AND SIMULATION OF EVENT-FLOW GENERATION

A reliable prediction of hydrograph responses in mountainous headwater catchments requires a mechanistic understanding of the coupled hydro-climatic processes in such regions This study shows that only a small fraction of the total area in a pre-Alpine headwater catchment actively regulates streamflow responses to hydro-climatic forcing, which facilitates the application of a parsimonious framework for hydrograph time-series prediction. Based on landscape analysis and hydrometric data from the upper Rietholzbach catchment (URHB, 0.94 km^2, NE Switzerland) a conceptual model was established. Here, rainfall event-driven contributions of surface runoff and subsurface flow (event flow) accounts for around 50 % of total discharge. This hydrograph component is generated from approximately 25 % of the entire area consisting of riparian zones (8 %) and hillslopes (17 %), each with characteristic streamflow-generating mechanisms. Baseflow generation is attributed to deep groundwater discharge from a fractured rock aquifer covering ~75 % of the catchment area. A minimalistic model, that represents event flow as depletion of two parallel linear reservoirs, verified the conceptual model of the URHB with adequate hydrograph predictions (R^2 = 0.67, *NSE* = 0.64). Hereby, the expansion of the event-flow contributing areas was found to be particularly significant during long and high-intensity rainfall events. These findings provide a generalized approach for the large-scale characterization of groundwater recharge and hydrological behavior of mountainous catchments with similar landscape properties.

JANA VON FREYBERG, P. SURESH C. RAO, DIRK RADNY, MARIO SCHIRMER (2015)
Hillslope groundwater dynamics and landscape functioning determine event-flow generation – a field study in the Rietholzbach catchment, Hydrogeology Journal, doi: 10.1007/s10040-015-1238-1 (*modified*[2]).

[2] Please note that this is the version of an article accepted for publication in *Hydrogeology Journal* in January 2015. Further modifications might be implemented in the formatting and editing process. For the final version consult the homepage of *Hydrogeology Journal*.

III – 1 INTRODUCTION

In many regions of the world mountainous headwater catchments maintain rivers and groundwater systems in the lowlands (VIVIROLI et al., 2003). Thus it is important to understand streamflow generation mechanisms to adequately predict hydrograph responses in such catchments. Mountainous headwater catchments, including the pre-Alpine catchment studied here, are often characterized by steep slopes, thin soil cover and high intensity precipitation that lead to flashy discharge responses and strong variability of streamflow. Further, their hydrology is controlled by the complex interaction of dynamic climatic processes (e.g., rainfall, radiation, evapotranspiration) and landscape properties (e.g., soil types, vegetation, topography) at various temporal and spatial scales. Consequently, hydrological modeling of these regions remains a challenging task (BLÖSCHL, 2011).

The discretization of catchments into functionally homogeneous landscape units with characteristic streamflow-generation processes provides an integrative approach that combines the advantages of lumped and fully distributed hydrological models (BASU et al., 2010; BEVEN and KIRKBY, 1979; SIVAPALAN, 2003). It is assumed that the landscape acts as hydrologic filter, integrating the coupled dynamic hydro-climatic processes at the local scale into the observed catchment-specific responses (e.g., CAREY et al., 2010; GALL et al., 2013; THOMPSON et al., 2011). Small-scale landscape properties and physical processes can then be described by macroscopic-effective parameters, for instance soil porosity, groundwater table depth, storage capacity or vegetation cover, in order to enhance modeling efficiency (e.g., (BASU et al., 2010; BOTTER et al., 2007; GHASEMIZADE and SCHIRMER, 2013).

Following MCGLYNN and SEIBERT (2003), riparian zones and hillslopes can be considered the most basic landscape units since they distinctly differ in their hydrological, biogeochemical and topographic properties. Spatiotemporal variability of the hydrologically active landscape units (e.g., BEVEN and KIRKBY, 1979; SEIBERT and MCGLYNN, 2005a) or groundwater storages (e.g., KIRCHNER, 2003; WINTER et al., 2003) that is triggered by soil moisture thresholds, rainfall intensities and heterogeneous subsurface properties (e.g., ALI et al., 2013; PENNA et al., 2011; ZEHE and SIVAPALAN, 2009) can cause nonlinear hydrological catchment behavior. Moreover, the hydrologic connectivity among the contributing landscape units and their connectivity to the river network both defines the probability distribution of groundwater residence times and alters the overall hydrologic catchment response (e.g., GUPTA et al., 1980; RINALDO et al., 2011; TETZLAFF et al., 2007). Numerous studies have focused on the experimental analysis of the spatiotemporal variability of hydrologically active landscape units with respect to streamflow generation (e.g., DAHLKE et al., 2009, GRAHAM et al., 2010; JAMES and ROULET, 2009) and solute export (e.g., DOPPLER et al., 2012; GBUREK et al., 2002; WOODBURY et al., 2014). The systematic delineation of hydrological landscape units can be based solely on the physical surface and subsurface features of the catchments, such as topography, soil type, geology and vegetation patterns (e.g., BEVEN and KIRKBY, 1979; GHARARI et al., 2011; GUPTA et al., 1980; MCGLYNN and SEIBERT, 2003). Additionally, groundwater-table variations in unconfined aquifers can serve as valuable proxies for dominant flow processes, for instance by analyzing typical time scales for infiltration and groundwater discharge (e.g., LYON et al., 2006b; MCGLYNN et al., 2004).

In the present study we evaluated the role of the two hydrological landscape units, riparian zones and hillslopes, for event-scale streamflow generation in mountainous headwater catchments. Here, event flow is defined as the rainfall-event driven contributions of surface runoff and subsurface flow to streamflow (i.e., corrected for baseflow), which is the most variable hydrograph component. We followed an integrative approach and combined digital elevation model based terrain analysis, experimentally derived subsurface properties and hydrometric measurements with a parsimonious modeling approach at a small pre-Alpine headwater catchment in NE Switzerland to address the following research questions: How can the dominant streamflow generating hydrological landscape units in the catchment be differentiated? How do landscape structure and subsurface properties control the dominant flow processes and event-flow generation? How is event flow generation affected by spatiotemporal variability of the contributing areas?

In order to answer these questions, this chapter first identifies important flow processes at the hillslope- and the catchment-scale to delineate the hydrologic landscape units (sections III - 4.1 and III - 4.2). This conceptual model is evaluated with a minimalistic, threshold-based model that assumes event-flow generation in parallel from two linear reservoirs (section III - 4.3). The role of variable contributing areas (VCA) for event-flow hydrograph simulations is systematically assessed in Section III - 4.4. Major limitations of the applied framework and concluding remarks are presented in sections III - 5 and III - 6.

III - 2 SITE DESCRIPTION

The Upper Rietholzbach sub-catchment (URHB, 0.94 km^2, Figure 18a and b) is a pre-Alpine headwater catchment located in the headwaters of the Swiss Thur river basin (1750 km^2, Figure 18a). It comprises the western part of the Rietholzbach catchment (RHB, 3.14 km^2) that has been subject of various hydro-meteorological studies since the late 1970's (e.g., GERMANN, 1981; GURTZ et al., 2003b; KOENIG et al., 1994; TEULING et al., 2010; VITVAR and BALDERER, 1997; VON FREYBERG et al., 2014) because its hydroclimatology is representative of the larger region of the Swiss north-eastern pre-Alps (SENEVIRATNE et al., 2012). The local climate is characterized by temperate humid conditions with high rainfall rates in late spring and summer (MeteoSchweiz METEOSWISS, 2013). Average annual sums of precipitation and evapotranspiration are around 1450 mm and 560 mm, respectively (based on data from 1976 – 2006 in EWEN et al. (2011)).

Elevations in the URHB range from 744 to 910 masl. Around 72 % of the land surface is used as pastureland, 19 % is forested, 4 % is settlement or streets and 5 % is covered by a wetland in the western central part of the URHB. The geology is composed of the Tertiary Upper Freshwater Molasse (UFM) that forms steep slopes and plateaus at higher elevations. The UFM consists of differentially permeable geologic strata, such as consolidated clastic sediments, marl, sand- and limestone, resulting in a large variability of hydraulic conductivities (1.7E-6 m s^{-1} to 1.1E-4 m s^{-1}, BALDERER (1983)).

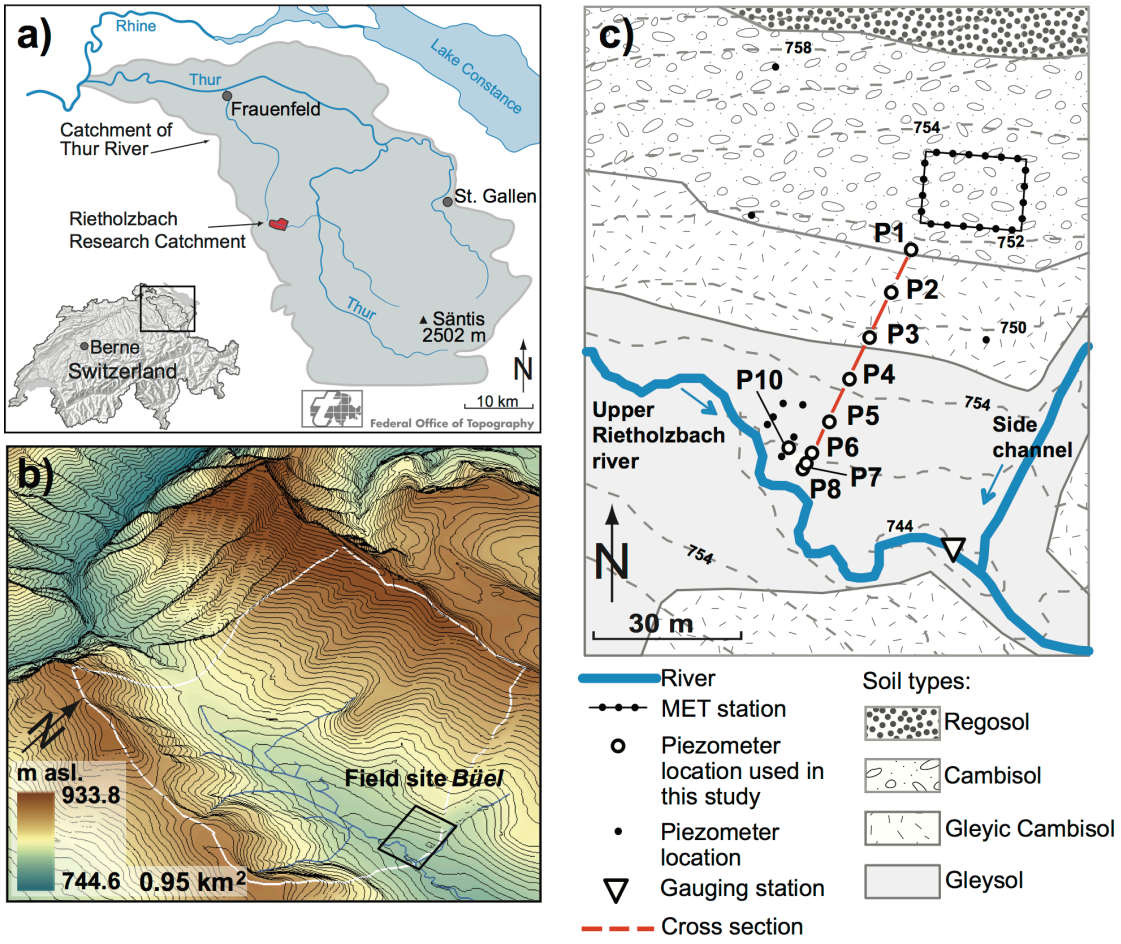

Figure 18 (a) Location of the Rietholzbach catchment (RHB) as part of the Thur basin in NE Switzerland; (b) Boundary of the Upper Rietholzbach sub-catchment (URHB) (white line) as the western part of the RHB and location of the Büel site (black square); (c) Büel site with observation network and main soil types (modified after KUHN (1980)); the side channel joins the URHB-river downstream of the gauging station.

Pleistocene Würm glacial moraine deposits (GMD) overlay the UFM in the valley bottom (Figure SI-3a and b). The GMD is characterized by a heterogeneous composition of conglomerates and quaternary gravel pockets (BALDERER, 1980). Hydraulic conductivities of the GMD-aquifer material were estimated by measuring the recovery rates of hydraulic head in several piezometers after a nearly instantaneous withdrawal of a groundwater volume (BOUWER and RICE, 1976). At the upper hillslope (piezometer locations P1, P2 and P3, Figure 18c) hydraulic conductivities range between 8E-6 m s^{-1} and 1E-4 m s^{-1} and become smaller towards the valley bottom with values between 1E-6 m s^{-1} and 3E-6 m s^{-1} (piezometer locations P5, P6 and P10, Figure 18c). Effective porosity in the GMD ranges from 0.05 to 0.1, as obtained from pumping tests in a neighboring catchment (BALDERER, 1980; VITVAR and BALDERER, 1997).

Soil core sampling and electrical resistivity tomography surveys revealed a several meters thick impermeable clay- and silt layer between GMD and UFM (VON FREYBERG et al., 2014). No groundwater was found beneath this layer, suggesting that the GMD is a perched aquifer, which is hydrologically disconnected from the UFM-aquifer in the valley bottom. The dominant soil types in the URHB are Regosols on the UFM, and Cambisols and Gleysols on

the lower slopes of the GMD and in the valley bottom areas, respectively (Figure 18c, Figure SI-3b). The soil texture of the Cambisol is gravely loam to clay loam with increasing clay contents towards the valley bottom (Mittelbach et al., 2012). After GERMANN (1981), soil depths range from less than 50 cm (Regosols) to up to 2 m (Cambisols).

III - 3 METHODS

III - 3.1 Monitoring and data processing

Near the catchment outlet the URHB is equipped with several 2"-piezometers for monitoring groundwater table responses at the hillslope-scale (Büel site, Figure 18c). Eight piezometers were installed in summer 2011 by Direct Push technology (*Geoprobe*®) along a 50 m-transect with the dimensions given in Table 6. In 7 piezometers of the transect groundwater table variations were recorded at 15 min-intervals with data loggers (*SensorTechnik Sirnach*, DL/N 70, accuracy 1 cm). During the study period, piezometer P7 served as the location for other experimental studies and, therefore, was not equipped with a data logger. The depth of the groundwater table below the soil surface (z_{gw} (L)) is denoted with positive values (Figure 19). The position of the deepest groundwater table recorded within the study period is symbolized with z_{min} (L) and the depth of the confining clay- and silt layer from the ground surface is z_{conf} (L).

Table 6 Properties of the piezometers installed at the Büel site in the URHB. The top edges of all piezometer pipes are between 8 cm to 22 cm below the ground surface (bsf).

Piezo-meter	Topographic height (m asl)	Installation depth (m bsf)	Depth of filtering (m bsf)	Depth to confining layer (m)	Distance to the river bank (m)	Data gaps due to logger failure (dd/mm/yy)
P1	751.64	5.2	1.2-4.2	5	53.3	-
P2	750.63	5.2	1.2-4.2	4.4	43.3	10/9-31/10/11
P3	749.75	4.2	1.2-3.2	3.8	33.3	
P4	748.28	3.1	1.1-2.1	2.4	23.3	6/9-30/10/12
P5	746.56	3.1	1.1-2.1	1.9[a]	13.3	10/5-4/6/12
P6	745.83	3	1.0-2.0	1.6[a]	6	1/7-26/7/11, 6/9-30/10/12
P7	745.59	3	1.0-2.0	1.5	4	-
P8	745.46	2.7	0.7-1.7	1.5	2.9	1/7-25/8/11

[a] No soil core was obtained. Depth was linearly interpolated from nearby measurements.

Because of the large measurement biases, up to 60 %, for solid precipitation in the URHB (GURTZ et al., 2003a), this study solely considers the snow-free periods from 1 March

to 31 October in 2011 and 2012. Time series of groundwater table depths are available the periods 1 July till 31 October, 2011 and 1 March till 31 October, 2012. Data gaps of up to 6 h were corrected by linear interpolation. Longer periods of missing groundwater table data are listed in Table 6.

Rainfall was recorded every 15 min at a meteorological station (MET) near the catchment outlet with a heated tipping bucket positioned 1.5 m above the ground (measurement error 3 – 15 %). Hourly sums of vertical percolation and actual evapotranspiration were obtained directly by mass-balance calculations from a weighting lysimeter (2.5 m deep and 2.0 m in diameter, measurement error 0.032 mm) following the post-processing procedure described in JAUN (2003). River discharge was monitored continuously every 15 min at the outlet of the URHB (*Ott Hydrometrie AG*, ODS4, measurement error up to 15 %). More information about the experimental set-up of the URHB can be found in SENEVIRATNE et al. (2012) and VON FREYBERG et al. (2014).

III - 3.2 A minimalistic, threshold-based model for the simulation of groundwater dynamics and event flow

To develop a simplistic yet robust method for the prediction of event streamflow generation in the URHB, we employ a parsimonious modeling approach that consists of two parallel, linear reservoirs (Figure 19).

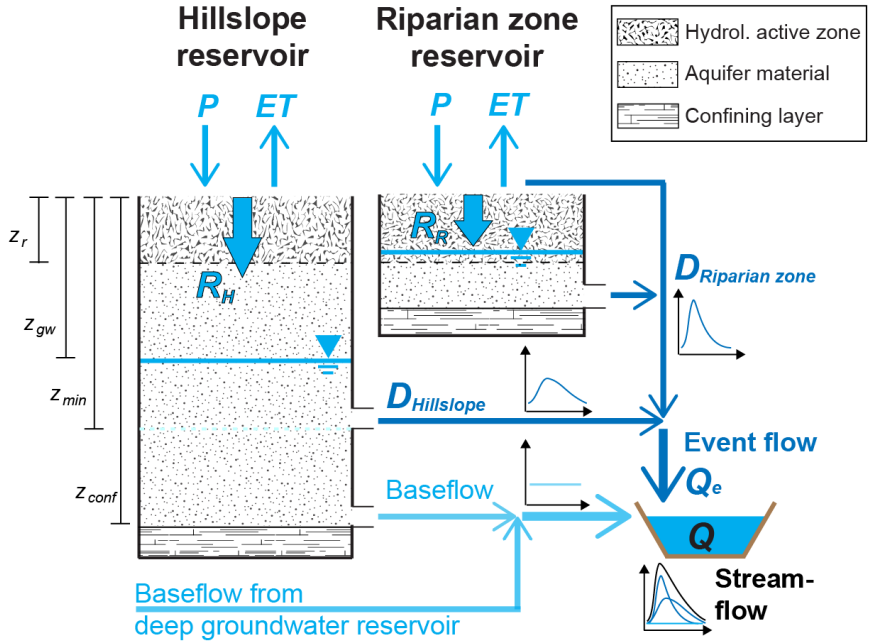

Figure 19 Schematic description of the minimalistic modeling concept consisting of two parallel, event-flow generating linear reservoirs (hillslope, riparian zone) and a baseflow reservoir. Following model parameters are presented: root zone depth (z_r); depth to groundwater table (z_{gw}); depth of the groundwater table (z_r); depth to the confining layer (z_{conf}); precipitation (P); actual evapotranspiration (ET); groundwater recharge (R); groundwater discharge (D); event flow (Q_e); total river streamflow (Q).

The reservoirs represent the hydrological landscape units (hillslope and riparian zone), and differ in terms of their subsurface properties that, in turn, define the dominant flow

processes. In the hillslope reservoir, infiltrating rainwater is assumed to percolate vertically to the groundwater aquifer and then as lateral matrix flow towards the river, resulting in a delayed and dampened groundwater discharge signal. For the riparian zone reservoir we simply assume that shallow subsurface stormflow and surface runoff is generated immediately when rainfall occurs.

The minimalistic model utilizes the linear soil-water balance model of RODRIGUEZ-ITURBE et al. (1999) to account for the competition between infiltration and evapotranspiration in the upper soil profiles of the two reservoirs. The storage capacity of this active soil layer is defined by its depth (z_r (L), typically the average rooting depth) and the soil porosity (φ_s (-)). The temporal evolution of relative soil water content (θ (-)) in the active soil layer is controlled by infiltration from rainfall, losses due to evapotranspiration and deep percolation beyond z_r.

The compensation of the daily soil water deficit (θ_{def} (-)) in the active soil layer triggers the occurrence of instantaneous deep percolation events (simulated groundwater recharge, R' (L T^{-1})). The daily soil water deficit (θ_{def} (-)) is the difference between the values of antecedent (θ_i (-)) and maximal soil moisture (θ^* (-)), which is typically between field capacity and full saturation. It is further assumed that the soil water content never falls below the wilting point θ_w. Accordingly, the water balance equation within the upper soil layer of a reservoir reads:

$$R'(t) = P(t) - ET(t) - z_r \cdot \theta_{def}(t) \tag{3}$$

where P (L T^{-1}) is rainfall, ET (L T^{-1}) is actual evapotranspiration and θ_{def} (-) is the soil water storage deficit at time t. Positive values of $R'(t)$ are defined here as simulated groundwater recharge with $R'(t) = 0$ when the right hand term of Eq. (1) becomes negative. A change of the unit-area groundwater volume ($\frac{dV_{gw'}(t,x)}{dt}$ (L T^{-1})) is presumed to depend linearly on recharge with the modulating factor φ (-) that is the effective porosity of the aquifer material:

$$\frac{dV_{gw'}(t,x)}{dt} = \frac{R'(t)}{\varphi} \tag{4}$$

Groundwater discharge is described with an exponential function to represent the recession of the groundwater storage (e.g., BEVEN, 2001; BRUTSAERT, 2005):

$$f(t) = c \cdot k_{gw} \cdot exp(-k_{gw} \cdot t) \tag{5}$$

In Eq. (5), c is a scaling constant to satisfy $\int f(t) = 1$ and k_{gw} is the inverse of the mean residence time of groundwater. The parameter k_{gw} can be estimated with the master recession curve separation tool of POSAVEC et al. (2010). The fully automated method fits sets of daily groundwater table recession curves that span at least 4 days to an overall exponential regression function. Unit-area groundwater discharge flux (D' (L T^{-1})) during two consecutive days (t_2, t_1) can then be simulated by convolution of the predicted recharge pulses ($R'(t)$) and the instantaneous unit hydrograph function ($f(t)$):

$$D'(t_2) = \int_0^t R'(t_2) f(t_2 - t_1) dt_1 \quad (6)$$

For the hillslope reservoir we assume an instantaneous infiltration of rainfall at the daily timescale, which makes the infiltration rate equal to the overall rainfall rate. Since an entirely rainfall-driven response of hillslope groundwater tables shall be simulated with this model, lateral influx of groundwater from other catchment areas is considered to be constant and can, therefore, be neglected (Figure 19).

For the riparian zone reservoir we assume that S_{def} is zero to simulate a direct runoff signal after rainfall occurs. Thus, Eq. (3) simplifies to $R'(t) = P(t) - ET(t)$ and k_{gw} = 1 d^{-1}, which corresponds to a mean residence time of 1 d, and the shortest time step in the model.

Total simulated event flow (Q_e' (L T^{-1})) is the sum of hillslope and riparian zone discharge (D_h', D_{rz}') from the areal portions (A_h, A_{rz} (-)) multiplied by α (-), which is the quotient of event-flow index (or 1 - baseflow index) and the portion of event-flow generating area (A_e (-)):

$$Q_e' = \alpha \cdot (A_h \cdot D_h' + A_{rz} \cdot D_{rz}') \quad (7)$$

III - 3.3 Estimation of hillslope groundwater recharge and discharge

Hillslope groundwater volume time series ($V_{gw}(x,t)$ (L^3 T^{-1})) were estimated from groundwater table observations to allow a robust evaluation of the minimalistic modeling concept:

$$V_{gw}(x,t) = l \cdot \varphi \cdot \int_{x=d_1}^{d_2} \int_{t=t_1}^{t_2} (z_{conf} - z_{gw}(x,t))\, dxdt \quad (8)$$

where l (L) denotes the width of the hillslope section, d_1 (L) and d_2 (L) mark its beginning and end perpendicular to l, t (T) indicates the time period from t_1 to t_2 and ($z_{conf} - z_{gw}$ (L)) is the saturated thickness of the aquifer above the confining layer (Figure 19). In order to consider only groundwater recharge and discharge relevant for event-flow generation, the observed depth to groundwater table (z_{gw}) in Eq. (8) is corrected for the deepest groundwater table recorded (z_{min}). It is assumed that leakage into the confining layer is negligible and that the composition of the aquifer is isotropic and homogeneous with an effective porosity φ (-).

Daily fluxes of hillslope groundwater recharge (R_h (L^3 T^{-1})) and discharge (D_h (L^3 T^{-1})) at the Büel site can then be estimated by the increase or decrease of groundwater volume over a time period (t_2-t_1), respectively:

$$\frac{V_{gw}(x,t_2) - V_{gw}(x,t_1)}{t_2 - t_1} = \begin{cases} > 0 \Leftrightarrow R_h(x,t) \\ < 0 \Leftrightarrow D_h(x,t) \end{cases} \quad (9)$$

An evaluation of the presented estimation method by means of streamflow- and lysimeter-seepage measurements will be carried out in section III - 4.2.

III - 4 RESULTS AND DISCUSSION

III - 4.1 Dominant flow processes and delineation of hydrological landscape units

The areal portions of the hillslope and riparian zone reservoirs are important model input parameters that depend on the hydrologic surface and subsurface properties of the catchment landscape. Thus, streamflow time series and groundwater table dynamics of the URHB were studied in detail and correlated to distinct landscape features.

III - 4.1.1 Streamflow analysis at the catchment scale

Overall, the hydrological regime of the URHB follows a distinct non-linear storage-discharge relationship (Figure SI-5) suggesting streamflow contributions from multiple storage reservoirs (MARTINA and ENTEKHABI, 2006). Deep groundwater discharge (baseflow) shows only minor temporal variability and comprises around 50 % of total annual streamflow (Figure SI-4). Baseflow-generation can be correlated to the substantial portion of Upper Freshwater Molasse (UFM) that underlies approximately 75 % of the URHB area (KOENIG et al., 1994; VITVAR and BALDERER, 1997). Since groundwater tables are deep in the UFM aquifer with mean residence times of more than one year (HEIDBÜCHEL et al., 2012; VITVAR and BALDERER, 1997), the baseflow signal is strongly dampened and not directly affected by climatic forcing (e.g., rainfall, evapotranspiration (Koenig et al., 1994)). This assumption is further supported by numerous perennial springs that originate from high-elevation regions of the URHB with underlying UFM (VON FREYBERG et al., 2014). The portion of baseflow was estimated with the recursive digital filter technique after NATHAN and MCMAHON (1990) by applying three passing times and a filter parameter of 0.95 to obtain a high degree of smoothing. Average baseflow indices of 0.5 from 1 March to 31 October 2011 and 0.6 from 1 March to 31 October 2012 were obtained, which are in good agreement with the long-term analysis (Figure SI-4), and thus can be considered representative for the long-term hydrological behavior of the URHB.

Streamflow rates above 2.8 mm d^{-1} (median flow) indicate a more dynamic hydrologic regime (Figure SI-4), which is mainly driven by rainfall events that activate quick groundwater fluxes and surface runoff. Source areas of this event-flow component of the hydrograph are therefore identified in the more permeable regions of the landscape adjacent to the river network, such as the valley bottom areas underlain by unconsolidated Quaternary GMD and on saturated or low-permeability soils that facilitate the generation of surface runoff (KOENIG et al., 1994).

III - 4.1.2 Groundwater dynamics at the Büel site

Water-table dynamics from 2011 and 2012 were analyzed with respect to the local surface- and subsurface properties at the Büel site in order to identify dominant event-flow

generating mechanisms in the GMD-unit. Figure 20 illustrates that the uppermost piezometer locations are characterized by deeper groundwater tables (z_{gw}) and a larger saturated thickness ($z_{conf} - z_{gw}$) compared to the near-stream piezometers (P4, P5, P6, P8). Steeper slopes of z_{gw}-distributions at low cumulative probabilities suggest rather dampened rainfall responses and a slow recession behavior of the groundwater tables at the uphill piezometers (P1, P2, P3). Therefore, slow vertical percolation though the vadose zone and lateral flux through the saturated soil matrix are likely to be the dominant groundwater flow pathways.

The near-stream groundwater tables showed a higher temporal variability, as is indicated by steeper slopes of the z_{gw}- and ($z_{conf} - z_{gw}$)-distributions in Figure 20. Further, generally small z_{gw}-values suggest the occurrence of full-saturation periods during rainfall events. At P5, the shallowest groundwater tables ($z_{gw}(P5) < 0.5$ m) occurred 13 % of the time (Figure 20a). A similar behavior was found for P4, P6 and P8 for $z_{gw} < 0.75$ m, although, the groundwater table did not reach the land surface. This indicates the existence of a high-transmissivity zone in the upper organic-rich soil layer that facilitates rapid lateral flux of shallow groundwater during rainfall (DAHLKE et al., 2012; LYON et al., 2006b). Such high-transmissivity zones can be formed by root channels, animal burrows and partially buried logs (BACHMAIR and WEILER, 2011).

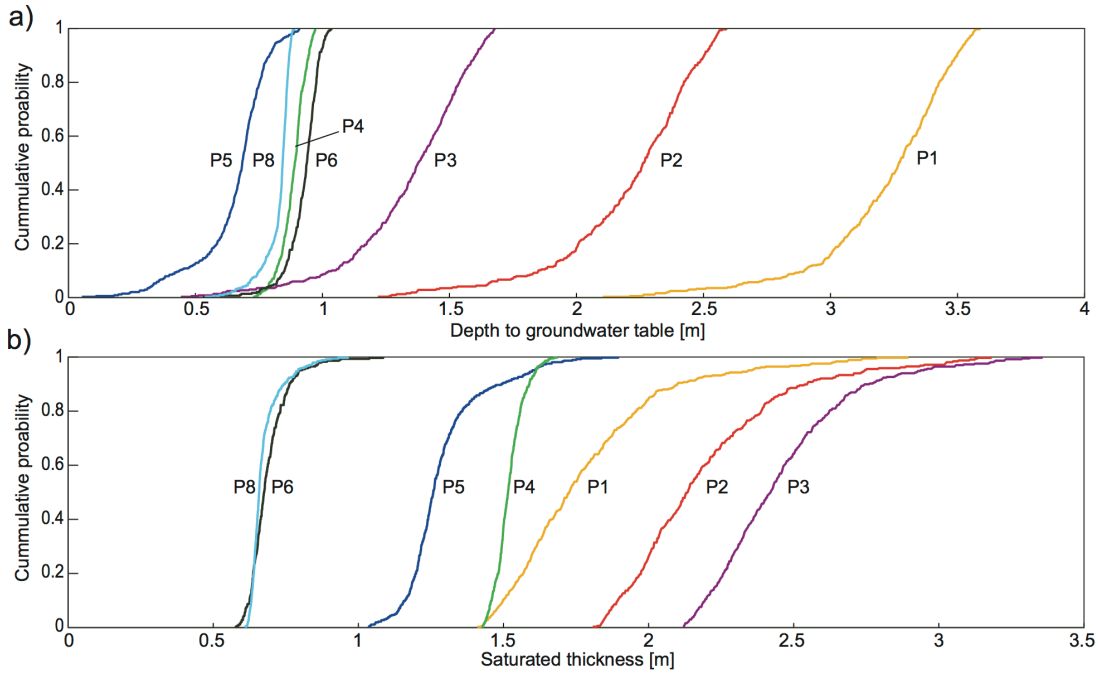

Figure 20 Cumulative probabilities of daily groundwater table dynamics at piezometer locations P1 to P6 and P8 during 1 July-31 October 2011 and 1 March-31 October 2012. (a) Groundwater tables below the ground surface (z_{gw}); (b) saturated thickness above the confining layer ($z_{conf} - z_{gw}$). Due to the shallow slope of the confining layer $z_{conf} - z_{gw}$ was largest around the middle of the transect (P2, P3) and not at the uppermost location (P1), where $z_{conf} - z_{gw}$ was on average 0.6 m smaller.

Measured infiltration rates ranged from 0 – 2.6E-5 m s^{-1}, with a distinct zone of low permeability at the flat bottom area of the Büel site that is underlain by Gleysol (infiltration rates 0 – 6.7E-6 m s^{-1}, arithmetic mean 3.7E-6 m s^{-1}, 5 plots). The permeability of the soil increased towards further uphill areas. At measurement locations near the MET, where

Cambisol can be found, infiltration rates were between 1.0E-5 and 2.6E-5 m s^{-1} (arithmetic mean 1.8E-5 m s^{-1}, 6 plots). This suggests that the storage deficit in the flat near-stream zone is very small, likely due to capillary rise from the shallow water table and low hydraulic permeability, that does not allow significant infiltration. Consequently, the absolute volume of groundwater recharge from percolating rainwater is presumably very small in this part of the Büel site. Instead, rainfall is likely to cause saturation excess, which triggers instantaneous overland flow and shallow subsurface stormflow in the uppermost soil layer (MCGRATH et al., 2007).

Accordingly, the Büel site can be discretized into the two hydrological landscape units: riparian zone (uphill piezometers P5, P6, P7, P8) and hillslope (near-stream piezometers P1, P2, P3) with piezometer P4 as the transition zone at a distance of 23.3 m from the riverbank. Similarly, the event-flow generating landscape units in the URHB are delineated as follows: shallow watershed areas (slopes < 7 °) adjacent to the river network underlain by peaty soils and Gleysols are assigned riparian zones, whereas Cambisols overlying the GMD in the intermediate area of fractured bedrock aquifer and riparian zones are allocated to hillslopes. Thus, riparian zones and hillslopes approximately cover 7.5 % (A_{rz}) and 17.7 % (A_h) of the URHB area, respectively. The remaining fraction of 74.8 % accounts for strongly damped discharge of deep groundwater (baseflow), which does not contribute to event-flow in the applied framework.

III - 4.2 Estimation of hillslope groundwater recharge and discharge from observed groundwater table data

To evaluate the representativeness of the hydrological landscape properties at the Büel site for the entire URHB, estimated hillslope groundwater volume (V_{gw}) and recharge (R) were compared to streamflow (Q) and lysimeter-seepage measurements. For this, Eq. (8) was applied with x = 23.3 m, d = 53.3 m (hillslope section from P1 to P4) and $\varphi = 0.075 \pm 0.025$ (BALDERER, 1980). Here, daily unit-area groundwater volume (V_{gw}) was calculated with respect to z_{min} to account solely for the event-flow generating portion of the hillslope groundwater storage (Figure 19).

A significant linear correlation between V_{gw} and Q was found for periods with $Q < 2.8$ mm d^{-1} ($R^2 = 0.64$, $p < 0.0001$, grey shaded areas in Figure 21) indicating that hillslope groundwater is the dominant source of streamflow during low and median-flow conditions (Figure SI-4). During high flow with $Q > 2.8$ mm d^{-1} the correlation becomes more scattered because most flood peaks occurred before the maximum hillslope groundwater volume was reached ($R^2 = 0.31$, $p < 0.0001$). Such extreme events can be attributed to non-stationary hydrological responses that were contingent on rainfall intensity and initial conditions of the streamflow contributing areas (e.g., local soil water storage deficit).

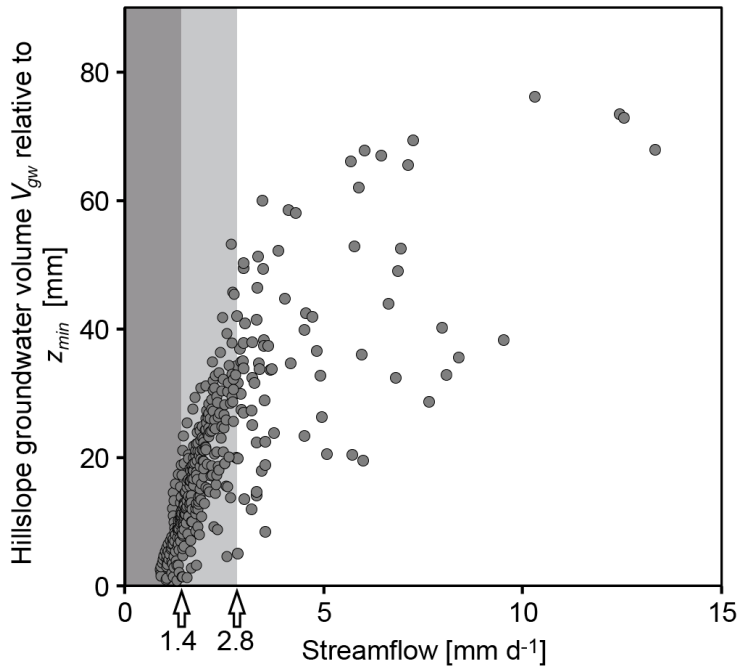

Figure 21 Daily streamflow of the URHB (Q, including baseflow) versus estimated hillslope groundwater volume V_{gw} (φ = 0.075) during 1 July-31 October 2011 and 1 March-31 October 2012. The grey shaded areas indicate baseflow (Q < 1.4 mm d^{-1}, dark grey) and conditions below median flow (Q < 2.8 mm d^{-1}, light grey). The same ranges of flow conditions are valid for porosities of φ = 0.05 and 0.1, respectively.

Further, the estimation method (section III - 3.3) is corroborated by a significant linear correlation between monthly estimated hillslope groundwater recharge (R) and lysimeter seepage ($R^2 = 0.97$, $p < 0.001$, data points of March and August 2012 were excluded in the linear regression, see caption of Figure 22). Slopes between 2.2 ($\varphi = 0.05$) and 1.3 ($\varphi = 0.1$) for the linear regression indicate an underestimation of R in relation to lysimeter seepage. This can be explained with the isolated soil column of the lysimeter that only allows vertical flow and prevents a hydraulic connection with the groundwater (GURTZ et al., 2003a). Thus, the open drainage collection system of the lysimeter base in 2.5 m depth allows quicker outflow of percolate compared to the surrounding undisturbed soil with a deeper zone of low-pressure head (e.g., median $z_{gw(P1)} > 3$ m) (HEALY and SCANLON, 2010). Nevertheless, since the differences between R and lysimeter seepage are consistent, Eq. (8) and (9) with $\varphi = 0.1$ are considered applicable for providing a basis of comparison with the results of the minimalistic model.

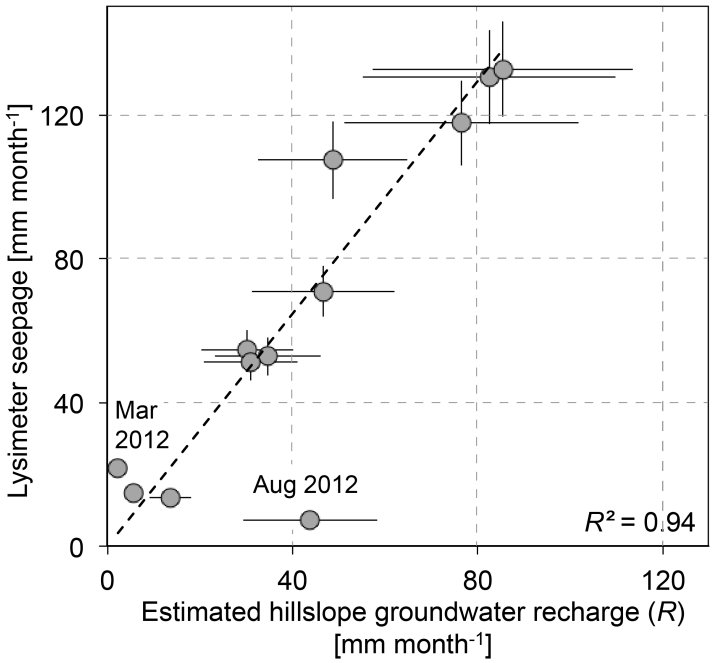

Figure 22 Estimated monthly mean hillslope groundwater recharge during 1 July-31 October 2011 and 1 March-31 October 2012. Whiskers of groundwater recharge describe the uncertainties for effective porosities (φ) ranging between 0.05 and 0.1 and for the lysimeter seepage a 10 % measurement uncertainty (SENEVIRATNE et al., 2012). The dashed line indicates the linear regression function with a slope of 1.62. The data point of March 2012 was excluded from the analysis due to logger failure at the lysimeter set-up. Further, the lysimeter seepage in August 2012 was considered unrepresentative since the physical properties of the weighting lysimeter lead to an anomalous high soil moisture deficit in this month compared to the surrounding environment (GURTZ et al., 2003a). Due to the absence of a groundwater table and the prevention of lateral groundwater flow into the lysimeter cylinder, a soil moisture deficit caused by evapotranspiration cannot be replenished by capillary rise and may persist over longer time periods. It is assumed that such a high soil moisture deficit developed in the lysimeter in July 2012, leading to very low seepage rates in August 2012, where only 12 % of the average seepage rate (59 mm month^{-1}) was measured.

III - 4.3 Simulation of hillslope groundwater dynamics

Hillslope groundwater dynamics were simulated with the minimalistic modeling approach (section III - 3.2) by utilizing daily rainfall and actual evapotranspiration data from the MET and following site-specific input parameters: z_r = 0.3 m, (GERMANN, 1981; SENEVIRATNE et al., 2012), θ^* = 0.34 and θ_w = 0.17 according to a clay loam (DINGMAN, 2002). The effective porosity of the aquifer material (φ) was set equal to 0.1 based on the above analysis. The hillslope reservoir was treated as a single hydrological unit with homogeneous subsurface properties and spatial uniform soil moisture deficit. The master recession curve separation tool of POSAVEC et al. (2010) was run with the estimated daily groundwater volume time series (V_{gw}) to obtain the parameter k_{gw} = 0.09 d^{-1}, which represents an average residence time of $1/k_{gw}$ = 11 d.

Figure 23a and b show that the hillslope reservoir model captured timing as well as amplitude for most of the recharge events as indicated by the synchronous behavior of the cumulative sums of R_h and R_h' as well as D_h and D_h'. For both years the modeled values were

only slightly below the estimates (2011: $\Sigma R_h - \Sigma R_h' = 8.2$ mm, $\Sigma D_h - \Sigma D_h' = 12.2$ mm, 2012: $\Sigma R_h - \Sigma R_h' = 5.7$ mm, $\Sigma D_h - \Sigma D_h' = 40.9$ mm). A few recharge responses after dry periods were underestimated by the model (e.g., October 2011, July to August 2012), suggesting that evapotranspirative losses entirely compensated incoming rainfall in the upper soil layer of the hillslope reservoir. Because the model does not account for capillary rise or groundwater influx from other reservoirs, soil moisture deficits are thus more persistent and recharge is smaller than the estimates from the Büel site.

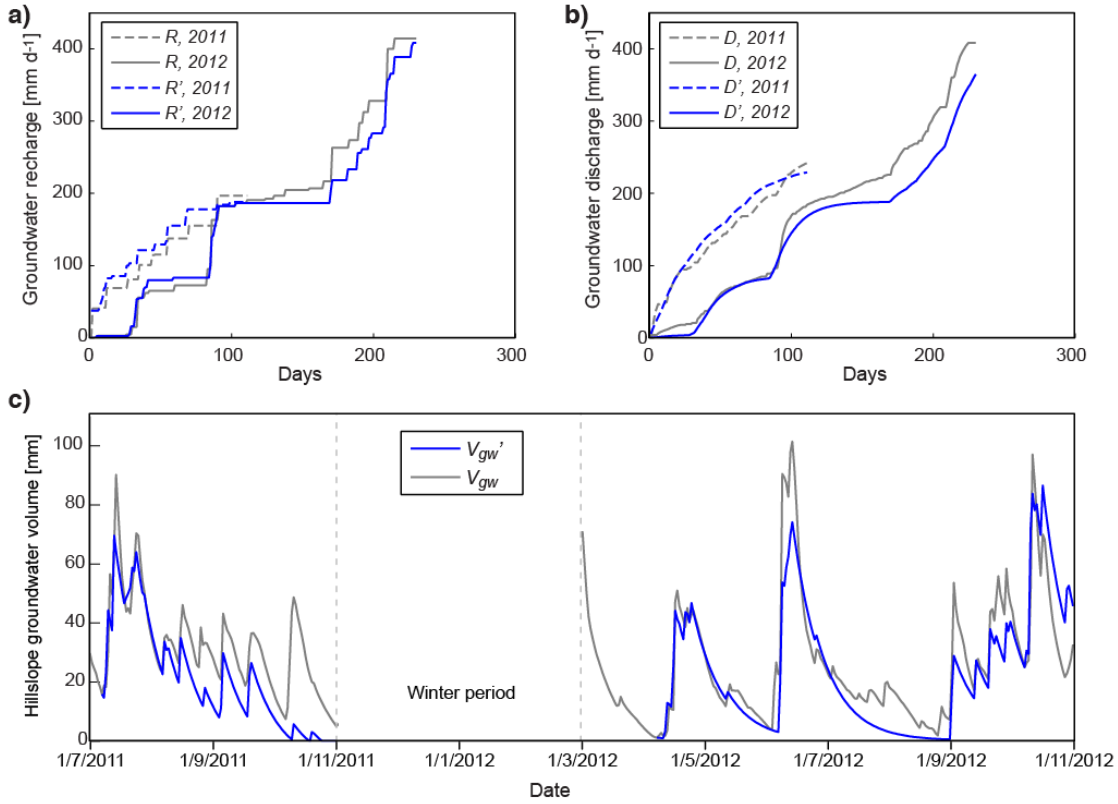

Figure 23 Comparison of cumulative sums of (a) estimated (R, grey) with simulated groundwater recharge (R', blue) and (b) estimated (D, grey) with simulated (D', blue) groundwater discharge per day and unit area from the hillslope reservoir during 15 July-31 October 2011 (dashed line) and 15 March-31 October 2012 (continuous line); the first 15 days of each simulation year were neglected; (c) Time series of estimated (V_{gw}, grey) and simulated (V'_{gw}, blue) groundwater volume; initial values of $V'_{gw}(t)$ were first observed minimum $V_{gw}(t)$ for each year (t = 7 July 2011 and t = 7 April 2012, respectively); effective porosity of the aquifer (φ) is 0.075.

Further, the evaluation of model performance with R^2, p-value, Nash-Sutcliffe efficiency (NSE) and percent bias (P_{bias}) shows that the hillslope reservoir model represents the groundwater dynamics in the hillslope aquifer sufficiently ($R^2 = 0.78$, $p < 0.001$, $P_{bias} = -34.0$, $NSE = 0.85$, Figure 23c). The general underprediction of V_{gw}' can be explained with the initial values in Eq. (3) used for each simulation year. Nevertheless, the minimalistic model was capable of reproducing rainfall responses and recession behavior of the observed groundwater table, particularly during large rainfall events (e.g., July to August 2011 and summer 2012).

III - 4.4 Simulation of event-flow hydrographs at the catchment scale

The minimalistic hydrological model with two linear reservoirs (riparian zones and hillslopes) was applied to simulate the event-flow hydrograph (Q_e) of the URHB during the snow-free periods in 2011 and 2012. First, event-flow was simulated with the lowest degree of (spatial) complexity and thus with fixed areal portions of the hydrological landscape units (constant contributing areas, CCA) based on the findings in section III - 4.1. Second, the role of spatial variability of the landscape units on the hydrologic regime was assessed by implementing the variable contributing areas concept (VCA) into the minimalistic model.

III - 4.4.1 Constant contributing areas (CCA)

The minimalistic model with CCA (A_{rz} = 7.5 % and A_h = 17.7 % of A_{tot}, respectively) provided a good fit between the observed and simulated event hydrograph with $R^2 = 0.67$, $p < 0.001$, $P_{bias} = 6.2$ and $NSE = 0.64$ (first months of each predicted year were used as initiation period and thus were excluded from this analysis, Figure 24b).

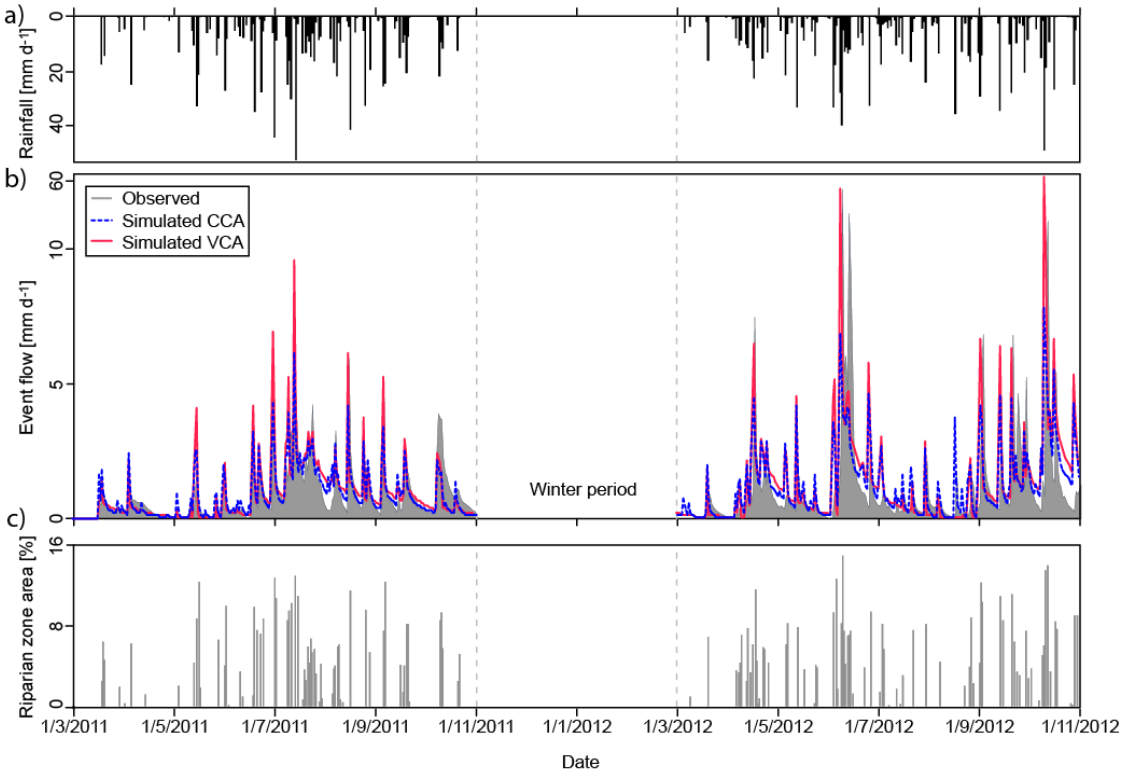

Figure 24 (a) Daily rainfall; (b) Event hydrograph predictions with CCA and VCA: Observed (grey shaded areas) and simulated event hydrographs with constant (blue dashed) and variable (red solid) portions of hydrological landscape during 15/3-31 October 2011 and 15/3-31 October 2012; event flow is streamflow minus baseflow, which was estimated by the recursive filter method of NATHAN and MCMAHON (1990); (c) Portion of riparian zone relative to the total catchment area.

Despite the invariant riparian-zones area, the temporal variability of this event-flow component was simulated adequately, i.e. a large contribution at the beginning of rainfall events due to surface runoff and shallow subsurface stormflow. The increasing wetness state of

the catchment during progressing rainfall was reproduced well by predicting delayed hillslope groundwater discharge that causes a slower recession of the event-flow hydrograph. However, large flood peaks ($Q_e > 4$ mm d^{-1}) during short, high-intensity rainfall events with more than 35 mm of rain were underpredicted by the minimalistic model and CCA (e.g., June 2011).

The simulated response to smaller rainfall events, however, often exceeded the observations (e.g., July-August 2012). This is likely to be caused by the initial values used in Eq. (3) and the assumption of an invariant riparian zone area that omits shrinking and expanding saturated areas during dry and wet periods, respectively (BEVEN and KIRKBY, 1979; DUNNE and BLACK, 1970).

Nevertheless, the applied delineation rule for hydrological landscape units (section III - 4.1) could be verified by fitting the simulation results of 2011 and 2012 to total observed Q_e. Presuming a total event-flow generating area of 25.2 % of A_{tot}, an optimal fit was obtained for A_{rz} = 8.8 % and A_h = 16.7 %, which is in line with the results presented in section III - 4.1.

III - 4.4.2 Variable contributing areas (VCA)

The VCA-concept was implemented into the minimalistic model with a non-linear relationship between the portion of the riparian zone (A_{rz}) and effective precipitation (P_e) following the modified SCS-CN equation approach of DAHLKE et al., (2009). With this, the area of the riparian zones varied between 0 % and 14 % of A_{tot} during the observation period (Figure 24c). Detailed calculations of the VCA are shown in the supplementary information of part III.

Similar to the CCA approach, the simulated event-flow hydrograph with VCA provided a slightly better fit with a smaller deviation to observed Q_e ($R^2 = 0.68$, $p < 0.001$, $P_{bias} = -3.3$, $NSE = 0.67$, first month of prediction excluded, Figure 24b). Since the single-valued indices R^2 and NSE are generally very sensitive to outliers and sample size (MORIASI et al., 2007), model performance was evaluated by comparing flow duration curves (*fdc*) of Q_e' with VCA and CCA against observed Q_e. A *fdc* captures the entire distribution of event flow rates that facilitates a more efficient assessment of model performance. Figure 25a indicates that the model with VCA generally captured the event-flow regime better than the model with CCA, i.e., over a wider range of streamflow conditions. Nevertheless, for event flow between 0.5 mm d^{-1} and 3 mm d^{-1} the model with VCA gave similar results as with CCA. The biggest flood events (90th percentile, $Q_e > 2.3$ mm d^{-1}), however, were captured more effectively when the model accounts for VCA (inset of Figure 25a). While the VCA concept provided a good fit during medium and high-event-flow conditions, streamflow responses to short and low-intensity rainfall events with $Q_e < 0.3$ mm d^{-1} were captured better by the CCA approach (Figure 25a). This can largely be correlated to the under-prediction of rainfall responses during July - August 2012 (Figure 24a) that results in a larger offset of the VCA-*fdc* during the 2012 observation period compared to the previous year (Figure 25b and c, Figure SI 8). Model performances with CCA or VCA are comparable, although, median- and peak-flow events were captured more efficiently when the model accounted for spatial variability of the landscape units. During long and high-intensity rainfall events that compensate the soil-water storage deficit in the adjacent lower hillslopes, the riparian zones expand and more shallow

subsurface stormflow and surface runoff is generated. Although the absolute range of spatial variability (0-14 %) was small compared to the total URHB-catchment area, it strongly affected the simulated event-flow hydrograph, particularly during extreme events. For average flow conditions, however, the areal portions of the landscape units can be considered invariant in time and the minimalistic model with CCA provides a sufficient representation of the event-flow regime of the URHB.

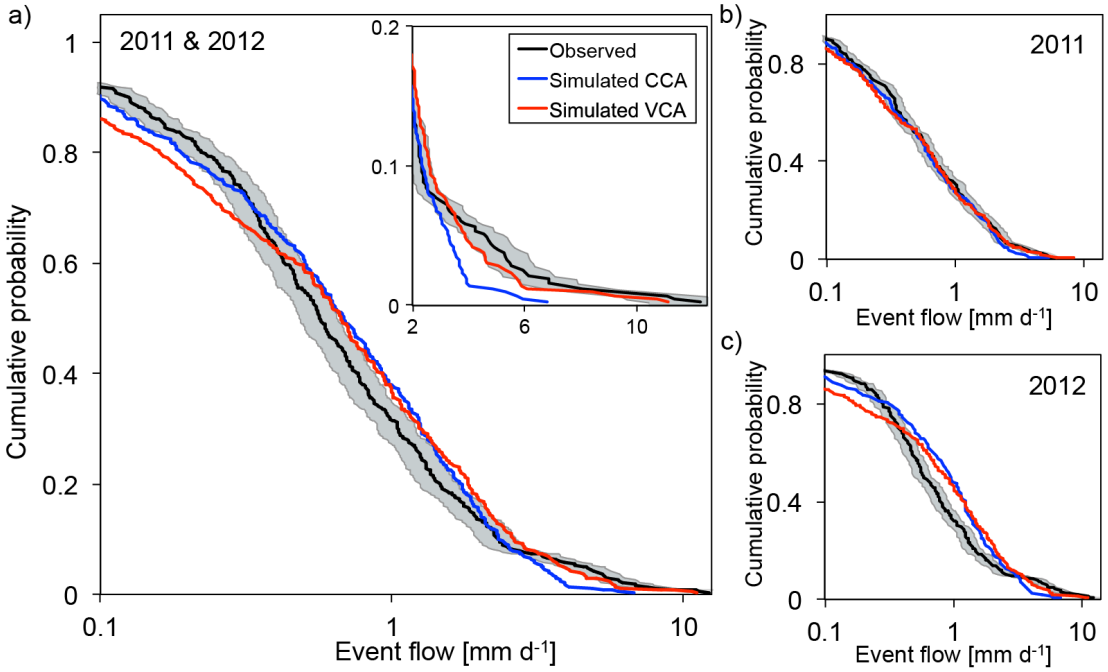

Figure 25 Comparison of flow duration curves (fdc) of observed (black line with uncertainty bounds of 15 % in grey) and simulated event flow assuming constant contributing areas (CCA, blue line) and variable contributing areas (VCA, red line); please note the logarithmic x-axis; (a) Whole observation period (1 March-31 October 2011 and 1 March-31 October 2012), each first month was used as initialization period in the model and was excluded from the analysis, the inset figure shows the fdc for the upper 20th percentile of event flow rates (linear x-axis); (b) 2011 observation period; (c) 2012 observation period.

III – 5 CRITICAL EVALUATION OF THE MODELING RESULTS AND IMPLICATIONS FOR THE CONCEPTUALIZATION OF MOUNTAINOUS CATCHMENT HYDROLOGY

A minimalistic framework was applied to test whether the hydrological behavior of a mountainous catchment can be explained by the event-flow generation at two landscape units. With only a limited number of parameters and no calibration the minimalistic model gave robust results with high predictive power. It captured the main hydro(geo)logical dynamics (e.g., timing and amplitude of hillslope groundwater volume re- and discharge, event-flow hydrograph) and provided insight into the effect of climate drivers on hillslope groundwater storage and surface runoff generation at distinct landscape units in a complex environment. In the case of the URHB, the utilization of such a minimalistic modeling scheme was facilitated

by the fact that only a small fraction of the area (~25 %) actively contributes to event flow. Similar observations were made in other mountainous headwater catchments (e.g., JAMES and ROULET, 2009; MCGLYNN and SEIBERT, 2003; PENNA et al., 2011) indicating that a consolidation of a complex landscape into hillslopes and riparian zones might provide a foundation for future studies at larger scales or at other sites. Major limitations of the minimalistic modeling framework that are determined by the initial assumptions, will be discussed hereafter and in the supplementary information of part III (Figure SI-7 and Figure SI 8).

III - 5.1 Sensitivity analysis

A qualitative sensitivity analysis of the model key parameters was carried out for both the CCA- and VCA-concept (Figure SI-7). It reveals that the soil-water content threshold value (θ^*) is the most important control on the hydrologic simulations, because it defines the maximum storage deficit in z_r, and thus the intensity of groundwater-recharge events. The model is less sensitive to the other soil-water storage properties, such as soil porosity (φ_s), root zone depth (z_r) and wilting point (θ_w), that dominantly control hillslope groundwater contributions to low- and medium flow events. The effects of the groundwater residence time (i.e., groundwater recession constant, k_{gw}) are more pronounced towards higher k_{gw}-values since a faster drainage of groundwater from the hillslope reservoir would result in an under-estimation of event flow.

Overall, the model with CCA shows a smaller sensitivity to the input parameters compared to the VCA-concept, where the hillslope- and riparian zone areas shrink or expand during heavy rainfall events, respectively, that may amplify parameter-induced model bias.

III - 5.2 Total event-flow generating area

A few of the larger peak flow events were not captured by the minimalistic model, both with the CCA- and VCA-concepts, such as the rainfall events between 31 May – 13 June 2012 and 19 - 27 September 2012 (Figure 24b). It may be that this is related to the conceptualization of a total event-flow generating area that comprises maximal 25.2% of A_{tot}. This may, in turn, limit the maximum areal portions of the hillslopes or riparian zones in the conceptual model.

In order to assess the possible spatial range of the event-flow generating area with respect to the saturated portion (A_{rz}), the runoff coefficients (Q_e/P) for a series of three rainfall events between 31 May – 13 June 2012 were analyzed in detail (see supplementary information of part III). Fitting of Q_e' with the areal estimates from section III - 4.4 (CCA) to observed Q_e revealed that the riparian zone area expanded from around ~5 % and ~7 % during the first two events to ~24 % of A_{tot} during the last rainfall period (Figure SI 8). This value seems reasonable under the assumption that shallow subsurface stormflow in the uppermost high-transmissivity soil zone also occurs on the hillslopes when antecedent soil-water conditions were highest, as was the case during the third event. Similar threshold-like behavior was observed at other experimental hillslopes (e.g., BACHMAIR and WEILER, 2011; DAHLKE et

al., 2012; LYON et al., 2006a). Implementation of this process into the modeling framework would require a variable storage parameter in the modified SCS-SN equation that also accounts for antecedent moisture conditions in the hillslopes (DAHLKE et al., 2012). The determination of such a highly non-linear relationship, however, is challenging and would significantly increase model complexity and uncertainty. Nevertheless, the minimalistic model with VCA captured the event-flow responses to most of the other high-intensity rainfall events adequately, despite the fact that an invariant event-flow generating area (25.2 % of A_{tot}) and a static storage parameter were presumed (Figure SI 8, Figure 25).

III – 6 CONCLUSIONS

Prediction of hydrograph responses in mountainous catchments requires the identification of surface and subsurface properties and a holistic understanding of the dominant streamflow-generating mechanisms. Therefore, the presented study systematically analyzed landscape features and hydrometric data during the snow-free periods of 2011 and 2012 and applied a minimalistic modeling approach to simulate groundwater storage dynamics at different hydrological landscape units and event-flow generation in the small URHB headwater catchment. The following dominant landscape units and related hydrological processes can be described:

- The spatial distribution of aquifer geology, slopes, soil types and -depths are the major surface and subsurface properties that determine the spatial extent of the hydrological landscape units where baseflow and rainfall event-driven flow (event flow) are generated.

- Deep groundwater discharge originates dominantly from the fractured UFM-aquifer that accounts for ~75 % of the URHB area. The event-flow generating area comprises the remaining ~25 % of the URHB, whereas riparian zones and hillslopes cover areas of ~8 % and ~17 %, respectively.

- During rainfall, hillslopes contribute shallow groundwater to the URHB-river, while riparian zones generate surface runoff and shallow subsurface stormflow due to a reduced infiltration capacity. The riparian zone discharge leads to very short response times of the event-flow hydrograph and is dominant during peak flow.

- A minimalistic threshold-based modeling scheme, that assumes event-flow generation from two parallel linear storage reservoirs with constant contributing areas (CCA), was found to be sufficient to predict the overall hydrological regime of the URHB.

- The area of the riparian-zones expands by up to 14 % when wet antecedent moisture conditions coincide with high-intensity rainfall periods. Consequently, implementation of the variable contributing area concept (VCA) into the minimalistic model improves the overall performance and large flood events can be simulated more effectively.

This study confirms previous observations that stress the important role of landscape properties and variable contributing areas as first-order controls on the hydrological functioning of mountainous headwater catchments. For this, the analysis of groundwater dynamics was shown to facilitate a better understanding of the relationships between climatic drivers (e.g., rainfall, evapotranspiration), subsurface properties and streamflow generation.

Prospective application of this framework could involve the identification of hydrological landscape units that coincide with areas of fertilizer application in agricultural catchments, allowing an efficient assessment of potential source areas of surface water pollution. Spatiotemporal variability of event-flow generating areas was found to strongly affect peak flow rates during larger rainfall events due to hydrologically activated hillslopes adjacent to riparian zones. Hence, this process can be expected to exacerbate pollutant export from agricultural areas. Because mountainous catchments serve as vital ecological habitats and important freshwater resources, future work is needed to address these concerns and to evaluate the role of shallow groundwater dynamics and variable contributing areas for the hydrologic and biogeochemical regime in these regions.

SUPPLEMENTARY INFORMATION OF PART III

Table SI-6 List of abbreviations and model parameters

Parameter	Symbol	Unit	Model input value
Soil moisture content	θ	-	-
Soil moisture deficit	θ_{def}	-	-
Soil moisture threshold	θ^*	-	0.34
Permanent wilting point	θ_w	-	0.17
Aquifer effective porosity	φ	-	0.05-0.1
Event-flow generating area	A_e	%	25.2
Areal portion of the hillslopes	A_h	%	17.7 (CCA), 2.7 – 17.7 (VCA)
Areal portion of the riparian zones	A_{rz}	%	7.5 (CCA), 0 - 14 (VCA)
Total catchment area	A_{tot}	L^3	944049 m^2
Estimated hillslope groundwater discharge	D_h	$L\,T^{-1}$	-
Simulated hillslope groundwater discharge	D_h'	$L\,T^{-1}$	-
Actual evapotranspiration	ET	$L\,T^{-1}$	-
Hillslope groundwater recession constant	k_{gw}	T^{-1}	0.09 d^{-1}
Depth to groundwater table	z_{gw}	L	-
Rainfall	P	$L\,T^{-1}$	-
Effective rainfall	P_e		-
Event flow (streamflow minus baseflow)	Q_e	$L\,T^{-1}$	
Simulated event flow	Q_e'	$L\,T^{-1}$	
Total URHB-river streamflow	Q	$L\,T^{-1}$	-
Estimated hillslope groundwater recharge	R_h	$L\,T^{-1}$	-
Simulated hillslope groundwater recharge	R_h'	$L\,T^{-1}$	-
Estimated hillslope groundwater volume	V_{gw}	$L^3\,T^{-1}$	-
Simulated hillslope groundwater volume	V_{gw}'	$L^3\,T^{-1}$	-
Depth to confining layer	z_{conf}	L	-
Depth of groundwater table	z_{gw}	L	-
Depth of active soil layer	z_r	L	300 mm

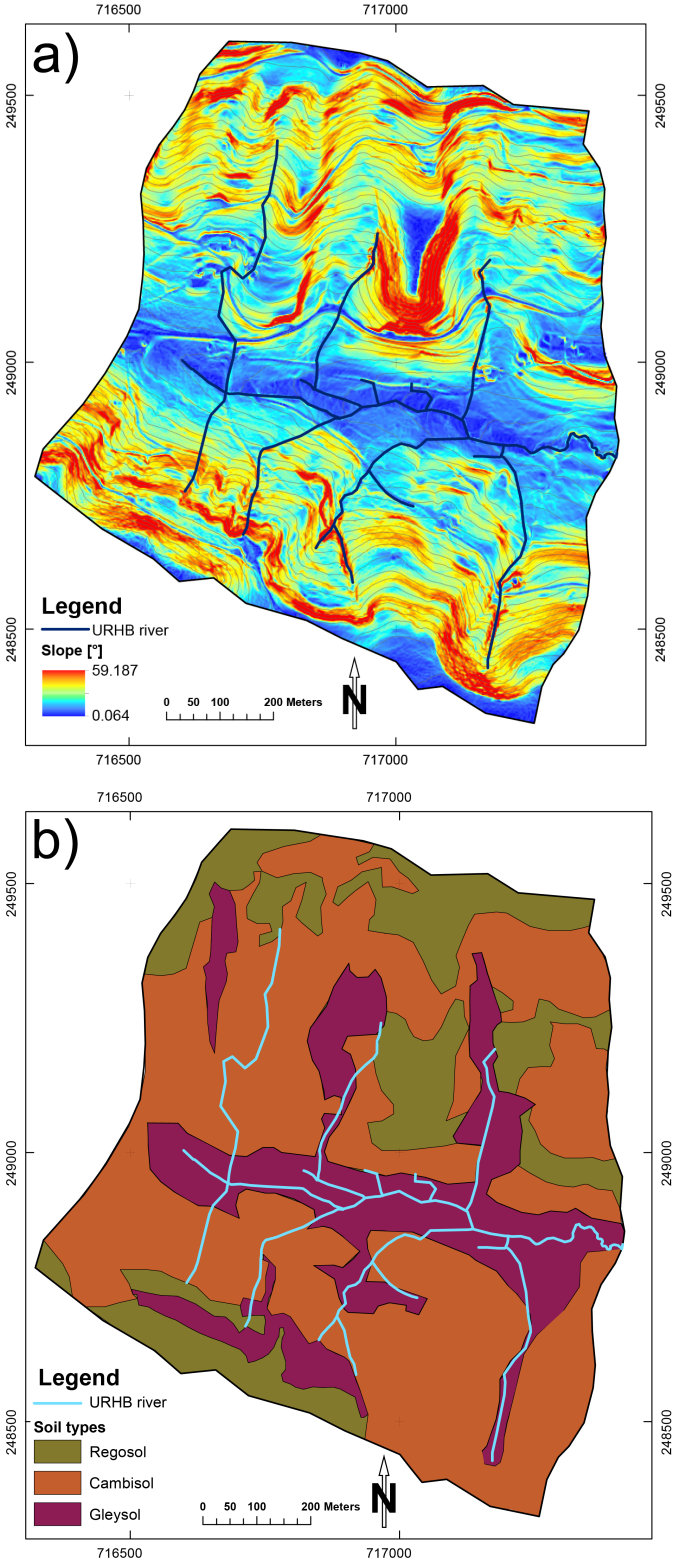

Figure SI-3 Landscape properties of the URHB. (a) slopes (°) of the URHB based on a 2 m × 2 m DEM; (b) soil types distribution in the URHB, adapted from KUHN (1980).

Flow duration curve analysis

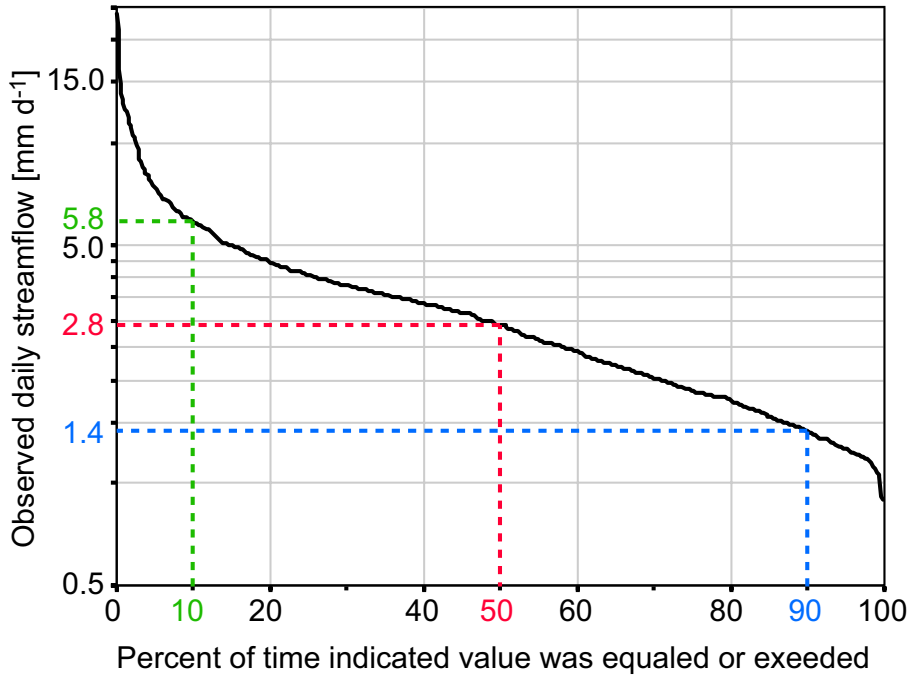

Figure SI-4 Flow duration curve of daily streamflow of the URHB per unit area for 1 March till 31 October (snow-free periods) of the years 2008 - 2012.

The visualization of streamflow data as flow duration curve (*fdc*) allows for identification of dominant effects of landscape properties on the overall hydrological response and facilitates an estimation of the groundwater contribution to catchment outflow (NATHAN and MCMAHON, 1990; SMAKHTIN, 2001). Figure SI-4 depicts the *fdc* of URHB-discharge from 1 March to 31 October (snow-free periods) of the years 2008 - 2012. The *fdc* shows a wide range of flow conditions with values of Q between 0.9 mm d^{-1} and 23.8 mm d^{-1}. The steep slope of the *fdc* between $Q_{0\%}$ and $Q_{10\%}$, with streamflow rates exceeding median flow up to one order of magnitude, suggests a large variability of flow during flood events. Small changes of flow beyond $Q_{10\%}$ indicate sustainable low-flow rates and a significant contribution of groundwater to the URHB streamflow hydrograph. Median flow ($Q_{50\%}$) of the 5-year time series was approximately 2.8 mm d^{-1}. The portion of deep groundwater can be estimated by the ratio $Q_{90\%}$: $Q_{50\%}$ (NATHAN and MCMAHON, 1990) that is approximately 50 % of total river discharge.

Analysis of streamflow recession behavior

The temporal evolution of discharge in relation to catchment storage was analyzed by studying the streamflow recession behavior, which reveals information about the properties of the groundwater reservoir (BRUTSAERT and NIEBER, 1977). This builds the foundation for the estimation of catchment storage and groundwater recharge (WITTENBERG, 1999).

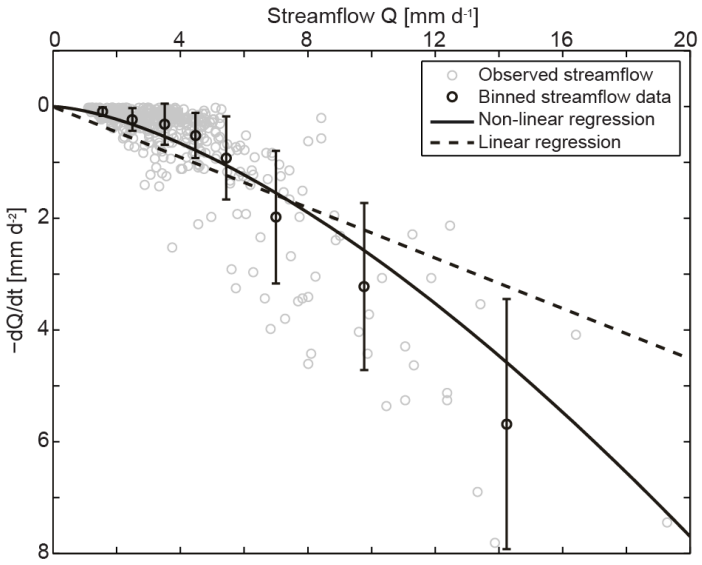

Figure SI-5 Binned streamflow recession rates versus average streamflow of two consecutive days (dots) and fitted linear (dashed line) and power law (solid line) recession curves of observed daily streamflow of the URHB for 1 March till 31 October (snow-free periods) of the years 2008 - 2012. Bin intervals of Q were chosen with respect to the density of data points and are (in mm d-1): 0.1-2, 2-3, 3-4, 4-6, 6-8, 8-12, 12-22. Error bars indicate the standard deviation of -dQ/dt within the bin intervals. The obtained recession curve analysis parameters are $k = 0.23\ d^{-1}$ *for the linear and* $b = 0.27\ cm\ d^{-2}$ *and* $a = 1.53$ *for the power law regression function, respectively.*

On a daily timescale, streamflow recession rates ($-dQ/dt$) can be estimated as the difference of Q between two consecutive days ($-dQ/dt = (Q_{t-\Delta t} - Q_t)/\Delta t$). By plotting the average streamflow ($Q = (Q_{t-\Delta t} + Q_t)/2$) against ($-dQ/dt$) a regression function with its characteristic parameters can be fitted to the data. Here, a linear ($-dQ/dt = k \times Q(t)$) as well as a power law function ($-dQ/dt = a \times Q(t)^b$) was fitted to the data by means of least square regression. Q and dQ/dt of the URHB-river cover a wide range of data and thus were binned according to Q to best visualize their mutual relationship (Figure SI-5, see figure caption for more details). Figure SI-5 indicates a better fit of the power-law regression function compared to the linear model that assumes exponential recession behavior. Especially, during both low and high flow conditions, the power law approximation provides a better representation of the observed trend of dQ/dt versus Q.

Parameterization of variable contributing areas (VCA)

To implement the variable contributing area concept (VCA, BEVEN and KIRKBY (1979) into the minimalistic hydrological model, the modified Soil Conservation Service Curve Number equation (SCS-CN) as presented in DAHLKE et al. (2009) was applied. It was adapted to represent the spatial decrease and increase of the saturated, surface runoff generating areas (riparian zones) depending on the actual storage conditions in the URHB. After USDA-SCS (1972) the SCS-CN equation is a widely used method to predict runoff with the fundamental equation:

$$Q_S = \frac{P_e^2}{P_e - S} \quad \text{(SI-1)}$$

where Q_s (L T^{-1}) is the runoff depth, S (L) is the average catchment-wide storage capacity of the active soil layer and P_e (L T^{-1}) is the effective precipitation (i.e., required rainfall depth until surface runoff begins). The value of S can be approximated by fitting Eq. (SI-1) to observed Q_s and P_e (STEENHUIS et al., 1995). After STEENHUIS et al. (1995), integration of Eq. (SI-1) yields a relationship that allows the estimation of the saturated, runoff-generating portion of a catchment (A_s, (-)):

$$A_S = 1 - \frac{S^2}{(P_e + S)^2} \quad \text{(SI-2)}$$

with the same parameters used as in Eq. (SI-1).

Originally, the SCS-CN runoff equation assumes constant values for S and the initial abstraction that is used to obtain P_e. A further developed SCS-CN runoff equation considers the temporal variability of initial abstraction (i.e., antecedent moisture deficit) that determines the amount of rainfall required to initiate surface runoff and thus the size of the runoff generating areas (DAHLKE et al., 2009). Average daily moisture deficit was calculated based on simple soil water balance equations (DAHLKE et al., 2009). For days with rainfall ($P(t)$) and no preceding precipitation the sum of actual evapotranspiration ($ET(t)$) defines the antecedent moisture deficit and $P_e(t)$ can be calculated with:

$$P_e(t) = P(t) - \sum_{t=1}^{n} ET(t) \quad \text{(SI-3)}$$

In case of previous rainfall the antecedent conditions were implemented as follows (DAHLKE et al., 2009):

$$P_e(t) = P(t) + P(t-1) - Q_S(t-1) - ET(t-1) - ET(t) \quad \text{(SI-4)}$$

Since Eq. (SI-3) and Eq. (SI-4) can give negative values for P_e, A_s is set to zero when $P_e \leq 0$ and to one when P_e approaches infinity. The hillslope area is the remaining portion of the event-flow generating area, which is one in the SCS-CN framework:

$$A_h = 1 - A_{rz} \quad \text{(SI-5)}$$

For the URHB, it is $A_s = A_{rz}$ in Eq. (SI-2) and the size of the hillslopes (A_h) can then be derived by subtracting A_{rz} from the portion of event-flow generating area, which is one in Eq. (SI-2) and represents 25.2 % of A_{tot} (section III - 4.1). A catchment-wide average storage capacity of the upper soil profile of S = 102 mm was presumed which is based on ($\theta^* \cdot z_r$) in the hillslope reservoir model (section III - 3.3). Plotting of P_e against observed Q_e (Figure SI-6) confirmed this value for S (Eq. (SI-2)). With this, the spatial variability of the riparian zones ranges from 0 % to 14 % for the rainfall events that occurred during the observation period.

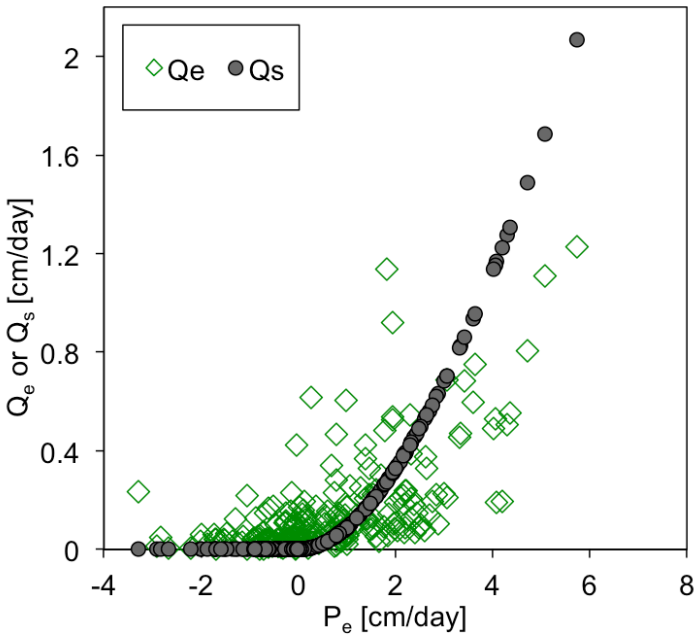

Figure SI-6 Effective rainfall (P_e) plotted against observed event flow (Q_e, green diamonds) and runoff (Q_s, grey circles) from the modified SCS-CN runoff equation after DAHLKE et al. (2009).

Sensitivity analysis

A sensitivity analysis of the model key parameters was carried out to evaluate their effects on the event-flow predictions with the minimalistic model and CCA and VCA. For this, the model was run each time with the value of one parameter increased or decreased by 25%, respectively. Predictions and data were compared as cumulative distributions, which allow an easy assessment of the model performance.

The plots in Figure SI-7 indicate that the soil moisture threshold value (θ^*) is the most sensitive parameter of the minimalistic modeling approach, because it defines the storage deficit in the upper soil layer, and thus the intensity of groundwater-recharge events. A 25%-smaller θ^*-value causes a significant overprediction of event flow, i.e., median values of $Q_e'(CCA)$ and $Q_e'(CCA)$ exceed observed Q_e' by more than 40%. A higher threshold value limits groundwater contributions from the hillslope reservoir, and thus, causes an underprediction particularly of the low-flow-component.

The simulation results are less controlled by the other soil properties, such as root zone depth (z_r) and wilting point (θ_w). Higher values of z_r and smaller values of θ_w describe a soil with higher storage capacity that would lead to less hillslope groundwater recharge.

Variations of the residence time (i.e., groundwater recession constant, k_{gw}) dominantly affect medium and low event-flow rates. Higher k_{gw}-values result in an underestimation of event-flow because the groundwater would drain faster from the hillslope reservoir. Although 25%-smaller k_{gw}-values still give reasonable results for high flow rates, the model would capture lowest event-flow less sufficiently.

Overall, there was a higher sensitivity on the input parameters for the model with VCA- compared to the CCA concept, where the hillslopes and riparian zones always account for 7.5 % and 15.7 % of the catchment area and do not shrink or expand during heavy rainfall events, respectively.

This analysis did not show any sensitivity on the event-flow generating area (A_e. not shown) because the model calculates the hillslope and riparian zone areas as fractions from A_e that are related to the baseflow index prior to the calculation of Q_e' (Eq. (9)). Therefore, a larger A_e-value gives a smaller α to relate the observed portion of event flow in the streamflow hydrograph to the event-flow generating area. To assess the possible range of A_e, a more detailed evaluation at the event-time scale was carried out below.

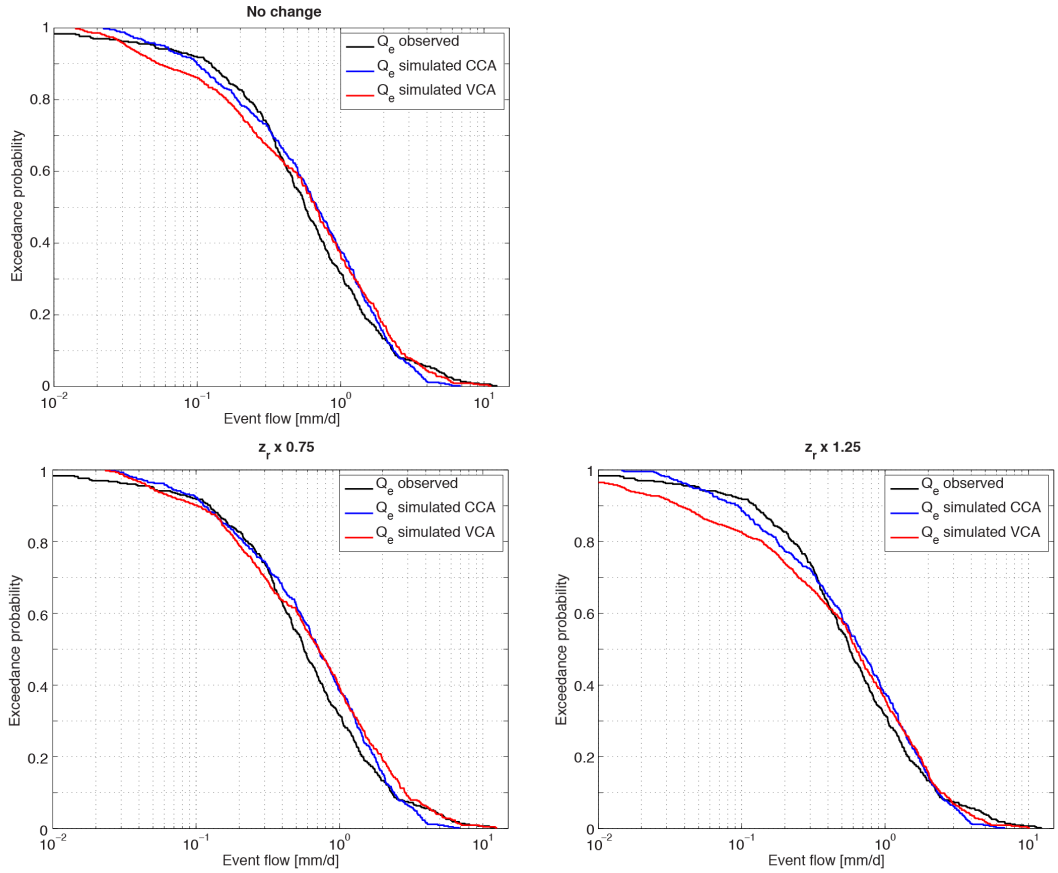

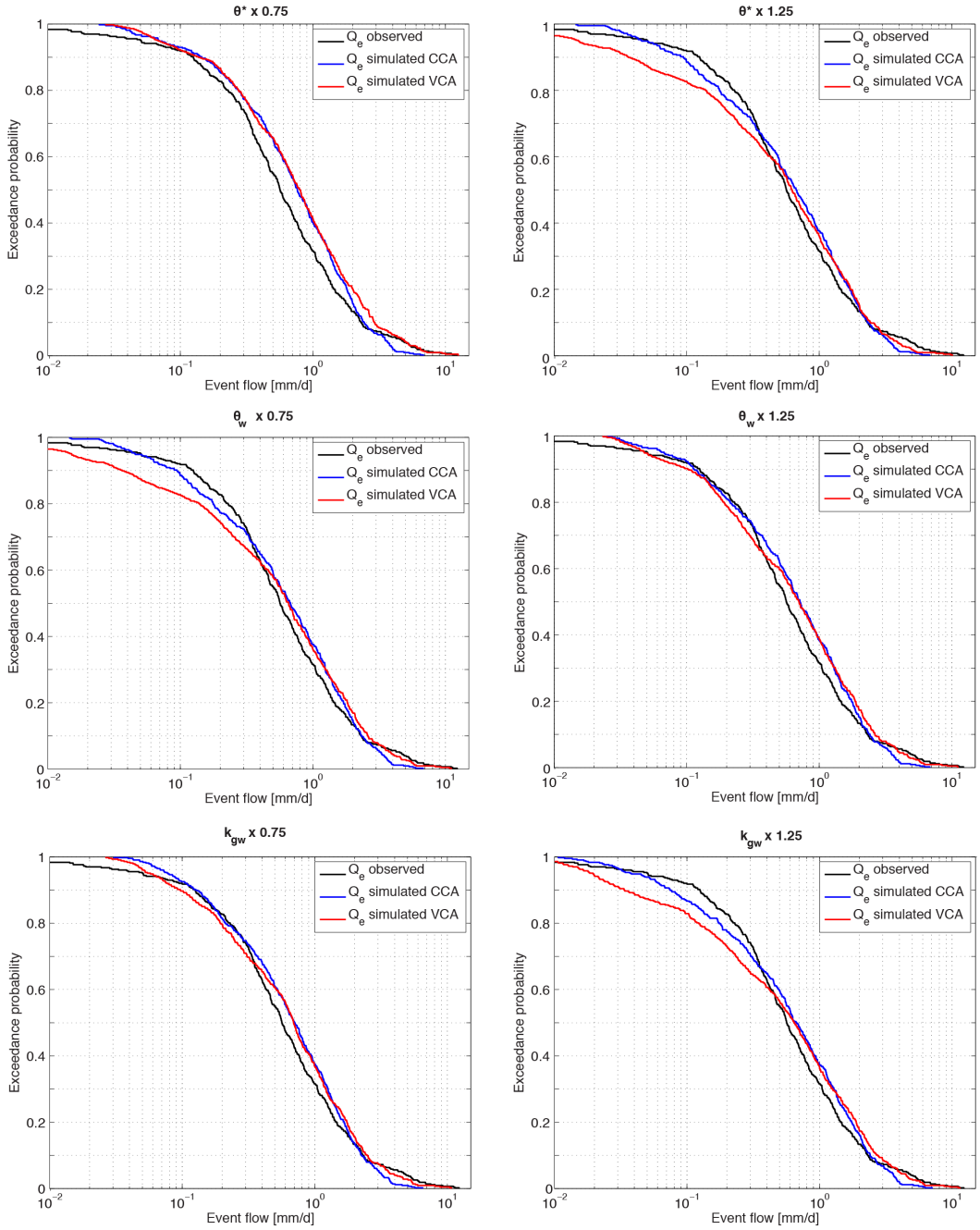

Figure SI-7 Comparison of flow duration curves (fdc) of observed (black line) and simulated event flow assuming constant contributing areas (CCA, blue line) and variable contributing areas (VCA, red line) for the periods 1 April-31 October, 2011 and 1 April-31 October, 2012 (each first month of the observation period was used as initialization period in the model and was excluded from the analysis). The graph titles indicate the changed input parameters and its relative change by ± 25%.

Analysis of total event-flow generating area during the rainfall event series 31 May – 13 June, 2012

The largest rainfall event within the observation period occurred between 31 May and 13 June, 2012 with total rainfall of 177.4 mm in 11 days. The minimalistic model only captured poorly the third pulse of peak flow (Figure SI 8). The first event mainly replenished the storage deficit in the URHB, as indicated by a rise of Q_e up to only 3 mm d^{-1} on 4 June 2012 and a small runoff coefficient of 0.1 (Table SI-7). The following rainfall period with the peak flow on 8 June 2012 led to a much stronger streamflow response and the runoff coefficient of 0.28 indicates an expansion of the event-flow generating area due to a higher catchment wetness state compared to the previous event. The third event around 12 June 2012 caused a similar streamflow response as the previous rainfall period, however, a runoff coefficient of 0.80 clearly suggests that surface runoff and shallow subsurface storm flow were the dominant sources of river discharge.

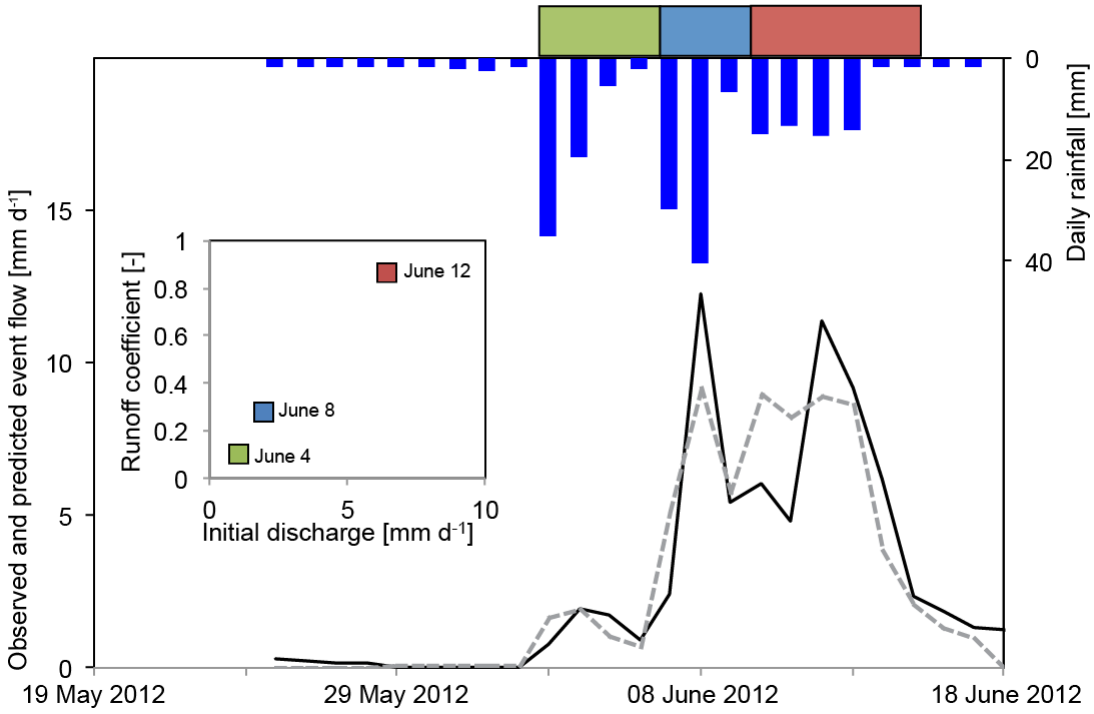

Figure SI 8 Rainfall events, observed (black solid line) and optimized (grey dashed line) event-flow of the URHB-river between 31 May, 2012 – 13 June, 2012. The inset figure shows the initial discharge (as a proxy for antecedent moisture conditions) and the corresponding runoff coefficient for each rainfall period. The colored areas indicate the time periods used to calculate the runoff coefficients and total event flow volume.

Table SI-7 Characteristics of the rainfall event series in the URHB during 31 May, 2012 – 13 June, 2012 and optimized riparian zone areas.

Time of peak flow	Total rainfall (mm)	Rainfall intensity (mm d^{-1})	Peak flow (mm d^{-1})	Runoff coefficient (-)	Optimized riparian zone area (% of A_{tot})
4/6/2012	54.9	13.7	3.0	0.10	4.8
8/6/2012	72.5	18.1	13.1	0.28	7.3
12/6/2012	50.10	12.5	12.4	0.80	24.1

GENERAL CONCLUSIONS AND OUTLOOK

In this section, the main results from the previous three chapters are revisited and put into a broader context. Since the experimental and modeling studies were carried out solely at one pre-Alpine headwater catchment, the question will be considered of whether and how the conclusions can be transferred to other sites and other scales. Finally, possible challenges for future research that arise from the findings of this PhD thesis are discussed.

The overall working hypothesis of this PhD thesis is that precipitation in mountainous catchments provides water inputs at different time scales and intensities, which are stored as soil- and groundwater in the subsurface and routed through complex flow pathways towards the valley bottom. Eventually this water feeds mountainous streams and lakes, which in turn significantly contribute to water flow in the lowlands. The importance of groundwater recharge and discharge in mountainous headwater catchments will increase in the future due to predicted earlier snow melt in spring and longer drought periods in summer and fall (e.g., BARNETT et al., 2005; ECKHARDT and ULBRICH, 2003; MAXWELL and KOLLET, 2008). A higher variability in climatic forcing functions, is expected to affect soil water processes, hydro(geo)logic responses and thus, groundwater-surface water interactions and groundwater storage in such regions. Adaption methods in the face of environmental changes (e.g., climate change, land use change), however, can only be successful when underpinned by a holistic understanding of the coupled physical processes.

Hence, this PhD thesis' primary objective was to enhance the existing knowledge of the role of groundwater for the hydrological functioning and solute transport in mountainous headwater catchments. This objective was addressed by a field-based study at a small pre-Alpine watershed in northeast Switzerland that focused on the investigation of the coupling between climatic drivers, landscape properties and responses of ground- and surface water. Four different aspects of catchment hydro(geo)logy in mountainous terrain were investigated at various spatiotemporal scales, which refer to the dominant drivers of groundwater recharge (i.e., climatic forcing and landscape properties) and to the responses due to groundwater discharge (i.e., streamflow generation and solute transport). The specific research objectives of this PhD thesis were formulated as:

- Investigation of groundwater recharge mechanisms through the systematic comparison of groundwater recharge estimation methods at different spatio-temporal scales and for average and extreme climatic conditions;
- Identification of dominant streamflow-generation mechanisms and threshold-responses with a focus on groundwater discharge;
- Evaluation of the impact of agricultural land use and related transport of solutes and nutrients towards the river by groundwater discharge.
- Development of a conceptual rainfall-runoff model at the hillslope- and the catchment scale, which is validated with an analytical model;

GENERALIZATION OF THE RESULTS

Previous studies pointed out that the reliable quantification of groundwater recharge at the plot- or the catchment scale is often challenging due to the large variety of modeling concepts and their sensitivity to the applied input parameters. Since in part I of this PhD thesis, the groundwater recharge (GR) estimation methods were reviewed within the context of climatic forcing functions and subsurface properties, some more specific guidelines could be provided that extend existing recommendations in the literature. Hence, future applications of

GR estimation methods in water management studies can benefit from the presented results, particularly under consideration of the predicted intensification of climatic extremes.

To increase the general significance and transferability of the results, long time series with a large variability of climatic condition were utilized and different methods were compared that are representative for a wide range of spatio-temporal scales. In addition, the GR estimation methods were applied with field- and literature based parameter sets, because a calibration to direct GR measurements is often not possible. Some of the strengths and limitations of the methods, however, are more representative for regions with similar hydro(geo)logic and climatic properties as the RHB, where feedback mechanisms between atmospheric processes and groundwater recharge take place at time scales of hours to days. Nevertheless, it could be shown that with increasing spatial and temporal scales, the limitations of the GR estimation methods become less important since small-scale processes are averaged out.

Based on the conceptual model developed in parts II and III of this PhD thesis, the URHB catchment can be discretized into a deep, fractured-rock aquifer system and a shallow, porous aquifer that is located in the valley bottom area. Due to continuous inflow of groundwater from the further uphill regions, groundwater tables in the valley bottom aquifer are shallow and the storage deficit in the unsaturated zone is low throughout the year. Consequently, the valley-bottom areas are prone to surface-runoff generation and subsurface stormflow, while groundwater discharge from the fractured-rock aquifer constitutes the baseflow fraction of the streamflow hydrograph. Although the valley bottom aquifer accounts for less than 30 % of the catchment area, it plays a major role in the timing and amplitude of flood events during precipitation events and generates on average 50 % of total streamflow. Similar findings in other studies indicate that this hydrologic behavior is typical for many mountainous catchments (e.g., BURT and PINAY, 2005; INAMDAR and MITCHELL, 2007; MCGLYNN and MCDONNELL, 2003).

The overall findings of this PhD thesis enhance the mechanistic understanding of hydro(geo)logic processes in mountainous regions that strongly control streamflow generation, water quality and catchment sensitivity to climatic forcing functions. This is of particular importance for the Swiss pre-Alps as they generally exhibit the highest flood disposition (i.e., ratio between the contributing area and the total catchment area) and larger runoff coefficients compared to catchments in the lowlands and at elevations above ~ 2000 m (WEINGARTNER, 1999). Whereas lowland catchments are mainly characterized by shallow hydraulic gradients, a low flood deposition in most alpine catchments is caused by comparably low precipitation input.

As the shallow valley-bottom aquifer plays a key role for the hydro(geo)logic responses in mountainous headwater catchments, detailed field-based investigations of the involved processes should focus on this part of the landscape. This would, in turn, clearly simplify the representative measurement of precipitation, groundwater dynamics and subsurface properties. As it was demonstrated above, observations of hydro(geo)logic responses and climatic variables as well as geomorphic analysis at the near-stream areas provided a sufficient foundation that allows for an identification of dominant controls on hydrological and biogeochemical catchment behavior. It was shown that groundwater-table

and streamflow responses could be simulated adequately for the entire catchment based only on observations at the plot- and hillslope scale. Hence, important indicators are provided on how groundwater dynamics in mountainous catchments can be effectively assessed and understood. This approach can be introduced into future research studies that tackle questions regarding hydrology, ecosystem functioning and land use management.

From a hydro-climatic point of view, a previous study in the Rietholzbach Research catchment, concluded that the site is representative for the larger region of north-east Switzerland (SENEVIRATNE et al., 2012). It was further shown by TEULING et al. (2010) that the RHB catchment behaves for the most part like the simple dynamical system described by KIRCHNER (2009). In this study, river discharge variations could be explained with a power-law relationship between streamflow and the change in catchment storage. In this PhD project, the physical mechanisms behind this conceptualization were identified and described in great detail, for instance by analyzing non-linear threshold responses (part II) and the source areas of streamflow (part III).

PERSPECTIVES

In this PhD thesis, the role of groundwater for streamflow generation and solute transport was systematically investigated at the mountainous Rietholzbach catchment. Because of the strong coupling between climatic forcing functions and surface and subsurface flow processes in such mountainous regions, a wide range of analytical and experimental approaches from different disciplines was utilized and several assumptions had to be made in the course of the analyses. These assumptions, however, provide interesting challenges for future research that may improve the presented results and conclusions.

Temporal sources of river water

In addition to the separation of the streamflow hydrograph with regard to the source areas (parts II and III), the travel times of ground- and river water could be assessed in future studies in order to verify and enhance the conceptual model. The presented results in part II already indicate that saturation dynamics are a key driver of nutrient mobilization from riparian zones (WEILER and MCDONNELL, 2006; MCGLYNN and MCDONNELL, 2003). Return flow is assumed to emerge as hillslope groundwater at the hillslope-riparian zone-interface when rainfall causes the groundwater tables to rise. Since this return flow often originates from agricultural hillslopes, it might bypass the riparian zone as surface runoff and could be a major source of nitrate and other solutes (BURT and PINAY, 2005). For this, natural tracers (e.g., isotopes or inorganic cations and anions) in ground- and river water could be measured at the event-time scale to carry out end-member mixing analysis. Preliminary analyses already showed markedly different hydrochemical signatures of hillslope- and riparian groundwater (e.g., silica and DOC). It would also be interesting to employ the long-term data sets of electrical conductivity, that were collected for the ground- and river water at high temporal resolution, in order to study the seasonal pattern and the short-term responses to agricultural land use.

Other source areas

In the conceptual model of the URHB the tile drain system was considered to be part of the riparian zones as both systems produce similarly quick streamflow signals. With respect to water quality, however, different responses can be expected because of different subsurface properties. While the riparian zones in the URHB are characterized by low permeability soils and low hydraulic gradients, the man-made tile drains are either open channels or screened pipes overlain with highly permeable material that allows for quick infiltration and discharge. Hence, the flow pathway of the discharged water from the riparian zones and the tile drains can vary considerably, and thus have a different hydrochemical signature. Because agricultural areas are generally drained artificially through pipes or ditches, it is likely that pollutants or nutrients are transported into the river where they may harm the aquatic ecosystem (DOPPLER et al., 2012). In order to evaluate the role of the tile drain system in the URHB, a future research project could identify and map the drained areas, for instance by utilizing high-resolution aerial images in combination with a decision tree classifier model (NAZ et al., 2009). Then, flow rates and water quality of the tile drain discharge would have to be monitored at representative locations. As the application of V-notch weirs in such a dynamic system is often difficult, temperature probes (e.g., *TidbiT v2 Water Temperature Logger – UTBI-001*) could be installed into the drainage canals and pipes (ZAJICEK et al., 2011). They allow for monitoring the point of time when tile drain discharge starts or stops by a detectable shift of water temperature. Additionally, with weekly and event-based drainage water sampling in the tile drains and the river, hydrograph separation into the different source zones of streamflow could be carried out.

Variable contribution areas

Water quality analyses at the event-time scale together with three-component end-member analysis after MCGLYNN and MCDONNELL (2003) could be carried out to further evaluate the variable contributing area concept that was introduced in part III of this thesis. The results in part II of this thesis indicate that the hydrochemical signal from the riparian zone distinctly differs from the groundwater discharging from the hillslopes (calcium and dissolved silicate). As an alternative, spatially distributed monitoring of shallow soil moisture along several transects at the interface between riparian zones and hillslopes or thermal infrared imaging (e.g., PFISTER et al., 2010) could be used to map regions with very shallow groundwater tables or return flow. Such a visual analysis is likely to be most efficient during the snowmelt period when groundwater and air temperatures are distinctly different.

Model transferability

Finally, the applicability of the minimalistic model at the larger scale should be evaluated in future investigations. Based on a study of BASU et al. (2010), where a similar modeling scheme was successfully applied at an agricultural catchment of around 700 km^2, the

transferability of the presented framework seems reasonable. In both cases, the application of such a simplistic modeling framework requires the identification and delineation of the hydrologically active regions of the landscape, as well as knowledge about the dominant hydrological processes. Hence, at a different site the local soil and topographic properties would have to be known, for instance from satellite images or field surveys. Other important input parameters, such as the average hillslope groundwater residence time ($1/k_{gw}$) or soil hydraulic properties could even be obtained from literature values or by calibration in case no direct measurements exist. In a second step it would be interesting to utilize the modeling framework for the simulation of non-reactive transport of solutes from the variable contributing areas into the river system. This would allow a first approximation of the loads of nutrients or other pollutants that become activated and are transported from the headwaters further downstream during precipitation events.

APPENDIX A

Published Conference Contributions

A1 UNDERSTANDING SUBSURFACE FLOW PROCESSES AND THEIR DRIVING FEEDBACK MECHANISMS

Oral presentation at the *ZHydro Conference*, November 15 2011, ETH Zurich, Switzerland.

Understanding subsurface flow processes is an ongoing task for a multitude of research areas such as hydro(geo)logy, ecology or biology. Many studies have been carried out to investigate groundwater - surface water - interaction near river sections, transport mechanisms of nutrients within hyporheic zones as well as groundwater flow directions in the shallow subsurface. A multidisciplinary approach can lead to a better understanding of interactions between these processes and help in defining their driving mechanisms.

In the pre-Alpine Rietholzbach catchment (Toggenburg, NE Switzerland) we perform a field-based process study where we simultaneously investigate spatial and temporal variations of groundwater - surface water - interactions over longitudinal and vertical cross sections. The existing field site near the Rietholzbach has been equipped with 16 piezometers along a hillslope and near the river bank. Other instrumentation available on site includes probes for electrical conductivity, temperature and hydraulic head. A well-equipped meteorological research station of ETH Zurich at the upper margin of the field site provides high-resolution hydrological and climatic data since 1975. The Rietholzbach is the lower boundary where runoff, electrical conductivity and temperature are continuously recorded at a gauging station. Apart from the groundwater head data, tracer tests, chemical water analyses and geophysical surveys will be carried out to characterize subsurface properties in the saturated zone.

The installed setup facilitates the investigation of annual, inter-seasonal as well as short-term (minutes to hours) dynamics of groundwater - surface water - interaction and provides the unique opportunity to explore temporal and spatial responses of complex subsurface flow systems within the broader context of climate change. Finally, structural and functional connectivity will be discussed and several processes will be explored through probabilistic dynamics.

A2 NATÜRLICHE RÜCKKOPPLUNGSPROZESSE BEI GRUNDWASSER-OBERFLÄCHEN-WASSER-INTERAKTIONEN

Oral presentation at the *Conference of the Hydrogeology Section of the German Geological Society* (Fachsektion Hydrogeologie in der Deutschen Gesellschaft für Geowissenschaften e.V. (FH-DGG)), May 16 – 20 2012, Dresden, Germany.

Die Grundwasserdynamik im Uferbereich von Flüssen spielt eine bedeutende Rolle für biologische und chemische Umwandlungs-prozesse und steht daher seit einigen Jahrzehnten im Fokus zahlreicher hydro(geo-)logischer Untersuchungen. Um Fließprozesse in der hyporheischen Zone jedoch umfassend beschreiben zu können, ist eine Einbeziehung aller beteiligten Faktoren (Klima, Topographie, Vegetation etc.) von großer Bedeutung. Ein

multidisziplinärer Ansatz kann deshalb zu einem besseren Verständnis der Wechsel-wirkungen zwischen natürlichen Prozessen führen und dazu beitragen, den Einfluss wesentlicher steuernder Faktoren zu quantifizieren (DETTY and MCGUIRE, 2010, WAINWRIGHT et al. 2011).

Mit Hilfe eines umfangreich ausgebauten Feldstandortes in dem voralpinen Einzugsgebiet des Rietholzbaches (NO Schweiz) sollen die oben genannten Wechsel-wirkungen genauer untersucht werden. Das Versuchsfeld befindet sich nahe eines Flussabschnitts und umfasst neben 16 Grundwassermessstellen mit Datenloggern auch Bodenfeuchtesensoren und Temperatur-lanzen, die im Flussbett installiert wurden. Um die variierenden hydraulischen Verhältnisse im Untergrund zu rekonstruieren, werden an diesem Feldstandort Tracerversuche, hydro-chemische Untersuchungen, geophysikalische Messungen sowie Isotopenanalysen durch-geführt. Eine meteorologische Messstation mit Wäge-Lysimeter, sowie eine Abflussmessstation des Instituts für Atmosphäre und Klima der ETH Zürich liefern zudem hochaufgelöste Langzeitdaten, wodurch ein ausführliches Bild des Wasserkreislaufs in diesem Einzugsgebiet generiert werden kann.

Ein Ziel dieser Arbeit ist es, wesentliche natürliche Rückkopplungsprozesse, v.a. zwischen Grund- und Oberflächenwasser, Bodenfeuchte und Atmosphäre aufzuzeigen. Zudem soll der Einfluss natürlicher Faktoren, welche Grundwasser-Oberflächenwasser-Interaktionen steuern, beschrieben und quantifiziert werden. Dazu werden die gewonnenen Daten zunächst innerhalb verschiedener räumlicher und zeitlicher Skalen miteinander korreliert (z. Bsp. Rangkorrelation nach Spearman, Kreuzkorrelation) und die Ergebnisse diskutiert. Eine numerische Simulation möglicher Fliesspfade des Grund-wassers sowie der daraus resultierenden Zusammensetzung des Gebietsabflusses erfolgt unter Verwendung des Modells Hydro-GeoSphere.

A3 A FIELD-BASED STUDY TO INVESTIGATE HYDROLOGIC CONNECTIVITY AND DRIVING MECHANISMS IN A SWISS PREALPINE RESEARCH CATCHMENT

Oral presentation at the 39th *IAH Congress*, September 16-21 2012, Niagara Falls, Canada.

In our research, we investigate the first-order controls on the formation of surface and subsurface hydrologic connectivity in a small (~3 km^2) pre-Alpine catchment. Our motivation is to understand how hydrologic connectivity evolves within the catchment during storm events and droughts to establish a general framework of interdisciplinary interest (e.g., ecology and climate science). In particular, we will focus on the identification of groundwater flow paths on local and regional scales and their effects on small-scale flow processes in the riparian zone as well as on the impact of tile drains as a significant contributor to event runoff. In order to incorporate hydrologic connectivity into our work it is necessary to apply a fully coupled model that simulates recharge and flow between surface, soil and aquifer. This will be accomplished by using the numerical code HydroGeoShere.

As groundwater in mountain headwaters sustain downstream baseflow in larger catchments, it plays an important role for water resource management in the densely populated lowlands of Switzerland as well as in many other parts of the world. Therefore, it is necessary to improve our understanding of the groundwater flow processes and their interactions with the ecosystem in high altitude watersheds, under explicit consideration of the joint behaviours and feedbacks of climate and groundwater.

We conduct our field-based study in the pre-Alpine Rietholzbach research catchment situated in northeastern Switzerland. It was equipped with a meteorological station, a lysimeter, 20 piezometers, 3 stream gauging stations and various soil moisture and temperature probes, which provide continuous measurements of atmospheric and hydrometeorological data. These measurements are used in combination with isotope analyses to determine groundwater residence times and streamflow composition. The installed setup facilitates the investigation of annual, inter-seasonal as well as short-term dynamics of water flow and its links to associated parameters describing atmospheric, surface and subsurface properties. Based on our first one-year time series, we will present a conceptual model of the complex groundwater flow processes and the involved feedback mechanisms, which explains the very dynamic streamflow response of the catchment.

A4 IMPLICATIONS OF HYDROLOGIC CONNECTIVITY BETWEEN HILLSLOPES AND RIPARIAN ZONES ON STREAMFLOW COMPOSITION

Poster presentation at the 8th *IAHS International Groundwater Quality Conference (GQ13)*, April 21-26 2013, University of Florida, Gainesville, USA.

In our research, we investigate the first-order controls on the formation of hydrologic connectivity between hillslopes and riparian zones in a small pre-Alpine catchment. Our motivation is to understand how hydrologic connectivity evolves during storm events and droughts to establish a general framework of interdisciplinary interest (e.g., ecology and climate science). In particular, we will focus on the identification of groundwater flow paths on local and regional scales and their effects on small-scale flow processes in the riparian zone. In order to incorporate hydrologic connectivity into our work it is necessary to apply a fully coupled model that simulates recharge and flow between surface, soil and aquifer. This will be accomplished by using the numerical code HydroGeoShere.

As groundwater in mountain headwaters sustains downstream baseflow in larger catchments, it plays an important role for water resource management in the densely populated lowlands of Switzerland as well as in many other parts of the world. Therefore, it is necessary to improve our understanding of the groundwater flow processes and their interactions with the ecosystem in high altitude watersheds, under explicit consideration of the joint behaviours and feedbacks of climate and groundwater.

We conduct our field-based study in the pre-Alpine Rietholzbach research catchment situated in northeastern Switzerland. It was equipped with a meteorological station, a lysimeter, a piezometer transect, 3 stream gauging stations and various soil moisture probes,

which provide continuous measurements of atmospheric and hydrometeorological data. Additionally, we collected ground- and surface water samples and installed probes with data loggers into the piezometers and the streams in order to record a one-year time series of ground- and surface water quality data (nutrients, main ions, electrical conductivity and temperature). These measurements are used to determine groundwater residence times and the effects of hydrologic connectivity between the hillslopes and riparian zones on streamflow composition. The installed setup facilitates the investigation of annual, inter-seasonal as well as short-term dynamics of water flow and its links to associated parameters describing atmospheric, surface and subsurface properties. Based on our first one-year time series, we will present a conceptual model of the complex groundwater flow processes and the involved feedback mechanisms, which explains the very dynamic streamflow response of the catchment.

A5 A FIELD STUDY IN THE SWISS RIETHOLZBACH BASIN TO UNDERSTAND LANDSCAPE FILTERING OF HYDRO-CLIMATIC DRIVERS AND ITS EFFECTS ON STREAMFLOW COMPOSITION

Poster presentation at the *AGU Fall Meeting*, December 9-13 2013, San Francisco, USA (received the Outstanding Student Paper Award (OSPA)).

Non-linear hydrological behavior of small mountainous watersheds is often attributed to variable streamflow contributions from different landscape units that differ in subsurface properties, vegetation cover and land use. Within this concept, the role of landscape can be seen as that of a filter, translating hydro-climatic drivers into particular streamflow signals – such as discharge rates or water quality.

Our research addresses the question of how hydrologic connectivity between the relevant landscape units evolves during storm events and droughts at headwater catchments and seeks to establish a general framework of interdisciplinary interest (e.g., ecology and climate science). We focus on the description of groundwater flow on the local and regional scale, since groundwater - surface water - interaction in the valley bottoms, transport mechanisms of nutrients within hyporheic zones, and groundwater flow dynamics in the shallow subsurface have all been identified as important processes in describing hydrologic catchment response and streamflow composition.

Our field-based study takes place in the pre-Alpine Rietholzbach research catchment (~ 3 km^2) in the headwaters of the Thur basin in NE Switzerland. We investigated the effects of landscape properties on river water quality and catchment hydrology over a two-year period. The Rietholzbach research catchment is equipped with a meteorological station, a weighting lysimeter, 20 piezometers, 3 stream gauging stations and various soil moisture and temperature probes, which provide continuous, high-frequency measurements of atmospheric and hydrometric data. These measurements are used in combination with hydro-chemistry data to determine groundwater residence times and streamflow composition. The installed setup facilitates the investigation of annual, inter-seasonal as well as short-term dynamics of water

flow and its links to associated parameters describing atmospheric, surface and subsurface properties.

We have identified three hydrological landscape units with very characteristic subsurface properties, with which the overall catchment behavior can be predicted by applying a parsimonious modeling approach. By implementing solute, electrical conductivity and temperature time series data from ground- and river water into the model, the spatio-temporal streamflow contribution from these landscape units reveals new insights into the hydrological functioning of the Rietholzbach catchment. The landscape units defined in our study are considered typical for the Swiss pre-Alps and, therefore, our results will provide valuable input for local and regional hydrological modeling studies in similar pre-Alpine watersheds.

A6 HYDROLOGICAL RESPONSES IN A PRE-ALPINE HEAD WATERSHED: THE ROLE OF HILLSLOPES AND RIPARIAN ZONES

Oral presentation at the *EGU General Assembly*, April 27 - May 29 2014, Vienna, Austria.

Mountainous watersheds are characterized by generally high precipitation inputs and very heterogeneous landscape properties, which make them very dynamic hydrologic systems that play an important role in the water cycle. Their groundwater systems sustain downstream baseflow in larger catchments in many parts of the world, particularly in the densely populated lowlands of Switzerland. Hillslope aquifers are often categorized as one of the dominant groundwater resources in mountainous watersheds. These aquifers may also act as source areas for pollutants in rivers due to intensive agricultural land use. In our study we seek to improve the understanding of the groundwater flow processes and runoff generation mechanisms in high altitude watersheds, under explicit consideration of the joint behaviors of climate and groundwater.

The role of the hillslope groundwater contribution to catchment outflow and streamflow composition was investigated in the pre-Alpine Rietholzbach catchment (~1 km^2) in northeast Switzerland. The field site, equipped with an extensive hydrometric setup, facilitates the monitoring of annual, inter-seasonal and short-term dynamics of water flow and composition, as well as its links to associated parameters describing atmospheric, surface and subsurface properties. In this study, we focused on the effects of antecedent moisture, rainfall characteristics and landscape properties on groundwater and river responses in order to develop a conceptual model of runoff generation.

Our observations indicate generally low hydraulic conductivities and average groundwater travel times of several months in the hillslope aquifers resulting from high clay-contents of the unconsolidated glacial Moraine deposits. Event analysis revealed that only a small portion of the total watershed area generates event discharge and we have identified the saturated valley bottom (riparian zones) and lower hillslopes as the two dominant hydrological landscape units. Runoff generation from the riparian zones is mainly driven by rainfall characteristics, whereas antecedent moisture conditions regulate groundwater discharge from the hillslopes.

In late summer, we could correlate an accumulation of nutrients in the riparian zones with agricultural land use on the hillslopes in combination with downhill groundwater flux. From this, we expect an increased flushing-out of nutrients from the near-stream areas into the river during rainfall events. In order to incorporate solute transport into our conceptual model, the ongoing research focuses on the role of rainfall characteristics and antecedent moisture conditions on the buffer-capacity of the riparian zones to filter the nutrient input from the hillslopes.

LIST OF REFERENCES

ALI G, OSWALD CJ, SPENCE C, et al. (2013) Towards a unified threshold-based hydrological theory: necessary components and recurring challenges. Hydrol Process 27: 313-318. doi: 10.1002/hyp.9560

ALLEN DM, CANNON AJ, TOEWS MW, SCIBEK J (2010a) Variability in simulated recharge using different GCMs. Water Resour Res 46. doi: 10.1029/2009wr008932

ALLEN DM, WHITFIELD PH, WERNER A (2010b) Groundwater level responses in temperate mountainous terrain: regime classification, and linkages to climate and streamflow. Hydrol Process 24: 3392-3412. doi: 10.1002/hyp.7757

ALLEN RG, PEREIRA LS, RAES D, SMITH M (1998) Crop evapotranspiration - Guidelines for computing crop water requirements - FAO Irrigation and drainage paper 56 FAO, Rome

ALLEN RG, SMITH M, PEREIRA LS, PERRIER A (1994) An update for the calculation of reference evaporation. ICID Bulletin 43: 35–92

ALLEN RG, SMITH M, PEREIRA LS, PRUITT WO (1997) Proposed revision to the FAO procedure for estimating crop water requirements. Acta Hortic: 17-33

ALLEY WM (1984) The Palmer Drought Severity Index: limitations and assumptions. Journal of Climate & Applied Meteorology 23: 1100-1109

ALLISON GB, GEE GW, TYLER SW (1994) Vadose-Zone Techniques for Estimating Groundwater Recharge in Arid and Semiarid Regions. Soil Sci Soc Am J 58: 6-14

ANDERSON AE, WEILER M, ALILA Y, HUDSON RO (2009) Subsurface flow velocities in a hillslope with lateral preferential flow. Water Resour Res 45: 1-15. doi: 10.1029/2008wr007121

ANDREADIS KM, CLARK EA, WOOD AW, HAMLET AF, LETTENMAIER DP (2005) Twentieth-century drought in the conterminous United States. J Hydrometeorol 6: 985-1001. doi: 10.1175/Jhm450.1

ARNOLD JG, ALLEN PM (1999) Automated methods for estimating baseflow and ground water recharge from streamflow records. J Am Water Resour Assoc 35: 411-424. doi: 10.1111/J.1752-1688.1999.Tb03599.X

BACHMAIR S, WEILER M (2011) New Dimensions of Hillslope Hydrology. In: Levia DF, Carlyle-Moses D, Tanaka T (eds) Forest Hydrology and Biogeochemistry, Synthesis of Past Research and Future DirectionsCaldwell MM, Heldmaier G, Jackson RB, Lange OL, Mooney HA, Schulze ED, Sommer U, Ecological Studies:455-481.

BADER S (2004) Die extreme Sommerhitze im aussergewöhnlichen Witterungsjar 2003 [The extreme summer heat in 2003]. In: MeteoSwiss (ed) Federal Office of Meteorology and Climatology (MeteoSwiss).

BAKKER M, BARTHOLOMEUS RP, FERRE TPA (2013) "Groundwater recharge: processes and quantification" Preface. Hydrol Earth Syst Sci 17: 2653-2655. doi: 10.5194/Hess-17-2653-2013

BALDERER W (1980) Hydrogeologie des Murgtales (Kt. Thurgau) [Hydrogeology of the Murg valley (Conton of Thurgau)]. 969 Ph.D., University of Neuchâtel, Switzerland

BALDERER W (1983) Hydrogeologie der Oberen Süßwassermolasse im Einzugsgebiet des Aubaches (Schweiz) [Hydrogeology of the Upper Freshwater Molasse in the Aubach catchment (Switzerland)]. Steirische Beiträge zur Hydrogeologie 34/35: 15-54

BALDERER W (1984) Hydrogeologische Gesamtsysteme in quartären Lockergesteinsablagerungen [Hydrogeological systems in quaternary unconsolidated deposits] Steirische Beiträge zur Hydrogeologie 36: 115-125

BARNETT TP, ADAM JC, LETTENMAIER DP (2005) Potential impacts of a warming climate on water availability in snow-dominated regions. Nature 438: 303-309. doi: 10.1038/Nature04141

BASU NB, RAO PSC, WINZELER HE, et al. (2010) Parsimonious modeling of hydrologic responses in engineered watersheds: Structural heterogeneity versus functional homogeneity. Water Resour Res 46. doi: 10.1029/2009wr007803

BENCALA KE, GOOSEFF MN, KIMBALL BA (2011) Rethinking hyporheic flow and transient storage to advance understanding of stream-catchment connections. Water Resour Res 47. doi: 10.1029/2010wr010066

BENISTON M, FOX DG (1996) Impacts of Climate Change on Mountain Regions. In: Watson RT, Zinyowera MC, Moss RH (eds) Climate Change 1995 - Impacts, adaptations and mitigation of Climate Change: Scientific-technical analyses: Contribution of Working Group II to the second assessment report of the intergovernmental Panel on Climate Change:193-213.

BEVEN K (2001) How far can we go in distributed hydrological modelling? Hydrol Earth Syst Sci 5: 1-12

BEVEN K (2007) Towards integrated environmental models of everywhere: uncertainty, data and modelling as a learning process. Hydrol Earth Syst Sci 11: 460-467

BEVEN K, KIRKBY MJ (1979) A physically based, variable contributing area model of basin hydrology. Hydrological Sciences-Bulletin 24: 43-69

BISHOP K, SEIBERT J, KOHER S, LAUDON H (2004) Resolving the Double Paradox of rapidly mobilized old water with highly variable responses in runoff chemistry. Hydrol Process 18: 185-189

BLÖSCHL G (2011) Scaling and Regionalization in Hydrology. In: Uhlenbrook S (ed) Treatise on Water Science:519-535.

BLUME T, ZEHE E, BRONSTERT A (2007) Rainfall-runoff response, event-based runoff coefficients and hydrograph separation. Hydrol Sci J-J Sci Hydrol 52: 843-862. doi: 10.1623/hysj.52.5.843

BÖHNER J, BLASCHKE T, MONTANARELLA L (2008) SAGA: System for an automated geographical analysis. In: Schickhoff UaB, J. (ed) Hamburger Beiträge zur Physischen Geographie und Landschaftsökologie.

BOND WJ (1998) Part 3: Soil Physical Methods for Estimating RechargeThe Basics of Recharge and Discharge.

BOTTER G, PORPORATO A, RODRIGUEZ-ITURBE I, RINALDO A (2007) Basin-scale soil moisture dynamics and the probabilistic characterization of carrier hydrologic flows: Slow, leaching-prone components of the hydrologic response. Water Resour Res 43. doi: 10.1029/2006wr005043

BOUGHTON WC (1987) Evaluating Partial Areas of Watershed Runoff. J Irrig Drain E-Asce 113: 356-366

BOUWER H, RICE RC (1976) A Slug Test Method for Determining Hy- draulic Conductivity of Unconfined Aquifers with Completely or Partially Penetrating Wells. Water Resour Res 12: 423-428. doi: 10.1029/WR012i003p00423.

BRUTSAERT W (2005) Hydrology - An Introduction Cambrige University Press

BRUTSAERT W, NIEBER JL (1977) Regionalized Drought Flow Hydrographs from a Mature Glaciated Plateau. Water Resour Res 13: 637-644. doi: 10.1029/Wr013i003p00637

BURLANDO P, PELLICCIOTTI F, STRASSER U (2002) Modelling Mountainous Water Systems Between Learning and Speculating Looking for Challenges Nordic Hydrology 33: 47-74

BURT TP, MATCHETT LS, GOULDING KWT, WEBSTER CP, HAYCOCK NE (1999) Denitrification in riparian buffer zones: the role of floodplain hydrology. Hydrol Process 13: 1451-1463

BURT TP, PINAY G (2005) Linking hydrology and biogeochemistry in complex landscapes. Progress in Physical Geography 29: 297-316. doi: 10.1191/0309133305pp450ra

CALANCA P (2007) Climate change and drought occurrence in the Alpine region: How severe are becoming the extremes? Glob Planet Change 57: 151-160. doi: 10.1016/j.gloplacha.2006.11.001

CAREY SK, TETZLAFF D, SEIBERT J, et al. (2010) Inter-Comparison of Hydro-Climatic Regimes Across Northern Catchments: Synchronicity, Resistance and Resilience. Hydrol Process 24: 3591–3602

CASTY C, WANNER H, LUTERBACHER J, ESPER J, BOHM R (2005) Temperature and precipitation variability in the european Alps since 1500. Int J Climatol 25: 1855-1880. doi: 10.1002/Joc.1216

COMBALICER E, LEE S, AHN S, KIM D, IM S (2008) Comparing groundwater recharge and base flow in the Bukmoongol small-forested watershed, Korea. Journal of Earth System Science 117: 553-566. doi: 10.1007/s12040-008-0052-8

CONRAD O (2006) SAGA - Entwurf, Funktionsumfang und Anwendung eines Systems für Automatisierte Geowissenschaftliche Analysen. Ph.D., Georg-August-University

COOK PG, HERCZEG AL (2000) Environmental tracers in subsurface hydrology Kluwer Academic Publishers, Boston

CROSBIE RS, BINNING P, KALMA JD (2005) A time series approach to inferring groundwater recharge using the water table fluctuation method. Water Resour Res 41: 1-9. doi: 10.1029/2004WR003077

CROSBIE RS, DAWES WR, CHARLES SP, et al. (2011) Differences in future recharge estimates due to GCMs, downscaling methods and hydrological models. Geophysical Research Letters 38. doi: 10.1029/2011gl047657

DAHLKE HE, EASTON ZM, FUKA DR, LYON SW, STEENHUIS TS (2009) Modelling variable source area dynamics in a CEAP watershed. Ecohydrology 2: 337-349. doi: 10.1002/Eco.58

DAHLKE HE, EASTON ZM, WALTER MT, STEENHUIS TS (2012) Field Test of the Variable Source Area Interpretation of the Curve Number Rainfall-Runoff Equation. J Irrig Drain E 138: 235-244. doi: 10.1061/(Asce)Ir.1943-4774.0000380

DETTY JM, MCGUIRE KJ (2010) Topographic controls on shallow groundwater dynamics: implications of hydrologic connectivity between hillslopes and riparian zones in a till mantled catchment. Hydrol Process 24: 2222-2236. doi: 10.1002/hyp.7656

DINGMAN SL (2002) Physical hydrology, 2nd edn Prentice Hall Upper Saddle River, N.J.

DOHERTY J (2011) PEST: Model-Independent Parameter Estimation, User Manual, Watermark Numer. Comput. [Available at http://www.pesthomepage.org/Downloads.php]

DOMAGALSKI JL, JOHNSON H (2012) Phosphorus and Groundwater: Establishing Links Between Agricultural Use and Transport to Streams: U.S. Geological Survey Fact Sheet 2012-3004

DOPPLER T, CAMENZULI L, HIRZEL G, et al. (2012) Spatial variability of herbicide mobilisation and transport at catchment scale: insights from a field experiment. Hydrol Earth Syst Sci 16: 1947-1967. doi: 10.5194/Hess-16-1947-2012

DOS SANTOS JÚNIOR AG, YOUNGS EG (1969) A study of the specific yield in land-drainage situations. Journal of Hydrology 8: 59-81. doi: http://dx.doi.org/10.1016/0022-1694(69)90031-6

DUNN SM, FREER J, WEILER M, et al. (2008) Conceptualization in catchment modelling: simply learning? Hydrol Process 22: 2389-2393. doi: Doi 10.1002/Hyp.7070

DUNNE T, BLACK RD (1970) Partial Area Contributions to Storm Runoff in a Small New-England Watershed. Water Resour Res 6: 1296-1311. doi: 10.1029/Wr006i005p01296

ECKHARDT K, ULBRICH U (2003) Potential impacts of climate change on groundwater recharge and streamflow in a central European low mountain range. Journal of Hydrology 284: 244-252. doi: 10.1016/j.jhydrol.2003.08.005

EWEN T, LEHNER I, SEIBERT J, SENEVIRATNE SI (2011) Climate patterns in the long-term hydrometeorological data series of the Rietholzbach catchment. Bodenkultur 62: 53-58

FEDDES RA, BRESLER E, NEUMAN SP (1974) Field-Test of a Modified Numerical-Model for Water Uptake by Root Systems. Water Resour Res 10: 1199-1206. doi: 10.1029/Wr010i006p01199

FENICIA F, KAVETSKI D, SAVENIJE HHG, et al. (2014) Catchment properties, function, and conceptual model representation: is there a correspondence? Hydrol Process 28: 2451-2467. doi: 10.1002/Hyp.9726

FINCH JW (1998) Estimating direct groundwater recharge using a simple water balance model - sensitivity to land surface parameters. Journal of Hydrology 211: 112-125. doi: 10.1016/S0022-1694(98)00225-X

FLINT AL, FLINT LE, KWICKLIS EM, FABRYKA-MARTIN JT, BODVARSSON GS (2002) Estimating recharge at Yucca Mountain, Nevada, USA: comparison of methods. Hydrogeol J 10: 180-204. doi: Doi 10.1007/S10040-001-0169-1

FREIBURGHAUS M (2012) Statische Übersicht über die Wasserversorgung in der Schweiz 2010. Aqua & Gas 3: 54-59

GABRIELLI CP, MCDONNELL JJ, JARVIS WT (2012) The role of bedrock groundwater in rainfall-runoff response at hillslope and catchment scales. Journal of Hydrology 450-451: 117-133. doi: 10.1016/j.jhydrol.2012.05.023

GALL HE, PARK J, HARMAN CJ, JAWITZ JW, RAO PSC (2013) Landscape filtering of hydrologic and biogeochemical responses in managed catchments. Landscape Ecol 28: 651-664. doi: 10.1007/S10980-012-9829-X

GBUREK WJ, DRUNGIL CC, SRINIVASAN MS, NEEDELMAN BA, WOODWARD DE (2002) Variable-source-area controls on phosphorus transport: Bridging the gap between research and design. J Soil Water Conserv 57: 534-543

GEE GW, HILLEL D (1988) Groundwater Recharge in Arid Regions - Review and Critique of Estimation Methods. Hydrol Process 2: 255-266. doi: 10.1002/Hyp.3360020306

GERMANN PF (1981) Untersuchungen über den Bodenwasserhaushalt im hydrologischen Einzugsgebiet Rietholzbach [Study about the soil water budget in the hydrological catchment Rietholzbach]. Mitteilungen der Versuchsanstalt für Wasserbau, Hydrologie und Glaziologie der ETH Zürich 51

GHARARI S, HRACHOWITZ M, FENICIA F, SAVENIJE HHG (2011) Hydrological landscape classification: investigating the performance of HAND based landscape classifications in a central European meso-scale catchment. Hydrol Earth Syst Sci 15: 3275-3291. doi: 10.5194/Hess-15-3275-2011

GHASEMIZADE M, SCHIRMER M (2013) Subsurface flow contribution in the hydrological cycle: lessons learned and challenges ahead-a review. Environ Earth Sci 69: 707-718. doi: 10.1007/S12665-013-2329-8

GODERNIAUX P, BROUYERE S, FOWLER HJ, et al. (2009) Large scale surface-subsurface hydrological model to assess climate change impacts on groundwater reserves. Journal of Hydrology 373: 122-138. doi: 10.1016/J.Jhydrol.2009.04.017

GRAHAM CB, WOODS RA, MCDONNELL JJ (2010) Hillslope threshold response to rainfall: (1) A field based forensic approach. Journal of Hydrology 393: 65-76. doi: 10.1016/J.Jhydrol.2009.12.015

GREEN TR, TANIGUCHI M, KOOI H, et al. (2011) Beneath the surface of global change: Impacts of climate change on groundwater. Journal of Hydrology 405: 532-560. doi: 10.1016/j.jhydrol.2011.05.002

GUPTA VK, WAYMIRE E, WANG CT (1980) A Representation of an Instantaneous Unit-Hydrograph from Geomorphology. Water Resour Res 16: 855-862. doi: 10.1029/Wr016i005p00855

GURTZ J, VERBUNT M, ZAPPA M, et al. (2003a) Long-term hydrometeorological measurements and model-based analyses in the hydrological research catchment Rietholzbach. Journal of Hydrology and Hydromechanics 51: 162-174

GURTZ J, ZAPPA M, JASPER K, et al. (2003b) A comparative study in modelling runoff and its components in two mountainous catchments. Hydrol Process 17: 297-311. doi: 10.1002/hyp.1125

HAGA H, MATSUMOTO Y, MATSUTANI J, et al. (2005) Flow paths, rainfall properties, and antecedent soil moisture controlling lags to peak discharge in a granitic unchanneled catchment. Water Resour Res 41. doi: 10.1029/2005wr004236

HARMAN CJ, RAO PSC, BASU NB, et al. (2011) Climate, soil, and vegetation controls on the temporal variability of vadose zone transport. Water Resour Res 47. doi: 10.1029/2010wr010194

HAUGHT DRW, MEERVELD HJ (2011) Spatial variation in transient water table responses: differences between an upper and lower hillslope zone. Hydrol Process 25: 3866-3877. doi: 10.1002/Hyp.8354

HEALY RW, COOK PG (2002) Using groundwater levels to estimate recharge. Hydrogeol J 10: 91-109. doi: 10.1007/S10040-001-0178-0

HEALY RW, SCANLON BR (2010) Estimating groundwater recharge Cambridge University Press, Cambridge ; New York

HEIDBÜCHEL I, TROCH PA, LYON SW, WEILER M (2012) The master transit time distribution of variable flow systems. Water Resour Res 48. doi: 10.1029/2011wr011293

HEILLWELL RC, BRITTON A, GIBBS S, FISHER J, AHERNE J (2008) Who Put the N in PristiNe? Impacts of Nitrogen Enrichment in Fragile Mountain Environments. Mt Res Dev 28: 210-215. doi: Doi 10.1659/Mrd.1043

HEIM RR (2002) A review of twentieth-century drought indices used in the United States. B Am Meteorol Soc 83: 1149-1165

HEPPNER CS, NIMMO JR (2005) A Computer Program for Predicting Recharge with a Master Recession Curve US Geological Survey Scientific Investigation Reports United States Geological Survey. .

HEPPNER CS, NIMMO JR, FOLMAR GJ, GBUREK WJ, RISSER DW (2007) Multiple-methods investigation of recharge at a humid-region fractured rock site, Pennsylvania, USA. Hydrogeol J 15: 915-927. doi: 10.1007/S10040-006-0149-6

INAMDAR S, MITCHELL MJ (2007) Contributions of riparian and hillslope waters to storm runoff across multiple catchments and storm events in a glaciated forested watershed. Journal of Hydrology 341: 116-130. doi: 10.1016/J.Jhydrol.2007.05.007

INAMDAR S, RUPP J, MITCHELL M (2009) Groundwater flushing of solutes at wetland and hillslope positions during storm events in a small glaciated catchment in western New York, USA. Hydrol Process 23: 1912-1926. doi: 10.1002/hyp.7322

IPCC (2007) Contribution of Working Group II to the Fourth Assessment Report of the Intergovernmental Panel on Climate Change, 2007 [M.L. Parry, O.F. Canziani, J.P. Palutikof, P.J. van der Linden and C.E. Hanson (eds)]IPCC Fourth Assessment Report: Climate Change 2007.

JACOBI J, PERRONE D, DUNCAN LL, HORNBERGER G (2013) A tool for calculating the Palmer drought indices. Water Resour Res 49: 6086-6089. doi: 10.1002/wrcr.20342

JAMES AL, ROULET NT (2007) Investigating hydrologic connectivity and its association with threshold change in runoff response in a temperate forested watershed. Hydrol Process 21: 3391-3408. doi: 10.1002/hyp.6554

JAMES AL, ROULET NT (2009) Antecedent moisture conditions and catchment morphology as controls on spatial patterns of runoff generation in small forest catchments. Journal of Hydrology 377: 351-366. doi: 10.1016/j.jhydrol.2009.08.039

JASPER K, CALANCA P, GYALISTRAS D, FUHRER J (2004) Differential impacts of climate change on the hydrology of two alpine river basins. Climate Research 26: 113-129. doi: 10.3354/cr026113

JENCSO KG, MCGLYNN BL (2011) Hierarchical controls on runoff generation: Topographically driven hydrologic connectivity, geology, and vegetation. Water Resour Res 47. doi: 10.1029/2011wr010666

JENCSO KG, MCGLYNN BL, GOOSEFF MN, BENCALA KE, WONDZELL SM (2010) Hillslope hydrologic connectivity controls riparian groundwater turnover: Implications of catchment structure for riparian buffering and stream water sources. Water Resour Res 46. doi: 10.1029/2009wr008818

JYRKAMA MI, SYKES JF (2007) The impact of climate change on spatially varying groundwater recharge in the grand river watershed (Ontario). Journal of Hydrology 338: 237-250. doi: 10.1016/J.Jhydrol.2007.02.036

KEESE KE, SCANLON BR, REEDY RC (2005) Assessing controls on diffuse groundwater recharge using unsaturated flow modeling. Water Resour Res 41. doi: 10.1029/2004wr003841

KIRCHNER JW (2003) A double paradox in catchment hydrology and geochemistry. Hydrol Process 17: 871-874. doi: 10.1002/Hyp.5108

KIRCHNER JW (2009) Catchments as simple dynamical systems: Catchment characterization, rainfall-runoff modeling, and doing hydrology backward. Water Resour Res 45: 34. doi: 10.1029/2008wr006912

KOENIG P, LANG H, SCHWARZE R (1994) On the runoff formation in the small pre-alpine research basin RietholzbachFRIEND: Flow Regimes from International Experimental

and Network Data (Proceedings of the Braunschweig Conference, October 1993) IAHS Publ. No. 221, pp. 391-398.

KUHN H (1980) Bodenkartierung HYDREX. Internal, unpublished report. Swiss Federal Institute of Technology (ETH), Zurich, pp. 64.

LAUDON H, SLAYMAKER O (1997) Hydrograph separation using stable isotopes, silica and electrical conductivity: an alpine example. Journal of Hydrology 201: 82-101. doi: http://dx.doi.org/10.1016/S0022-1694(97)00030-9

LEHMANN P, HINZ C, MCGRATH G, TROMP-VAN MEERVELD HJ, MCDONNELL JJ (2007) Rainfall threshold for hillslope outflow: an emergent property of flow pathway connectivity. Hydrol Earth Syst Sci 11: 1047-1063

LEIBUNDGUT C, SEIBERT J (2011) Tracer Hydrology. In: Uhlenbrook S (ed) The Science of HydrologyWilderer P, Treatise on Water Science:215-236.

LERNER DN, ISSAR AS, SIMMERS I (1990) Groundwater Recharge: A Guide to Understanding and Estimating Natural Recharge Heise, Hannover, Germany

LYON SW, MCHALE MR, WALTER MT, STEENHUIS TS (2006a) The impact of runoff generation mechanisms on the location of critical source areas. J Am Water Resour Assoc 42: 793-804. doi: 10.1111/J.1752-1688.2006.Tb04493.X

LYON SW, SEIBERT J, LEMBO AJ, WALTER MT, STEENHUIS TS (2006b) Geostatistical investigation into the temporal evolution of spatial structure in a shallow water table. Hydrol Earth Syst Sci 10: 113-125. doi: 10.5194/hess-10-113-2006

MARÉCHAL JC, DEWANDEL B, AHMED S, GALEAZZI L, ZAIDI FK (2006) Combined estimation of specific yield and natural recharge in a semi-arid groundwater basin with irrigated agriculture. Journal of Hydrology 329: 281-293. doi: 10.1016/j.jhydrol.2006.02.022

MARTINA MLV, ENTEKHABI D (2006) Identification of runoff generation spatial distribution using conventional hydrologic gauge time series. Water Resour Res 42. doi: 10.1029/2005wr004783

MAXWELL RM, KOLLET SJ (2008) Interdependence of groundwater dynamics and land-energy feedbacks under climate change. Nature Geoscience 1: 665-669. doi: 10.1038/ngeo315

MCGLYNN BL, MCDONNELL JJ (2003) Quantifying the relative contributions of riparian and hillslope zones to catchment runoff. Water Resour Res 39. doi: 10.1029/2003wr002091

MCGLYNN BL, MCDONNELL JJ, SEIBERT J, KENDALL C (2004) Scale effects on headwater catchment runoff timing, flow sources, and groundwater-streamflow relations. Water Resour Res 40. doi: 10.1029/2003wr002494

MCGLYNN BL, SEIBERT J (2003) Distributed assessment of contributing area and riparian buffering along stream networks. Water Resour Res 39. doi: 10.1029/2002wr001521

MCGRATH GS, HINZ C, SIVAPALAN M (2007) Temporal dynamics of hydrological threshold events. Hydrol Earth Syst Sci 11: 923-938

MCGUIRE KJ, MCDONNELL JJ (2010) Hydrological connectivity of hillslopes and streams: Characteristic time scales and nonlinearities. Water Resour Res 46. doi: 10.1029/2010wr009341

METEOSWISS (2009) Klimabulletin Jahr 2009 [Clima Bulletin of the year 2009] Swiss Federal Office of Meteorology and Climatology MeteoSwiss.

METEOSWISS (2011) Klimabulletin Jahr 2011 [Clima Bulletin of the year 2011] Swiss Federal Office of Meteorology and Climatology MeteoSwiss.

METEOSWISS (2013) Climate Scenarios - A Regional Survey [Klimaszenarien Schweiz - eine regionale Übersicht]Fachbericht MeteoSchweiz Nr 243 Swiss Federal Office of Meteorology and Climatology MeteoSwiss, pp. 36.

MEYER JL, STRAYER DL, WALLACE JB, et al. (2007) The contribution of headwater streams to biodiversity in river networks. J Am Water Resour Assoc 43: 86-103. doi: 10.1111/j.1752-1688.2007.00008.x

MIDDELKOOP H, DAAMEN K, GELLENS D, et al. (2001) Impact of climate change on hydrological regimes and water resources management in the rhine basin. Clim Change 49: 105-128. doi: 10.1023/a:1010784727448

MILLARES A, POLO MJ, LOSADA MA (2009) The hydrological response of baseflow in fractured mountain areas. Hydrol Earth Syst Sci 13: 1261-1271

MISHRA AK, SINGH VP (2010) A review of drought concepts. Journal of Hydrology 391: 204-216. doi: 10.1016/J.Jhydrol.2010.07.012

MITTELBACH H (2011) Soil moisture in Switzerland. Analyses from the Swiss soil moisture experiment. Doctoral Thesis, Swiss Federal Institute of Technology (ETH)

MORIASI DN, ARNOLD JG, VAN LIEW MW, et al. (2007) Model evaluation guidelines for systematic quantification of accuracy in watershed simulations. T Asabe 50: 885-900

MUNZ N, LEU C, WITTMER I (2012) Pestizidmessungen in Fliessgewässern. Aqua & Gas 11: 32-41

NACHABE MH (2002) Analytical expressions for transient specific yield and shallow water table drainage. Water Resour Res 38. doi: 10.1029/2001wr001071

NASH JE, SUTCLIFFE JV (1970) River flow forecasting through conceptual models part I - A discussion of principles. Journal of Hydrology 10: 282-290. doi: http://dx.doi.org/10.1016/0022-1694(70)90255-6

NATHAN RJ, MCMAHON TA (1990) Evaluation of Automated Techniques for Base-Flow and Recession Analyses. Water Resour Res 26: 1465-1473. doi: 10.1029/Wr026i007p01465

NAZ BS, ALE S, BOWLING LC (2009) Detecting subsurface drainage systems and estimating drain spacing in intensively managed agricultural landscapes. Agricultural Water Management 96: 627-637. doi: 10.1016/j.agwat.2008.10.002

NIMMO JR (2003) Aquifer recharge. In: Steward BA, Howell TA (eds) Encyclopedia of Water Science:1-4.

OCAMPO CJ, SIVAPALAN M, OLDHAM C (2006) Hydrological connectivity of upland-riparian zones in agricultural catchments: Implications for runoff generation and nitrate transport. Journal of Hydrology 331: 643-658. doi: 10.1016/j.jhydrol.2006.06.010

ORDENS CM, POST VEA, WERNER AD, HUTSON JL (2014) Influence of model conceptualisation on one-dimensional recharge quantification: Uley South, South Australia. Hydrogeol J 22: 795-805. doi: 10.1007/S10040-014-1100-X

PALMER WC (1965) Meteorological Drought In: Connor JT (ed) U.S. Deparment of Commerce, Weather Bureau, Washington, D.C., pp. 65.

PEARSON K (1895) Note on Regression and Inheritance in the Case of Two Parents. Proceedings of the Royal Society of London 58: 240-242. doi: 10.1098/rspl.1895.0041

PENNA D, TROMP-VAN MEERVELD HJ, GOBBI A, BORGA M, DALLA FONTANA G (2011) The influence of soil moisture on threshold runoff generation processes in an alpine headwater catchment. Hydrol Earth Syst Sci 15: 689-702. doi: 10.5194/hess-15-689-2011

PFISTER L, MCDONNELL JJ, HISSLER C, HOFFMANN L (2010) Ground-based thermal imagery as a simple, practical tool for mapping saturated area connectivity and dynamics. Hydrol Process 24: 3123-3132. doi: 10.1002/hyp.7840

PIONKE HB, GBUREK WJ, SHARPLEY AN, SCHNABEL RR (1996) Flow and nutrient export patterns for an agricultural hill-land watershed. Water Resour Res 32: 1795-1804. doi: Doi 10.1029/96wr00637

PLATE E (1998) Socio-economic factors in headwater land management. Hydrology, Water Resources and Ecology in Headwaters: 523-533

POSAVEC K, PARLOV J, NAKIC Z (2010) Fully Automated Objective-Based Method for Master Recession Curve Separation. Ground Water 48: 598-603. doi: 10.1111/J.1745-6584.2009.00669.X

PRINGLE C (2003) What is hydrologic connectivity and why is it ecologically important? Hydrol Process 17: 2685-2689. doi: 10.1002/hyp.5145

RINALDO A, BEVEN KJ, BERTUZZO E, et al. (2011) Catchment travel time distributions and water flow in soils. Water Resour Res 47. doi: 10.1029/2011wr010478

RISSER DW, GBUREK WJ, FOLMAR GJ (2005) Comparison of methods for estimating ground-water recharge and base flow at a small watershed underlain by fractured bedrock in the eastern United States U.S. Geological Survey, Reston, Va.

RODHE A, SEIBERT J (2011) Groundwater dynamics in a till hillslope: flow directions, gradients and delay. Hydrol Process 25: 1899-1909. doi: 10.1002/hyp.7946

RODRIGUEZ-ITURBE I, PORPORATO A, RIDOLFI L, ISHAM V, COX DR (1999) Probabilistic modelling of water balance at a point: the role of climate, soil and vegetation. P Roy Soc a-Math Phy 455: 3789-3805

RORABAUGH MI (1964) Estimating changes in bank storage and groundwater-contribution to streamflow. International Association of Scientific Hydrology: 432-441

ROY JW, HAYASHI M (2009) Multiple, distinct groundwater flow systems of a single moraine-talus feature in an alpine watershed. Journal of Hydrology 373: 139-150

RUTLEDGE AT (2002) Considerations for use of the RORA program to estimate ground-water recharge from streamflow records Open-File Report 00-156 U.S. Geological Survey, pp. 44.

RUTLEDGE AT (2007) Update on the use of the RORA program for recharge estimation. Ground Water 45: 374-382. doi: 10.1111/J.1745-6584.2006.00294.X

RUTLEDGE AT, DANIEL CC (1994) Testing an Automated-Method to Estimate Groundwater Recharge from Streamflow Records. Ground Water 32: 180-189. doi: 10.1111/J.1745-6584.1994.Tb00632.X

SAVENIJE HHG (2004) The importance of interception and why we should delete the term evapotranspiration from our vocabulary. Hydrol Process 18: 1507-1511. doi: Doi 10.1002/Hyp.5563

SCANLON BR, HEALY RW, COOK PG (2002) Choosing appropriate techniques for quantifying groundwater recharge. Hydrogeol J 10: 18-39. doi: 10.1007/S10040-001-0176-2

SCANLON BR, KEESE KE, FLINT AL, et al. (2006) Global synthesis of groundwater recharge in semiarid and arid regions. Hydrol Process 20: 3335-3370. doi: 10.1002/hyp.6335

SCHAAP MG, LEIJ FJ, VAN GENUCHTEN MT (2001) ROSETTA: a computer program for estimating soil hydraulic parameters with hierarchical pedotransfer functions. Journal of Hydrology 251: 163-176. doi: 10.1016/S0022-1694(01)00466-8

SCHÄR C, JENDRITZKY G (2004) Climate change: Hot news from summer 2003. Nature 432: 559-560. doi: 10.1038/432559a

SEIBERT J, GRABS T, KOHLER S, et al. (2009) Linking soil- and stream-water chemistry based on a Riparian Flow-Concentration Integration Model. Hydrol Earth Syst Sci 13: 2287-2297

SEIBERT J, MCGLYNN BL (2005) Landscape Element Contributions to Storm Runoff. In: Anderson MG (ed) Encyclopedia of Hydrological Sciencees:1751-1761.

SENEVIRATNE SI, LEHNER I, GURTZ J, et al. (2012) Swiss prealpine Rietholzbach research catchment and lysimeter: 32 year time series and 2003 drought event. Water Resour Res 48: W06526. doi: 10.1029/2011wr011749

SHAH N, ROSS M (2009) Variability in Specific Yield under Shallow Water Table Conditions. J Hydrol Eng 14: 1290-1298. doi: 10.1061/(asce)he.1943-5584.0000121

SIDLE RC, TSUBOYAMA Y, NOGUCHI S, et al. (1995) Seasonal hydrologic response at various spatial scales in a small forested catchment, Hitachi-Ohta, Japan Jounal of Hydrology 168: 227-250. doi: 10.1016/0022-1694(94)02639-s

SIMMERS I (1998) Groundwater recharge: An overview of estimation "problems" and rechent developments. In: Robins NS (ed) Groundwater pollution, aquifer recharge and vulnerability Geological Society special publication 130.

SIMONI S, PADOAN S, NADEAU DF, et al. (2011) Hydrologic response of an alpine watershed: Application of a meteorological wireless sensor network to understand streamflow generation. Water Resour Res 47. doi: 10.1029/2011wr010730

SIMUNEK J, VAN GENUCHTEN MT (2008) Modeling nonequilibrium flow and transport processes using HYDRUS. Vadose Zone Journal 7: 782-797. doi: 10.2136/vzj2007.0074

SIVAPALAN M (2003) Process complexity at hillslope scale, process simplicity at the watershed scale: is there a connection? Hydrol Process 17: 1037-1041. doi: 10.1002/Hyp.5109

SKLASH MG, FARVOLDEN RN (1979) The role of groundwater in storm runoff. Journal of Hydrology 43: 45-65. doi: 10.1016/0022-1694(79)90164-1

SMAKHTIN VU (2001) Low flow hydrology: a review. Journal of Hydrology 240: 147-186. doi: 10.1016/S0022-1694(00)00340-1

SOPHOCLEOUS MA (1991) Combining the Soilwater Balance and Water-Level Fluctuation Methods to Estimate Natural Groundwater Recharge - Practical Aspects. Journal of Hydrology 124: 229-241. doi: 10.1016/0022-1694(91)90016-B

SORENSEN JPR, FINCH JW, IRESON AM, JACKSON CR (2014) Comparison of varied complexity models simulating recharge at the field scale. Hydrol Process 28: 2091-2102. doi: 10.1002/hyp.9752

STEENHUIS TS, WINCHELL M, ROSSING J, ZOLLWEG JA, WALTER MF (1995) SCS Runoff Equation Revisited for Variable-Source Runoff Areas. J Irrig Drain E-Asce 121: 234-238. doi: 10.1061/(Asce)0733-9437(1995)121:3(234)

STIEGLITZ M, SHAMAN J, MCNAMARA J, et al. (2003) An approach to understanding hydrologic connectivity on the hillslope and the implications for nutrient transport. Global Biogeochemical Cycles 17. doi: 10.1029/2003gb002041

STRAHM I, MUNZ N, LEU C, WITTMER I, STAMM C (2013) Landnutzung entlang des Gewässernetzes. Aqua & Gas 5: 36-44

STUMPP C, MALOSZEWSKI P (2010) Quantification of preferential flow and flow heterogeneities in an unsaturated soil planted with different crops using the environmental isotope delta O-18. Journal of Hydrology 394: 407-415. doi: 10.1016/J.Jhydrol.2010.09.014

SURRIDGE BWJ, HEATHWAITE AL, BAIRD AJ (2007) The Release of Phosphorus to Porewater and Surface Water from River Riparian Sediments. J Environ Qual 36: 1534-1544. doi: 10.2134/jeq2006.0490

TALLAKSEN LM, HISDAL H, VAN LANEN HAJ (2009) Space-time modelling of catchment scale drought characteristics. Journal of Hydrology 375: 363-372. doi: 10.1016/J.Jhydrol.2009.06.032

TALLAKSEN LM, MADSEN H, CLAUSEN B (1997) On the definition and modelling of streamflow drought duration and deficit volume. Hydrol Sci J-J Sci Hydrol 42: 15-33. doi: 10.1080/02626669709492003

TALLAKSEN LM, VAN LANEN HAJ (2004) Hydrological drought: processes and estimation methods for streamflow and groundwater Elsevier, London

TARBOTON DG (1997) A new method for the determination of flow directions and upslope areas in grid digital elevation models. Water Resour Res 33: 309-319. doi: 10.1029/96wr03137

TETZLAFF D, SOULSBY C, BACON PJ, et al. (2007) Connectivity between landscapes and riverscapes - a unifying theme in integrating hydrology and ecology in catchment science? Hydrol Process 21: 1385-1389. doi: 10.1002/hyp.6701

TEULING AJ, LEHNER I, KIRCHNER JW, SENEVIRATNE SI (2010) Catchments as simple dynamical systems: Experience from a Swiss prealpine catchment. Water Resour Res 46. doi: 10.1029/2009wr008777

THOMPSON JJD, DOODY DG, FLYNN R, WATSON CJ (2012) Dynamics of critical source areas: Does connectivity explain chemistry? Sci Total Environ 435: 499-508. doi: 10.1016/J.Scitotenv.2012.06.104

THOMPSON SE, BASU NB, LASCURAIN J, AUBENEAU A, RAO PSC (2011) Relative dominance of hydrologic versus biogeochemical factors on solute export across impact gradients. Water Resour Res 47. doi: 10.1029/2010wr009605

TROCH PA, CARRILLO GA, HEIDBŰCHEL I, et al. (2009) Dealing with Landscape Heterogeneity in Watershed Hydrology: A Review of Recent Progress toward New Hydrological Theory. Geography Compass 3: 375-392. doi: 10.1111/j.1749-8198.2008.00186.x

TROMP-VAN MEERVELD HJ, MCDONNELL JJ (2006a) On the interrelations between topography, soil depth, soil moisture, transpiration rates and species distribution at the hillslope scale. Advances in Water Resources 29: 293-310. doi: 10.1016/J.Advwatres.2005.02.016f

TROMP-VAN MEERVELD HJ, MCDONNELL JJ (2006b) Threshold relations in subsurface stormflow 2. The fill and spill hypothesis. Water Resour Res 42. doi: 10.1029/2004WR003800

TROMP-VAN MEERVELD HJ, MCDONNELL JJ (2006c) Threshold relations in subsurface stormflow: 1. A 147-storm analysis of the Panola hillslope. Water Resour Res 42. doi: 10.1029/2004wr003778

U.S. Department of Agriculture - Soil Conservation Service (USDA-SCS) (1972) Estimation of Direct Runoff from Storm Rainfall National Engineering Handbook.

VAN GENUCHTEN MT (1980) A Closed-Form Equation for Predicting the Hydraulic Conductivity of Unsaturated Soils. Soil Science Society of America Journal 44: 892-898

VAN ROOSMALEN L, SONNENBORG TO, JENSEN KH (2009) Impact of climate and land use change on the hydrology of a large-scale agricultural catchment. Water Resour Res 45. doi: 10.1029/2007wr006760

VAN VERSEVELD WJ, MCDONNELL JJ, LAJTHA K (2009) The role of hillslope hydrology in controlling nutrient loss. Journal of Hydrology 367: 177-187. doi: 10.1016/j.jhydrol.2008.11.002

VANHAM D, FLEISCHHACKER E, RAUCH W (2009) Impact of an extreme dry and hot summer on water supply security in an alpine region. Water Sci Technol 59: 469-477. doi: 10.2166/Wst.2009.887

VIDON P, ALLAN C, BURNS D, et al. (2010) Hot Spots and Hot Moments in Riparian Zones: Potential for Improved Water Quality Management1. JAWRA Journal of the American Water Resources Association 46: 278-298. doi: 10.1111/j.1752-1688.2010.00420.x

VIDON P, SMITH AP (2007) Upland controls on the hydrological functioning of riparian zones in glacial till valleys of the Midwest. J Am Water Resour Assoc 43: 1524-1539. doi: 10.1111/j.1752-1688.2007.00125.x

VITVAR T, BALDERER W (1997) Estimation of mean water residence times and runoff generation by O-18 measurements in a pre-Alpine catchment (Rietholzbach, eastern Switzerland). Applied Geochemistry 12: 787-796

VIVIROLI D, WEINGARTNER R, MESSERLI B (2003) Assessing the hydrological significance of the world's mountains. Mt Res Dev 23: 32-40. doi: 10.1659/0276-4741(2003)023[0032:Athsot]2.0.Co;2

VON FREYBERG J, RADNY D, GALL HE, SCHIRMER M (2014) Implications of hydrologic connectivity between hillslopes and riparian zones on streamflow composition. Journal of Contaminant Hydrology 169: 62-74. doi: http://dx.doi.org/10.1016/j.jconhyd.2014.07.005

VON FREYBERG J, RAO PSC, RADNY D, SCHIRMER M (2015) The impact of hillslope groundwater dynamics and landscape functioning in event-flow generation: a field study in the Rietholzbach catchment, Switzerland. Hydrogeol J (*accepted for publication*). doi: 10.1007/s10040-015-1238-1

WALTER MT, BROOKS ES, MCCOOL DK, et al. (2005) Process-based snowmelt modeling: Does it require more input data than temperature-index modeling? Journal of Hydrology 300: 65-75. doi: Process-based snowmelt modeling: Does it require more input data than temperature-index modeling?

WEILER M, MCDONNELL JJ (2006) Testing nutrient flushing hypotheses at the hillslope scale: A virtual experiment approach. Journal of Hydrology 319: 339-356. doi: http://dx.doi.org/10.1016/j.jhydrol.2005.06.040

WEINGARTNER R (1999) Analyses of regional hydrology - Fundamental principles and applications [Regionalhydrologische Analysen- Grundlagen und Anwendungen]Beiträge zur Hydrologie der Schweiz, Berne.

WEINGARTNER R, BARBEN M, SPREAFICO M (2003) Floods in mountain areas - an overview based on examples from Switzerland. Journal of Hydrology 282: 10-24. doi: 10.1016/S0022-1694(03)00249-X

WIENHÖFER J, GERMER K, LINDENMAIER F, FARBER A, ZEHE E (2009) Applied tracers for the observation of subsurface stormflow at the hillslope scale. Hydrol Earth Syst Sci 13: 1145-1161. doi: 10.5194/hess-13-1145-2009

WINTER TC, ROSENBERRY DO, LABAUGH JW (2003) Where Does the Ground Water in Small Watersheds Come From? Ground Water 41: 989-1000. doi: 10.1111/j.1745-6584.2003.tb02440.x

WITTENBERG H (1999) Baseflow recession and recharge as nonlinear storage processes. Hydrol Process 13: 715-726. doi: 10.1002/(Sici)1099-1085(19990415)13:5<715::Aid-Hyp775>3.0.Co;2-N

WOODBURY JD, SHOEMAKER CA, EASTON ZM, COWAN DM (2014) Application of Swat with and without Variable Source Area Hydrology to a Large Watershed. J Am Water Resour Assoc 50: 42-56. doi: 10.1111/Jawr.12116

WOODWELL GM (2004) Mountains: Top down. Ambio: 35-38

XU CY, CHEN D (2005) Comparison of seven models for estimation of evapotranspiration and groundwater recharge using lysimeter measurement data in Germany. Hydrol Process 19: 3717-3734. doi: 10.1002/Hyp.5853

YOUNG MH, WIERENGA PJ, MANCINO CF (1996) Large weighing lysimeters for water use and deep percolation studies. Soil Sci 161: 491-501. doi: 10.1097/00010694-199608000-00004

ZAJICEK A, KVITEK T, KAPLICKA M, et al. (2011) Drainage water temperature as a basis for verifying drainage runoff composition on slopes. Hydrol Process 25: 3204-3215. doi: 10.1002/hyp.8039

ZEHE E, SIVAPALAN M (2009) Threshold behaviour in hydrological systems as (human) geo-ecosystems: manifestations, controls, implications. Hydrol Earth Syst Sci 13: 1273-1297. doi: 10.5194/hess-13-1273-2009

ZIERL B, BUGMANN H (2005) Global change impacts on hydrological processes in Alpine catchments. Water Resour Res 41. doi: 10.1029/2004wr003447

ZLOTNIK VA, CARDENAS MB, TOUNDYKOV D (2011) Effects of Multiscale Anisotropy on Basin and Hyporheic Groundwater Flow. Ground Water 49: 576-583. doi: 10.1111/j.1745-6584.2010.00775.x